



UiT The Arctic University of Norway

Faculty of Science and Technology
Department of Physics and Technology

Pulsating Aurora: Optical observations and modelling of the time-variation of ionospheric response to precipitation of pitch-angle-scattered electrons from the magnetosphere

Silje Moe Stangstuen

FYS-3931 Master's thesis in Space Physics 30 SP
January 2024

Abstract

This thesis explores the mechanisms governing pulsating auroras by combining observational analysis with theoretical simulations using the AURORA model. The AURORA model simulates electron transport and ionospheric responses, playing a key role in replicating the abrupt onset precipitation of electrons from source altitudes at $3 R_E$, $4.4 R_E$, $6.1 R_E$, and $7.6 R_E$. Eight events of pulsating aurora were selected between October 2006 and March 2007, with a focus on emissions at 4278 \AA , 6730 \AA , 7774 \AA , and 8446 \AA . The observational part of the thesis examines distinct pulsations, highlighting differences in intensity and noise levels across these eight events. The theoretical study aligns with observed pulsation characteristics, establishing a clear link when comparing observational results with theoretical findings. Furthermore, it emphasises the necessity of specific source altitudes for achieving abrupt onsets in the ionosphere. The research findings indicate that, for an abrupt pulsation onset in the ionosphere over Tromsø, the source altitude along the magnetic field line must fall within the range of $6.1 R_E$ and $7.6 R_E$. The study highlights the importance of combining both observational and theoretical approaches to advance our understanding of the onset characteristics of pulsating aurora.

Acknowledgements

I would like to thank my supervisor Professor Björn Johan Gustavsson for invaluable guidance during the entire process of working with this master's thesis. Keeping me on track and providing feedback whenever I needed it.

A big thanks to Dr Daniel Whiter for generously providing me with the necessary data to conduct this research.

I want to express my gratitude to Etienne Gavazzi for preparing and sharing the necessary MATLAB code for conducting the theoretical study, as well as for engaging in valuable conversations.

Additionally, I want to thank my family, friends and fellow students for continuous support and encouragement. Making the past five and a half years an enjoyable experience.

Lastly, I would like to extend special thanks to Amalie Gjelsvik for proofreading this thesis.

Contents

Abstract	i
Acknowledgements	iii
List of Figures	vii
List of Tables	ix
1 Introduction	1
2 Theory	3
2.1 Pulsating Aurora	3
2.2 Time-Dependent Electron Transport Equation	6
2.2.1 Discretized Transport Equation	8
2.2.2 Pitch Angle Streams	9
3 Instruments	11
3.1 Auroral Structure and Kinetics	11
3.2 All Sky Camera	13
3.3 Magnetometer	15
4 Observational Study	21
4.1 Events	21
4.1.1 Event 1	23
4.1.2 Event 2	26
4.1.3 Event 3	30
4.1.4 Event 4	33
4.1.5 Event 5	37
4.1.6 Event 6	41
4.1.7 Event 7	44
4.1.8 Event 8	47
4.2 Results	51
5 Theoretical Study	55

5.1 Intensity Modulation	55
5.2 Intensity Ratio	59
6 Discussion	61
7 Summary	63
Bibliography	65
A Python Code	69
B Matlab Code	93

List of Figures

3.1	Keogram - ASK	13
3.2	ASC NIPR	15
3.3	IMF event 1, 2, 3, 4	16
3.4	IMF events 5, 6, 7, 8	17
3.5	Magnetometer plots from ground	18
4.1	Event 1: Main event plots	23
4.2	Event 1: pseudocolour plot of emission 6730 Å	24
4.3	Event 1: pseudocolour-plot of emission 7774 Å	24
4.4	Event 1: Specific onset gradient	25
4.5	Event 1: Incorrect onset example	25
4.6	Event 1: Regression line plot	26
4.7	Event 2: Main event plots	27
4.8	Event 2: pseudocolour plot 5620 Å	28
4.9	Event 2: pseudocolour plot 7774 Å	28
4.10	Event 2: Specific onset gradient	29
4.11	Event 2: Incorrect onset example	29
4.12	Event 2: Regression line plot	30
4.13	Event 3: Main event plots	31
4.14	Event 3: pseudocolour plot r2	31
4.15	Event 3: pseudocolour plot r3	32
4.16	Event 3: Specific onset gradient	32
4.17	Event 3: Incorrect onset example	33
4.18	Event 3: Regression line plot	33
4.19	Event 4: Main event plots	34
4.20	Event 4: pseudocolour plot 6730 Å	35
4.21	Event 4: pseudocolour plot 7774 Å	35
4.22	Event 4: Specific onset gradient	36
4.23	Event 4: Incorrect onset example	36
4.24	Event 4: Regression line plot	37
4.25	Event 5: Main event plots	38
4.26	Event 5: pseudocolour plot 6730 Å	38
4.27	Event 5: pseudocolour plot 7774 Å	39
4.28	Event 5: Specific onset gradient	39

4.29 Event 5: Incorrect onset example	40
4.30 Event 5: Regression line plot	40
4.31 Event 6: Main event plots	41
4.32 Event 6: pseudocolour plot 6730 Å	42
4.33 Event 6: pseudocolour plot 7774 Å	42
4.34 Event 6: Specific onset gradient	43
4.35 Event 6: Incorrect onset example	43
4.36 Event 6: Regression line plot	44
4.37 Event 7: Main event plots	45
4.38 Event 7: pseudocolour plot 6730 Å	45
4.39 Event 7: pseudocolour plot 7774 Å	46
4.40 Event 7: Specific onset gradient	46
4.41 Event 7: Incorrect onset example	47
4.42 Event 7: Regression line plot	47
4.43 Event 8: Main event plots	48
4.44 Event 8: pseudocolour plot 6730 Å	49
4.45 Event 8: pseudocolour plot 7774 Å	49
4.46 Event 8: Specific onset gradient	50
4.47 Event 8: Incorrect onset example	50
4.48 Event 8: Regression line plot	51
4.49 Regression slopes w/uncertainties	53
5.1 Column integration for all altitudes	57
5.2 Column integration for all emissions	57
5.3 Comparison of pulsation onsets at 6730 Å	58
5.4 Comparison of pulsation onsets at 6730 Å	58
5.5 Intensity Ratio	59

List of Tables

3.1	ASK Camera Overview. The symbol " marks equivalence to the reference above.	12
3.2	Campaign log for the selected events	12
4.1	Event overview. The symbol " marks equivalence to the reference above.	22
4.2	Slope of the regression lines and their variance for each event.	52
4.3	y-axis intercept of the regression line for the events.	52



Introduction

The objective of the master's thesis is to analyse optical observations of pulsating aurora and model the time-variation of the ionospheric response to precipitation of pitch angle scattered electrons from the magnetosphere.

The work consists of two main parts, a data analysis part and a modelling part. The data analysis includes studying optical observations in keogram form of observations made by the Auroral Structure Kinetics (ASK) instrument, located at the European incoherent scatter (EISCAT) radar in Ramfjordmoen during the time period October 2006 to March 2007.

Calculations using a time-dependent electron transport model has been done to model the ionospheric response to electron precipitation at onset of pulsations. Since the electron precipitation varies at sub-second time-scales, an electron transport model has to take time-off-flight into account to properly model the pulsating aurora. In the context of electron transport models and simulations, the term "time-of-flight" refers to the time it takes for the particles to travel from a source region to a particular location within the ionosphere or atmosphere and is crucial regarding the ionospheric response.

The model that will be used for this purpose is called AURORA. It is a time-dependent multi-stream electron transport model, developed to model dynamic auroral phenomena such as pulsating aurora (Gustavsson, 2022). The model is intended to study the auroral emission rates, by investigating precipitation that has significant variations on sub-second timescales. AURORA accounts for

the time-of-flight, scattering, energy loss of the precipitating electrons and the production of secondary electrons. Previously, the model has been used to study flickering aurora, by making models and simulations. It has been used to model intensity variations of auroral emissions at the wavelengths 4278 Å, 6730 Å, 7444 Å and 8446 Å in flickering aurora (Gustavsson, 2022). In this study I use AURORA to calculate the intensity variations after the onsets with subsecond time resolution.

In this thesis, AURORA has been employed to capture Maxwellian energy spectra with a prompt onset of a pulse. The abrupt onset of loss-cone filling is set at different source altitudes up along the magnetic field-line at 3, 4.4, 6.1 and 7.6 earth radii, and is assumed to occur simultaneously at all energies. The goal of the thesis is to compare the onset characteristics from the data analysis with the onset characteristics obtained with AURORA.

In Chapter 2, essential background theory on pulsating auroras and the time-dependent electron transport equation is presented, providing knowledge regarding the use of the AURORA model in the theoretical part of the thesis. The instruments used to gather data for investigation in the observational part of the thesis are presented in Chapter 3. The observational study is detailed in Chapter 4, where selected events are described, and the results for each of them are presented. This is followed by the theoretical study in Chapter 5, where the results obtained from the AURORA model are presented. Chapter 6 consists of a discussion reflecting on the results. Finally, in Chapter 7, there is a summary of the thesis.

/2

Theory

In this chapter the theoretical framework used in the thesis is presented. In Section 2.1 the background theory on pulsating aurora is introduced, followed by an introduction of the Time-dependent electron transport equation used in the AURORA model found in Section 2.2. In Section 2.2.1 the discretized transport equation is discussed, and then in Section 2.2.2 the pitch angle streams are described.

2.1 Pulsating Aurora

The aurora is a captivating natural phenomenon, among the most dramatic spectacles in nature (Johnstone, 1978). The dynamics of the interaction between the Sun and magnetosphere of the Earth, is directly displayed in the aurora (Gustavsson, 2022). The solar wind interacts with the magnetosphere, which start multiple different processes that leads to the precipitation of particles into the atmosphere of the Earth. The particles consists of ions and electrons (Grono and Donovan, 2019). Plasma waves induce pitch angle scattering, leading to the precipitation of energetic electrons (Miyoshi et al., 2010). Energetic electrons experience random angular deviations, when they get scattered by the atmosphere (Rees, 1968). They collide with atoms and molecules present in the upper atmosphere, generating auroral pulsations (Kasahara et al., 2018). Most of the electrons injected into the inner magnetosphere from the magnetotail plasma sheet, typically reside outside of the loss cone and are trapped between

their mirror points (Yu et al., 2023). They can be trapped in the magnetosphere at closed magnetic field-lines, where the particles will bounce back and forth between their magnetic mirror points. As the particles bounce between the mirror points, the magnetic field makes the particles change direction, and by that also altering their pitch angle. The pitch angle is the angle between the direction of the magnetic field line and the velocity of the particle. This occurs as a result the field-aligned component of the Lorentz-force, which averaged over a gyro-period will push particles away from their mirror-points. If the particle has a mirror point in the lower thermosphere or below, it can start to interact with the atmosphere and ultimately be lost (Grono and Donovan, 2019).

The loss cone is described as the pitch angle range where particles are no longer trapped by the magnetic mirror force, but lost into the atmosphere of the Earth (Grono and Donovan, 2019). Particles that come from the plasma sheet and radiation belts, can be accelerated or scattered into the loss cone. It will eventually collide with atmospheric particles, and by doing so, excite different species in the polar atmosphere and create aurora (Tesema et al., 2020).

The particles can also be scattered into the loss cone through interaction with whistler-mode and chorus waves, by means of cyclotron resonances (Yu et al., 2023). The cyclotron resonance instability trigger the chorus wave activity through the injection of plasma sheet electrons into the magnetosphere. This occur at the same time as geomagnetic activity, and so the precipitation occur in the equator-ward section of the auroral oval (Partamies et al., 2017). Chorus waves are generated at the equator and propagate to higher latitudes, where they interact with particles in both hemispheres. The waves induce a Lorentz force that scatter electrons, making some of them align with the magnetic field of the Earth. As a result the electrons fall into the loss cone, and then start to interact with the upper atmosphere (Kasahara et al., 2018).

The two main types of aurora are discrete- and diffuse aurora. We can classify the aurora by the different processes which cause the particles to move into the loss cone. In other words, how the aurora is created (Grono and Donovan, 2019). Discrete aurora is observed when particles are accelerated into the loss cone by an increased field-aligned velocity, caused by the magnetic field-aligned electric field (Grono and Donovan, 2019). The electric field increases the kinetic energy of the particles parallel to the magnetic field, which ends up altering their pitch angle into the loss cone. The discrete auroral arc is an example of discrete aurora (Grono and Donovan, 2020). Diffuse aurora is observed when the particles are scattered into the loss cone due to either the magnetic field curvature or interactions with plasma-waves (Grono and Donovan, 2019). The electromagnetic waves that dominates the pitch angle scattering are the whistler-mode and chorus waves (Kasahara et al., 2018). The

plasma sheet induced precipitation has no additional acceleration in the low-altitude magnetosphere causing diffuse aurora. It is a region of glow, that does not contain bright large-scale sharp structures, such as the formation of rays, shear or rotational motion (Nishimura et al., 2020) sometimes seen in dynamic discrete aurora.

The pulsating aurora (PsA) is a type of diffuse aurora (Nishiyama et al., 2011). It is one of the most frequently observed types of auroras (Demekhov and Trakhtengerts, 1994). The PsA represents the optical expressions of particles precipitating into the atmosphere in a transient and burst-like manner at high latitudes (Arnoldy et al., 1982). Its characteristic feature is the on and off intensity variation, often displayed in distinctive structures (Tesema et al., 2020). The PsA usually occurs during the early morning hours after midnight, following an auroral expansion, while the recovery phase of the sub-storm is taking place (Yamamoto, 1988). The pulsating auroral patches that is observed during the sub-storm expansion phases tend to increase in size, while mainly decrease in size during recovery phase (Nishimura et al., 2020). Optical observations of PsA have shown that the size in latitudinal and longitudinal directions is ranging from 10 km to 200 km (Nishiyama et al., 2011). Bright, dynamic arcs swiftly move towards the poles, characterized as dim, diffuse auroral patches (Nishimura et al., 2020). The pulsations are quasi-periodic (Miyoshi et al., 2015), displaying a rapid and usually rhythmical fluctuation in luminosity, where the timescale range from between less than 1 s and up to several minutes (Royrvik and Davis, 1977). The timescales are typically just of a few to some tens of seconds, yet the time it takes for a pulse to come and go are often very short (Dahlgren et al., 2017). The PsA emission regions can vary in size, from the usual arc-like structure to irregular patches. The pulsation period can vary significantly during the same event. Even within a singular structure, the periodicity can be rather irregular (Partamies et al., 2017).

There is at least three types of PsA which describe the different features of the PsA, mainly categorised by their pulsation and structure. These are amorphous pulsating aurora (APA), patchy pulsating aurora (PPA), and patchy aurora (PA). APA usually shows a complete absence of persistent structure at the 3-second pace, captured by the Time History of Events and Macroscale Interactions during Substorms (THEMIS) all-sky imagers (ASIs). At this rate, identifying the amorphous auroral features between the successive images taken are generally difficult, if not impossible. Both PPA and PA, has a persistent, patchy structure that moves along with ionospheric convection. The main difference between them, is the PA's overall lack of pulsation compared to the PPA (Grono and Donovan, 2019).

During PsA, the high-energy electrons can ionize neutral particles down to below 100 km. The EISCAT radar has observed that the electron density has an

enhancement in the D region (80 km to 95 km), while there is an ongoing PsA event. It has been reported that the maximum altitude of electron density is 10 km lower during pulsation onsets, than for the off-periods. Enhancements under 70 km that have been observed by the EISCAT radar, imply that electron precipitation related to PsA can have energies in the range of tens to hundreds of keV (Tesema et al., 2020). These numbers have also been shown through multiple in situ measurements of the particles, which studied the cause of PsA (Jones et al., 2013). The time it takes for electrons to travel from the magnetosphere to the ionosphere is dependent on their energy level. Consequently, an observable energy dispersion of precipitating electrons occur in the topside ionosphere. The observations of such energy dispersion are frequently linked to PsA (Miyoshi et al., 2010).

A possible way to study the PsA is by using a high-resolution multi-spectral optical and incoherent scatter radar data. The energy and flux are both found to be reduced during each off period when compared to the on period. Estimates indicate a decrease in the flux of higher-energy electrons (Dahlgren et al., 2017). The high-resolution optical data presents the presence of dips in luminosity below the diffuse background level, which occur immediately after the end of an onset period. In the study of Dahlgren et al. (2017), they found that each dip had a duration of approximately one second, during which the brightness decreased by up to 70 % before returning to a stable background level. Their observations reveal that pulsations frequently exhibit asymmetry, characterized by either a gradual increase in brightness or a slower decline (Dahlgren et al., 2017).

2.2 Time-Dependent Electron Transport Equation

The time-dependent electron transport used in AURORA (Gustavsson, 2022) is given by:

$$\begin{aligned} \frac{1}{v(E)} \frac{\partial I(E, s, \mu, t)}{\partial t} + \mu \frac{\partial I(E, s, \mu, t)}{\partial s} = & -AI(E, s, \mu, t) \\ & + B(E, s, \mu, t, I) \\ & + Q(E, s, \mu, t, I) \\ & + n_e \frac{\partial (L_{ee}(E)I(E, s, \mu, t))}{\partial E} \end{aligned} \quad (2.1)$$

The left-hand-side of Equation 2.1 contains the electron-flux variation with time, as seen in the first term. Where v represents the velocity, E is energy, s is distance, μ is the pitch angle, I is the electron flux and time is denoted t . Distance along the magnetic field-line is expressed in the second term. Looking on the right hand side of Equation 2.1, the first term represent the loss of electron flux I from energy E , pitch angle μ , at altitude s and time t . The electron collisions can be either elastic or inelastic. The elastic ones change the pitch angle and the inelastic change the energy, which also could alter the pitch angle. According to Gustavsson (2022), we have:

$$A = \sum n_k(s) \sigma_k^{total}(E) \quad (2.2)$$

Here, $\sigma_k^{total}(E)$ is the total cross section of electron collisions at energy E and density n_k for atoms of the k 'th species. The second term represents the elastic scattering of electrons from pitch angles μ' to μ (Gustavsson, 2022) which can be expanded to:

$$B(E, s, \mu, t, I) = \sum n_k(s) \sigma_k^{elastic}(E) \cdot \int_{-1}^1 p_k^{elastic}(E, \mu' \rightarrow \mu) I(E, s, \mu', t) d\mu' \quad (2.3)$$

In this expression, $p_k^{elastic}(E, \mu' \rightarrow \mu)$ is the probability from where an electron that has pitch angle μ' and energy E , scatters to pitch angle μ , because of the elastic collisions it has with the k 'th species. The third term on the right hand side of Equation 2.1, represents the internal sources of energetic electrons. It includes the production of photo electrons and secondary electrons, as well as electrons that originate from a higher energy (ϵ), which declines to an energy E through inelastic collisions. This is given (Gustavsson, 2022):

$$\begin{aligned} Q(E, s, \mu, t, I) = & Q_{local}(E, s, \mu, t) + \\ & \sum_k n_k(s) \sum_j \sigma_k^j(\epsilon \rightarrow E) \int_{-1}^1 p_k^j(\epsilon, \mu' \rightarrow \mu) I(\epsilon, s, \mu', t) d\mu' + \\ & \sum_k n_k(s) \int_{E+E^*}^{\infty} \sigma_k^{ion}(\epsilon \rightarrow E) \int_{-1}^1 p_k^{ion}(\epsilon, \mu' \rightarrow \mu) I(\epsilon, s, \mu', t) d\mu' d\epsilon \end{aligned} \quad (2.4)$$

The summations in this equation iterates through the excited states j of the k 'th species. An electron loses some of its energy when it excites an atom or

molecule, corresponding to the excitation energy ΔE . Electrons with energy ϵ colliding in-elastically, add to the second term in 2.4. It does so from a series of discrete energies $\epsilon = E + \Delta E_k^j$, corresponding to the excitation threshold of the neutral k 'th species. The sum of energies coming from the ionization energy and secondary electrons, express the energy loss happening as a result of the ionizing collisions of the primary electron. This is shown in the third term in Equation 2.4 (Gustavsson, 2022).

By examining 2.1, it becomes evident that the fourth term on the right-hand side encapsulates the losses in electron fluxes. These losses, stemming from the depletion of electron flux, are fundamentally rooted in the process of energy transfer to ambient thermal ionospheric electrons. The ambient electrons has density $n_e(s)$ and temperature T_e . As the flux $I(E, s, \mu, t)$ depends on fluxes at both higher energies and fluxes with other pitch angles, when calculating with Equation 2.1, it is necessary to use the same time for all the different pitch angles. This requirement can be addressed by solving a set of coupled partial differential equations (PDEs), while applying the corresponding initial and boundary conditions to each pitch angle (Gustavsson, 2022).

2.2.1 Discretized Transport Equation

By using the discretized energy and pitch angles ranging from 0° to 180° , the discretized transport equation can be solved. To get a discretized version of Equation (2.1), the energy differential needs to be adapted so it describes the collisions between the electrons.

A modified version of Equation (2.1) can be written as:

$$\begin{aligned} \frac{1}{v(E_i)} \frac{\partial I^{\mu_i}(E_i, s, t)}{\partial t} + \tilde{\mu}_i \frac{\partial I^{\mu_i}(E, s, t)}{\partial s} = & - A' I^{\mu_i}(E_i, s, t) \\ & + \sum_{\mu_k} B'(E, s, \mu_k \rightarrow \mu_i) I^{\mu_k}(E_i, s, t) \\ & + Q'(E_i, s, \mu_i, t) \end{aligned} \quad (2.5)$$

The equation is now altered to show of the pitch angle cosines in the stream μ_i , go from $\tilde{\mu}_i$ to $\tilde{\mu}_{i+1}$. In the pitch angle stream there is an electron flux, which is assumed of being distributed uniformly within its boundaries. The pitch angle cosine for electrons has an average in stream i , which is specified by $\tilde{\mu}_i$ (Gustavsson, 2022):

$$\tilde{\mu}_l = \frac{\int_{\theta_l}^{\theta_{l+1}} \cos \theta \sin \theta d\theta}{\int_{\theta_l}^{\theta_{l+1}} \sin \theta d\theta} \quad (2.6)$$

In Equation 2.5 A' represents the electron-on-electron loss rate, the total of neutral densities and the total of collision cross-sections. B' represents the discretization of μ as well as the degradation of energy as a result of the inelastic collisions. B' will be able to resolve the scatter from all the pitch angles in stream μ_l and μ_l (Gustavsson, 2022) as seen in the following equation::

$$\begin{aligned} B'(E_i, s, \mu_l \rightarrow \mu_l) &= \sum_k n_k(s) \sigma_k^{el}(E_i) \int_{\tilde{\mu}_l}^{\tilde{\mu}_{l+1}} \int_{\tilde{\mu}_l}^{\tilde{\mu}_{l+1}} p_k^{el}(E_i, \mu' \rightarrow \mu) I(E_i, s, \mu', t) d\mu' d\mu \\ &+ \sum_k n_k(s) \sum_j \sigma_k^j(E_i) \int_{\tilde{\mu}_l}^{\tilde{\mu}_{l+1}} \int_{\tilde{\mu}_l}^{\tilde{\mu}_{l+1}} p_k^j(E_i, \mu' \rightarrow \mu) I(E_i, s, \mu', t) d\mu' d\mu \\ &\max(0, 1 - \Delta E_k^j / \Delta E_i) \end{aligned} \quad (2.7)$$

2.2.2 Pitch Angle Streams

To be able to solve for all the pitch-angle-streams at the same time, the discretized Equation (2.5) is needed. It will be used to solve this simultaneously with a set of equations that is shared across all the streams μ_l . This allows us to express the equation for all pitch angles, as illustrated below (Gustavsson, 2022):

$$\frac{1}{v} \frac{\partial}{\partial t} \begin{bmatrix} I^1 \\ I^2 \\ \vdots \\ I^n \end{bmatrix} + \frac{\partial}{\partial s} \begin{bmatrix} \bar{\mu}_1 I^1 \\ \bar{\mu}_2 I^2 \\ \vdots \\ \bar{\mu}_n I^n \end{bmatrix} = \begin{bmatrix} -A' + B'_{11} & B'_{21} & \cdots & B'_{n1} \\ B'_{12} & -A' + B'_{22} & \cdots & B'_{n2} \\ \vdots & \vdots & \ddots & \vdots \\ B'_{1n} & B'_{2n} & \cdots & -A' + B'_{nn} \end{bmatrix} \begin{bmatrix} I^1 \\ I^2 \\ \vdots \\ I^n \end{bmatrix} + \begin{bmatrix} Q^1 \\ Q^2 \\ \vdots \\ Q^n \end{bmatrix} \quad (2.8)$$

Here A' represent the total collision cross-section which vary with altitude. B'_{jl} represent scattering as a result of collisions coming from stream j to stream l . The preservation of electron energy between energy levels that range from E_i to $E_i + \Delta E_i$, results from the total of both elastic collisions and fragments produced by the inelastic collisions (Gustavsson, 2022).

To integrate Equation 2.8, a modified version of a standard Crank-Nicolson method is applied (Gustavsson, 2022). The modified version has been altered so it uses the upstream spatial differences instead of centralized spatial differences. It is necessary to implement boundary conditions applied to the initial and final component in each of the sub-arrays I^k . To secure the stability of the solution for any type of discontinuity that can occur within the sub-arrays, it is essential to modulate the time step (Gustavsson, 2022).

The time step of the integration that is selected, will ensure that the Courant-number stay less than one for all the levels of energy. Δs represent the change of distance along the magnetic field, and it has to be less than the mean free path of the electron. This condition is fulfilled by the use of a 150 m interval in altitude, ranging from 100 km and up to 140 km. By making these steps, the interval will grow exponentially with a maximum altitude of 649 km (Gustavsson, 2022).

This system has two primary outcomes. The first outcome is that the interval becomes very short in time for high-energy electrons, which results in it being physically irrelevant to calculate for every time step in the integration. As a solution to this problem, the outcome is instead recorded by a time resolution that vary from 1 ms to 20 ms. The second outcome of the system is that making models of the precipitation that has energies larger than 10 keV is complicated. The operation would require the lower boundary to be less than 100 km, which would be the point where the mean-free-path of electrons rapidly decrease. To handle this problem, a more elaborate altitude grid is required, to reduce the time step utilized by the Crank-Nicolson integration (Gustavsson, 2022).

Consequently, a typical desktop computer from 2016, is able to efficiently manage around 10 pitch angle streams. The 10 pitch angle streams used in this context has the following pitch angle boundaries of: 0° , 10° , 30° , 60° , 80° , 100° , 120° , 150° , 170° and 180° (Gustavsson, 2022).

/ 3

Instruments

In this chapter, the instruments that made the observations during the pulsating aurora used in the thesis will be introduced. Initially, information regarding the Auroral Structure and Kinetics is found in Section 3.1, followed by Section 3.2 where the All Sky Camera is presented. Lastly, the Magnetometer is described in Section 3.3.

3.1 Auroral Structure and Kinetics

Auroral Structure and Kinetics (ASK) is the source of the optical data presented in this study, which is a the multi-spectral instrument operated by the Space Environment Physics Group at the University of Southampton (Whiter et al., 2023). During the 2006-2007 winter ASK was located at the EISCAT Tromsø site. It was used to analyse 8 events of PsA that was observed over Tromsø.

ASK takes measurements of low energy auroral electron precipitation as well as plasma flows with a greater accuracy of resolution than previously achievable (Whiter et al., 2023). The instrument consists of three low-light imaging systems. Each system is equipped with an electron multiplying charge coupled device (EMCD) with an optical system giving a $3.1^\circ \times 3.1^\circ$ field of view. The cameras have three narrow-band (~ 1 nm) interference filters designed to select a narrow portion of the visible light spectrum. The time is synchronized between the three imagers, and it captures images of the aurora at magnetic

zenith at a rate of 25 frames per second during standard operations, and 32 frames per second during campaigns (Dahlgren et al., 2017).

The cameras filtered different wavelengths. For camera r1, the filter was changed during the winter 2006 to 2007. Event number 1, had camera r1 and interference filter at wavelength 6730 Å, with target emission from N^2 . Event number 2, had camera r1 and interference filter at wavelength filter 5620 Å, with target emission from O_2^+ . The wavelength filter used for camera r2 was 6730 Å and for camera r3 it was 7774 Å, with the target emissions being N_2 and O . So for this thesis, the two camera filters used was for wavelengths 6730 Å and 7774 Å, except for Event 2 which used 5620 Å and 7774 Å. The cameras used during these 8 events, along with their respective filters, can be found in table 3.1.

Event	Date	Camera	Wavelength (Å)	Target Emission
1	2006-10-22	r1, r3	6730, 7774	N_2 and O
2	2006-12-14	"	5620, 7774	O_2^+ and O
3 and 4	2007-01-19	r2, r3	6730, 7774	N_2 and O
5 and 6	2007-01-30	"	"	"
7	2007-02-15	"	"	"
8	2007-03-09	"	"	"

Table 3.1: ASK Camera Overview. The symbol " marks equivalence to the reference above.

The full documentation of the ASK instrument can be found on the ASK website: (Whiter et al., 2023). For the chosen events, the campaign log regarding the PsA events studied in this thesis, is presented in Table 3.2:

Event	EISCAT Campaign Log
1	23:04 UT Keogram showing pulsating aurora, about 20s intervals
2	Morning: clouds on and off, pulsating aurora at 01 UT, 2:50-3:10 UT
3	21:00UT Bright aurora, not much structure. Some pulsations, getting stronger after aurora at 21:50UT
4	Pulsations weakening about 22:45UT, but getting stronger again about 23:50UT for 20 min
5	Aurora followed by pulsations at 02:17 - 05:20
6	Aurora followed by pulsations at 02:17 - 05:20
7	More aurora over the night. Pulsating in the morning
8	Clear, aurora all night

Table 3.2: Campaign log for the selected events

Keograms are generated by extracting the central column of pixels from each mean image (an average over 2 seconds) and aligning them horizontally. Time progresses from left to right, and each keogram typically spans a duration of 20 minutes. These visual representations provide a concise overview of the ASK data (Whiter et al., 2023).

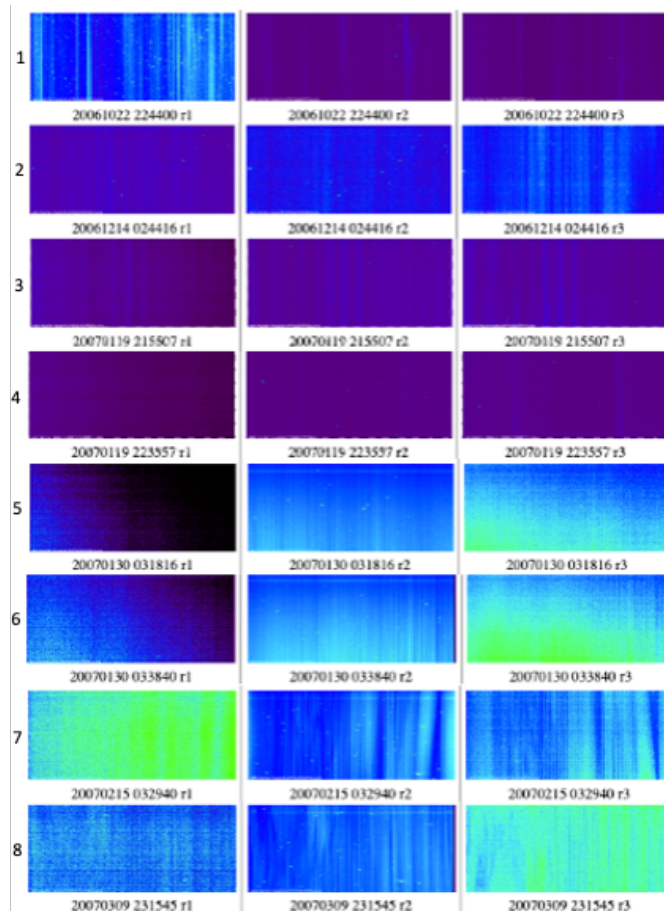


Figure 3.1: Keograms of the selected events from ASK website.

In Figure 3.1, the keograms of the eight selected events is shown as they appear on the ASK website (Whiter et al., 2023).

3.2 All Sky Camera

The All Sky Camera (ASC) utilized, is the one operated by the National Institute of Polar Research (Tokyo, Japan) (NIPR) in Ramfjorden during the winter season 2006 to 2007. The information was personally shared with me during

the following events.

In August 2023, I reached out to Magnar Gullikstad Johnsen (Johnsen, 2023) from Tromsø Geophysical Observatory. I was told they did not have any all sky measurements from this period, however, they provided me with the contact information to Michael Kosch (Kosch, 2023), chief scientist and SRA manager at the South African National Space Agency (SANSA). I was also informed about a NIPR-operated camera that was possibly in use during that particular season.

When talking with Michael Kosch (Kosch, 2023), they told me they used to run an ASC in Skibotn, but it unfortunately was stopped before my year of interest, and did not have suitable optical data for my purpose. I was then given information about Santonori Nozawa (Nozawa, 2023) and Shin-ichiro Oyama (Oyama, 2023), both from the Institute for Space-Earth Environmental Research (ISEE), Nagoya University, Japan, who possibly had optical data from a Japanese imager located at EISCAT during that time.

Both Shin-ichiro Oyama (Oyama, 2023) and Satonori Nozawa (Nozawa, 2023) provided me with contact information to Professor Yasunobu Ogawa (Ogawa, 2023) from NIPR.

Through communication with Yasunobu Ogawa (Ogawa, 2023), I was informed that they had examined and maintained old image data from an ASC operating in Ramfjorden, and I was provided with links to nine events from that season. Fortunately, two of my selected events was included in this batch. Screenshots from the videos can be seen in Figure 3.2.

Event 2 has thumbnail images that can be found en on (NIPR, a), and video found on (NIPR, b). Event 3 has thumbnail images found on (NIPR, c) and video found on (NIPR, d). Event 2 and Event 7 has movies and images taken by an all sky camera operated by NIPR.

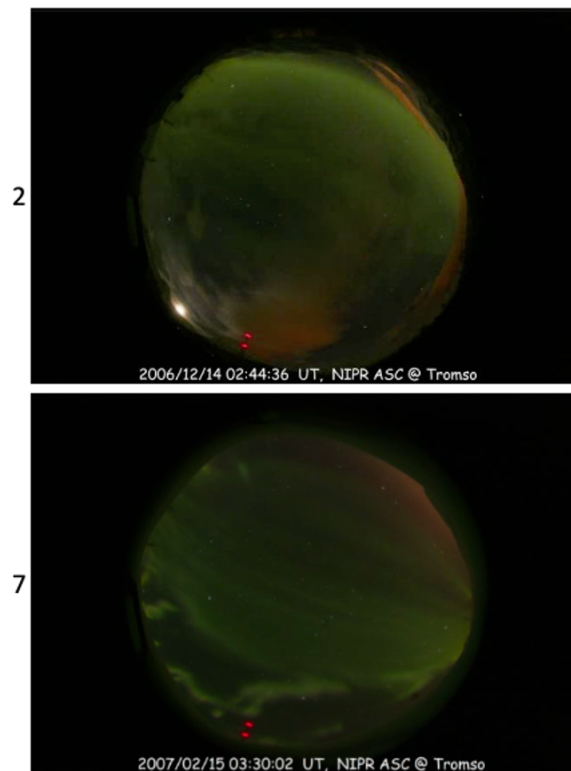


Figure 3.2: Images from videos taken by NIPR ASC when the equipment was located in Ramfjorden, Tromsø. The images take place in the beginning of event 2 and 7

3.3 Magnetometer

The ACE Magnetometer (MAG) (Ness et al., 2022), is an experiment that consist of two triaxial fluxgate magnetometers. ACE orbits around the Lagrange-point between Earth and Sun, measuring the solar-wind and IMF-parameters approximately 1 hour up-stream of Earth's magnetosphere. The magnetometers are positioned on booms that stretch four meter out from the ACE-spacecraft center, beyond the solar panels. The sensors has a wide sensitivity range and measure three vector components of the magnetic field. It utilizes twin magnetometer sensors to perform weak interplanetary magnetic field measurements. The data collected by MAG, includes average magnetic field vectors from primary and secondary sensors. The primary is "snap-shot-memory" data, that capture 30 vectors per second and is transmitted at 48 bps. The secondary is Fast Fourier Transform (FFT) data, transmitted at 32 bps. The average vector transmission include 216 bps, which relate to the six vectors per second (Ness

et al., 2022).

In this thesis, data from MAG is used to compare the solar wind activity with the selected PsA events.

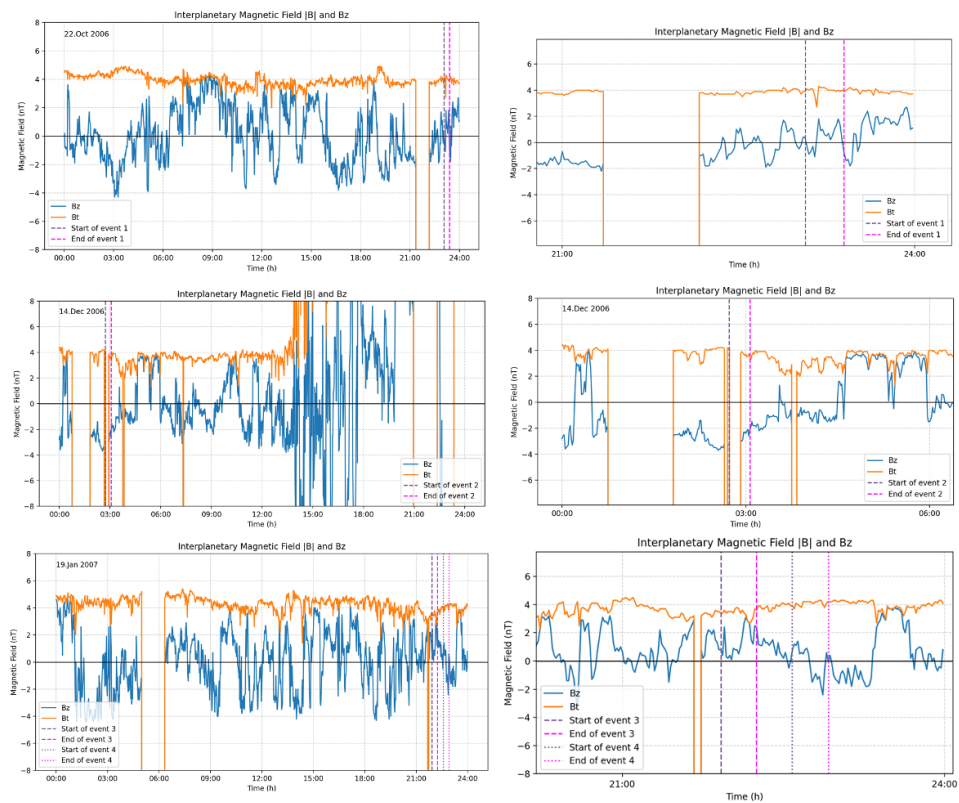


Figure 3.3: Interplanetary magnetic field plots of of the selected events 1, 2, 3 and 4 from ACE Magnetometer shown to the left, and the respective zoomed in plots to the right.

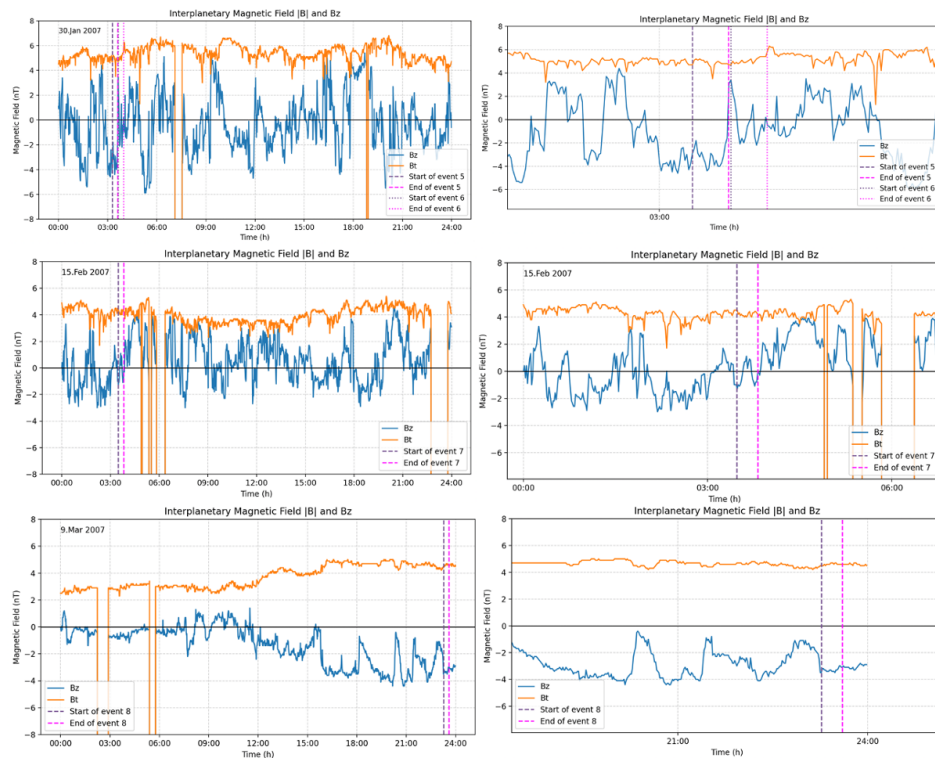


Figure 3.4: Interplanetary magnetic field plots of the selected events 5, 6, 7 and 8 from ACE Magnetometer shown to the left, and the respective zoomed in plots to the right.

Figure 3.3 and 3.4, show the interplanetary magnetic field (IMF) activity from each of the selected events, as numbered. When the B_z graph goes from being negative to positive is when we experience a sub-storm in the magnetosphere of Earth. This is a dominant feature in all events, except from event number 8, which has a lot less activity compared with the rest.

Additional ground based magnetometer measurements

Measurements with a ground based magnetometer has been used to study the magnetic field variations measured from geomagnetic observatories located in Longyearbyen, Tromsø, Rørvik and Dombås.

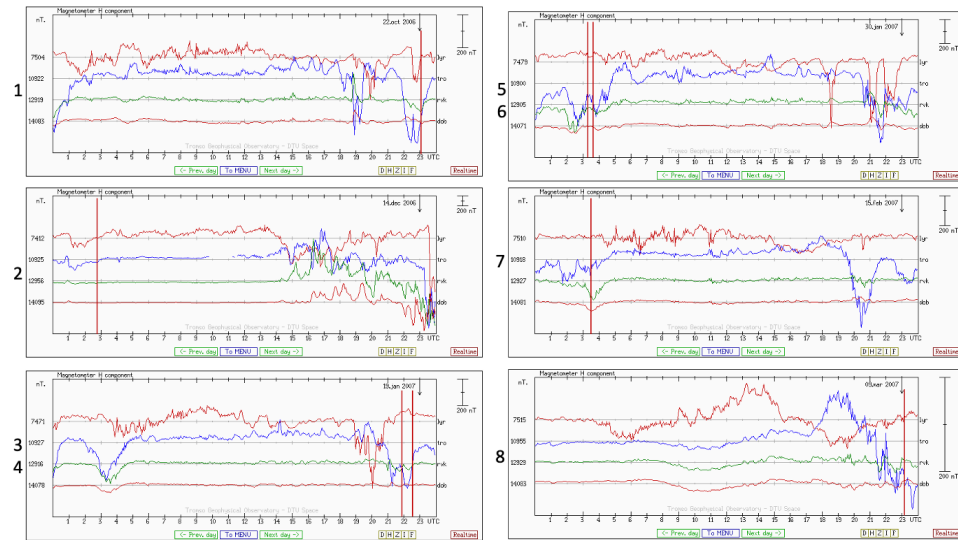


Figure 3.5: Magnetometer plots from the different ground observatories of the magnetic field variations during the events. The red lines in the plots marks the beginning of each event. And the numbers on the left side of each plot represent the number of event.

As seen in Figure 3.5, the eight selected events are shown. As event 3 and 4, and 6 and 7 occur during the same day, the solar events prior to their respective PsA events are shown in the same plot as numbered. All events has increased magnetic events at the end of the day, from 18:00 UTC to 23:00 UTC. There is also some events in the beginning of the days around 02:00 UTC to 03:00 UTC.

When comparing Figure 3.5 with 3.3 and 3.4, the event reveals a correlation between the Interplanetary Magnetic Field (IMF) and the generation of substorms. These sub-storms appear around midday, another at 18:00, and a potential one starting at 21:00. In the ground observatory plots, these events manifest as storms slightly after their impact on Earth. Notably, significant activity is observed around 18:30 and then again from 22:00 onwards. Event 1 initiates at approximately 23:00.

The day of Event 2 displayed increased activity around 15:00 and onwards, evident as some fluctuations in the Earth's magnetosphere observed by ground-based observatories around 16:00 and later. However, the activity during this event is not as pronounced as that observed in Event 1. Event 2 took place in the morning hours, but in these plots, the observations do not seem to contain pulsations with significant activity evident during that time.

On the days of events 3 and 4, the IMF magnetometer indicates activity starting

at 00:00, with a new event emerging at 03:00. Additionally, a series of events is observed consistently from 09:00 throughout the day. The ground-based observatory data reveals activity occurring after 03:00, and another episode in the evening around 20:00. Notably, events unfold between the time 22:00 and 23:00, possibly correlating with the outcomes of these events.

The magnetometer data for the days of events 5 and 6 reveals significant events throughout the day, with the most prominent ones occurring in the morning hours around 00:00, 02:00, and 03:00. There is also some activity noted in the evening around 21:00. The ground-based data confirms these observations, indicating activity around 03:00 and again at 22:00. Notably, events 5 and 6 occur between 03:18 and 04:00, aligning well with the magnetometer activities depicted in the figures.

On the day of event 7, the IMF plot indicates some activity in the morning sector between 00:00 and 02:00. However, this activity is not as pronounced in the ground-based plots. Additionally, there is more substantial activity in the evening on the IMF plot, starting around 20:00. Interestingly, this evening activity appears to be more prominent in the ground-based plot, showing major activity from around 20:00. Unfortunately, event 7 occurs at 03:30, missing the capturing of the evening events that seem to be more promising based on the observed patterns.

During event 8, the IMF plots display weak activity with some fluctuations during midday and a slight increase in the evening. Despite the subdued nature of these activities in the IMF plots, the ground-based plots reveal the weak peaks in Bz values starting from around 18:00 and continuing thereafter. Notably, the Bz values persistently remain negative throughout the entire evening. Event 8 takes place from 23:15.

/4

Observational Study

I started the observational study by looking through the keogram images on the ASK website (Whiter et al., 2023). Next, I selected the events which looked promising to contain PsA. I then contacted Dr. Whiter (Whiter, 2023) from the University of Southampton, who provided me with the data from the selected events. I created programs to process all the data received. And after that was finished, I started to analyse the plots and investigated each event separately. After embarking on a digital quest to unveil the truths surrounding a perceived all-sky camera operating in Tromsø during the 2006-2007 season, I stumbled upon a Japanese imager. Subsequently, I obtained both images and movies that correlated with two of my documented events, sent to me by very helpful scientists mentioned in Section 3.2.

In this chapter, selected events are outlined in section 4.1, which includes a description of the procedure used for data analysis. In section 4.1.1 to 4.1.8, the results from the eight selected events is presented. This chapter concludes with a short summary of the results in Section 4.2.

4.1 Events

After reviewing the event logs and correlating keograms, I ultimately selected eight events for further investigation. These are presented in Table 4.1:

Event	Year	Time	Camera	Wavelength (Å)	Target Emission
1	2006-10-22	23:04:24	r1, r3	6730, 7774	N_2 and O
2	2006-12-14	02:44:16	"	5620, 7774	O_2^+ and O
3	2007-01-19	21:55:07	r2, r3	6730, 7774	N_2 and O
4	2007-01-19	22:35:57	"	"	"
5	2007-01-30	03:18:16	"	"	"
6	2007-01-30	03:38:40	"	"	"
7	2007-02-15	03:29:40	"	"	"
8	2007-03-09	23:15:45	"	"	"

Table 4.1: Event overview. The symbol " marks equivalence to the reference above.

The process of analysing the data began by creating the main event plots, where I proceeded to select intervals where the pulsations were located. Subsequently, I plotted these selected intervals and marked each onset of the pulse manually. The resulting intervals and onset values were then stored in both text files and Matlab files.

Line plots depicting the onsets and events, pseudocolour-plots, and individual line plots for each pulse were created. A program was then implemented to save onset values separately for intensity and time into text files, along with saving the maximum and median of the onsets, as well as their respective gradients. Further steps involved the creation of a code to generate event plots encompassing both cameras used by ASK, with onset markers displayed in the plots. Onset plots were paired, and the paired onset indexes were saved into text files. Subsequently, a program was designed to plot the paired onsets, showcasing them separately matched from both cameras.

The previously selected onsets were then removed, and a new text file for the paired onset values was generated for only the best onset selections. These paired onsets were plotted, first with all the selected onsets and then with the new onset version, only containing the most distinct onsets. This is represented in a gray color for the previously selected onsets and in the color teal for the best onsets, as seen in Figure 4.6. The figure shows the peak pulsation intensity as a function of peak intensity gradient at emission 6730 Å and 7774 Å.

A regression line has been incorporated into the intensity ratio plots, and the gradient value of this regression line, along with its variance, has been stored. The regression line serves as a representation of the relationship between the intensity ratios of the emissions, giving a model for the data trend. This enables us to make predictions and conduct analyses on the relationship between the variables.

This process was repeated for all eight selected events, and the regression gradient values that was stored for all events were plotted in a single graph. This final plot illustrated the regression gradient alongside the respective standard deviation of each regression line from the preceding plots. I also plotted the emissions 6730 Å and 7774 Å from all source altitudes into a plot together with a pulsation onset to compare the results. These plots can be seen in Figure 5.3 and Figure 5.4.

4.1.1 Event 1

The event is a 20 minute window starting 23:04:24, October 22nd, 2006. Within the main event plots depicted in Figure 4.1, the chosen onset is denoted by black dots. The process of selecting these onsets involved a meticulous examination of pulsation intervals, where each unique pulse's initiation point was identified and marked.

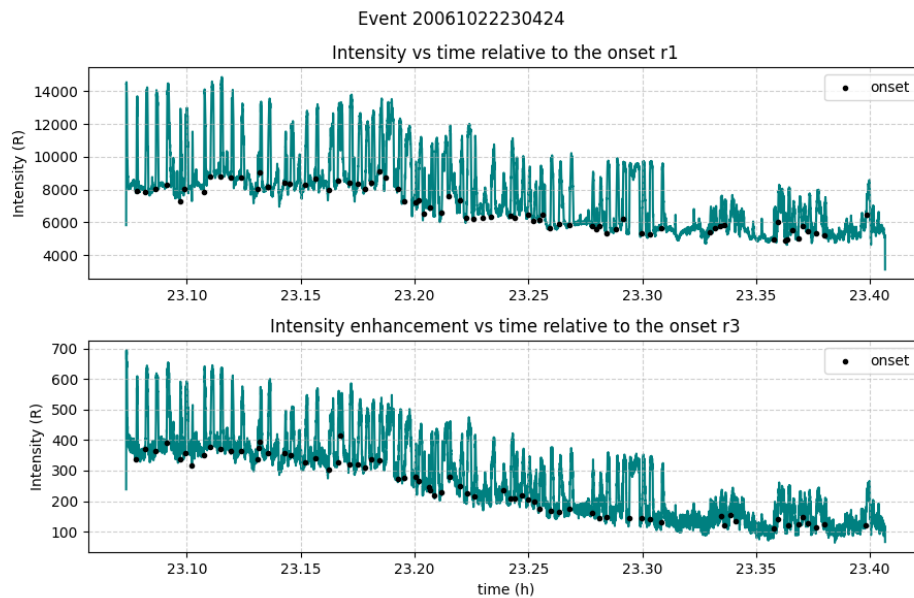


Figure 4.1: Event 1: Main event plots, showing both emissions with black onset markers.

In Figure 4.2 and 4.3, the main event plots are presented in a pseudocolour plot, departing from the previous line plot, for both cameras. Within these plots, all selected onsets are visually highlighted by the colorbar showing the increased intensity in yellow color. The onset time has been set to zero as a standard, ensuring that all onsets are aligned. The total number of samples corresponds to the quantity of selected onsets, approximately totaling around 70 in this

particular figure.

In both figures, the upper graph illustrates the intensity versus time concerning the selected onsets. Meanwhile, the middle graph depicts the intensity enhancement versus time relative to the onset, and the bottom graph showcases the intensity gradient versus time, all in relation to the onset. Consequently, the yellow sections at time 0 in the figures serve to visually represent the intensity increase, while the onset intensity decrease is perceptible as a darker blue immediately succeeding the same onset.

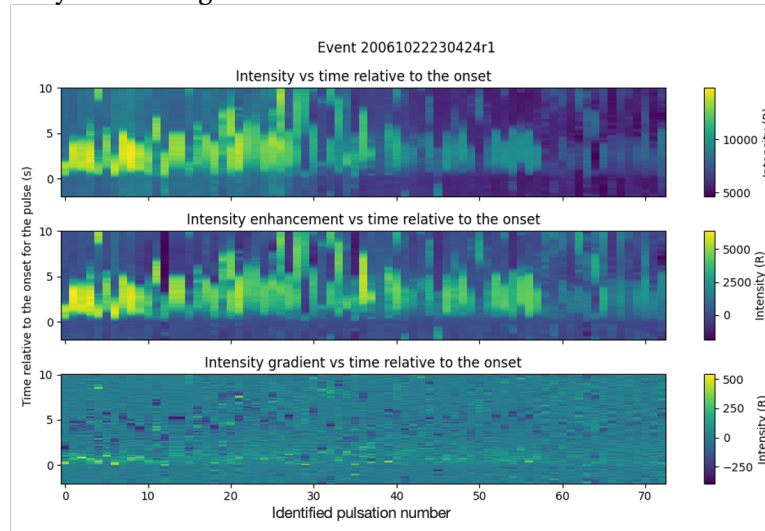


Figure 4.2: Event 1: pseudocolour plot of emission 6730 Å from camera r2.

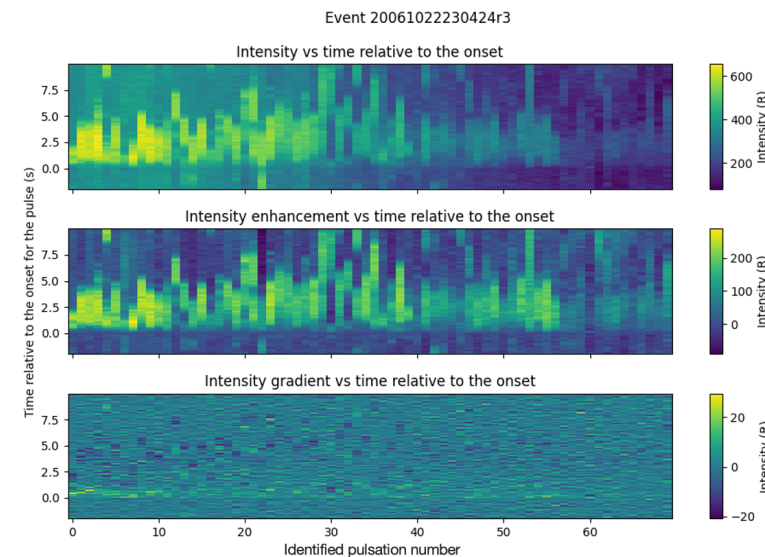


Figure 4.3: Event 1: pseudocolour plots of emission 7774 Å from camera r3.

The line plots depicted in Figure 4.4 present the intensity enhancement versus time relative to the onset seen on the top in Figure 4.4, compared with the intensity gradient versus time relative to the onset seen on the bottom in Figure 4.4. These plots illustrate a clear pattern, showing the gradient turning positive during intensity increase and negative when the intensity decreases. This trend is evident for both cameras.

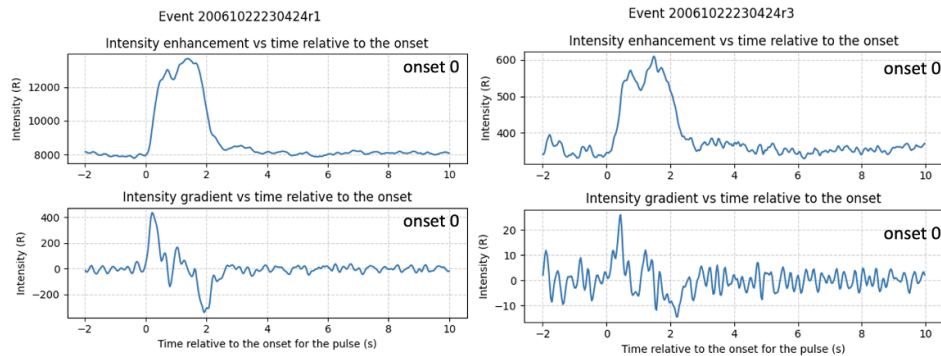


Figure 4.4: Event 1: gradients of onsets shown as line plots. Emission 6730 \AA from camera r2 on the left, and 7774 \AA from camera r3 on the right.

In Figure 4.4, two distinct onsets are showcased in the top of both plots. While Figure 4.5 shows an increase in intensity that could indicate a weak pulsation or some other form of intensity increase. For the analysis conducted here, I chose to include only the pulsation onsets that are distinct and clearly defined to ensure the accuracy of the plots featuring the regression lines.

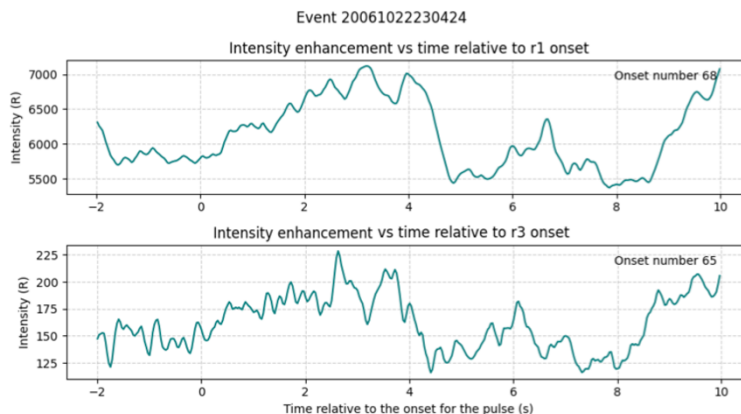


Figure 4.5: Example of a selected onset of varying quality from event 1.

As depicted in Figure 4.6, the top three gray plots displays the data incorpo-

rating all the initially selected onsets. After eliminating onsets of questionable quality, the resulting teal plot at the bottom emerges. As evident from the plots, the elimination of inadequately selected onsets transforms the regression line from a decreasing to an increasing trend for this event. In this particular event, 23 out of the initially selected 67 onsets were removed during this process.

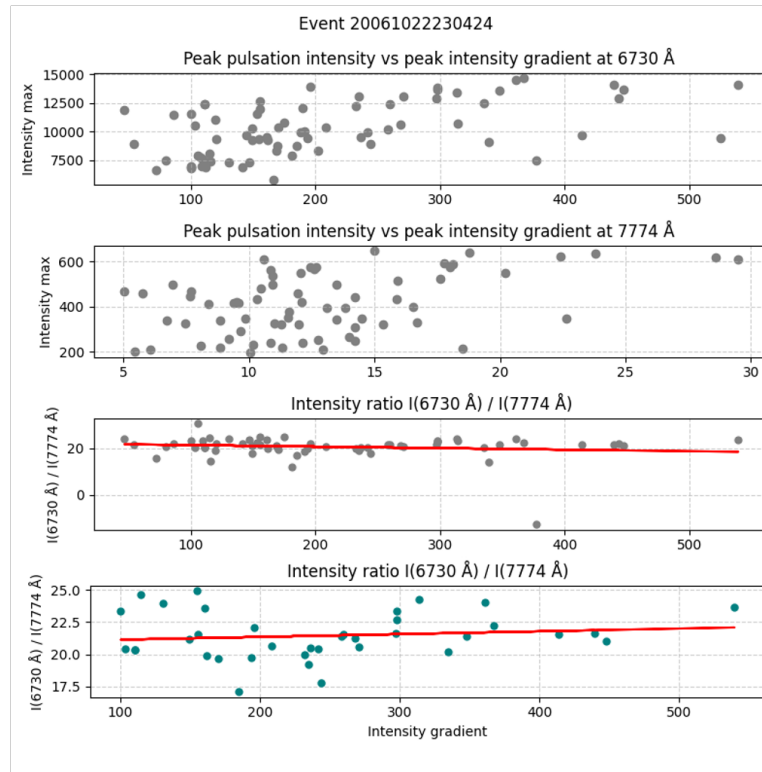


Figure 4.6: Event 1: Peak pulsation intensity vs peak intensity gradient for both 6730 Å and 7774 Å, shown in the two top plots. The two bottom plots show the intensity ratio between the intensity at 6730 Å and 7774 Å.

4.1.2 Event 2

The main event plots shown in Figure 4.7, illustrates the 20 minute event starting at 02:44:16 on December the 14 th, 2006. The manually selected onsets are denoted by black dots. Compared to Event 1, this event appear to have less distinct pulses, and more noise.

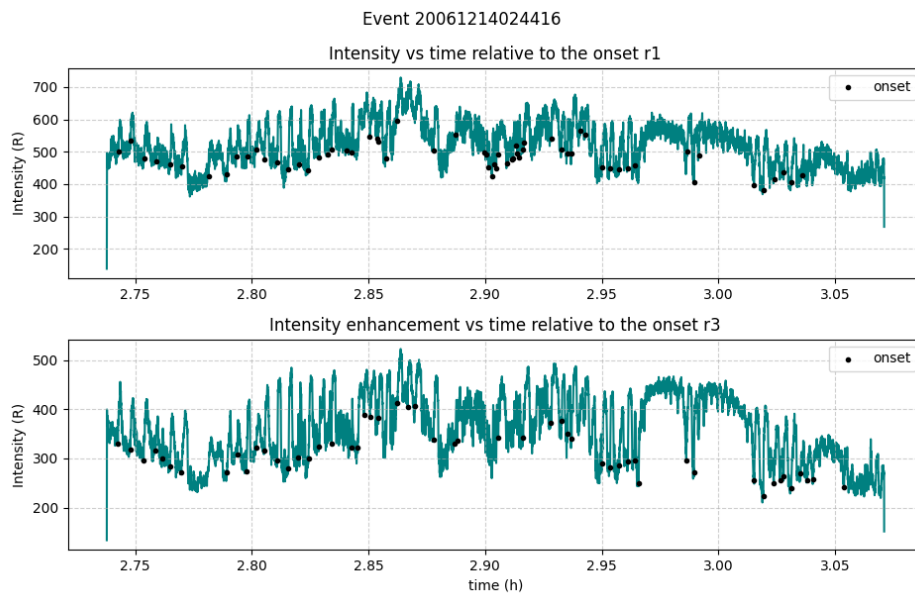


Figure 4.7: Event 2: Main event plots, showing both emissions with black onset markers.

In Figure 4.8 and 4.9, the primary event plots are showcased in a pseudocolour plot, with the total number of samples aligning with the quantity of selected onsets, approximately 60 in this event. As depicted in the plots, the onsets appear to lack clarity and definition. They exhibit a less distinct nature, lacking sharp onsets. This characteristic is evident in their softer and less defined appearance compared to Event 1. Moreover, the onset-to-offset gradient is nearly imperceptible in these instances, as seen in the intensity gradient versus time relative to the onset plot at the bottom.

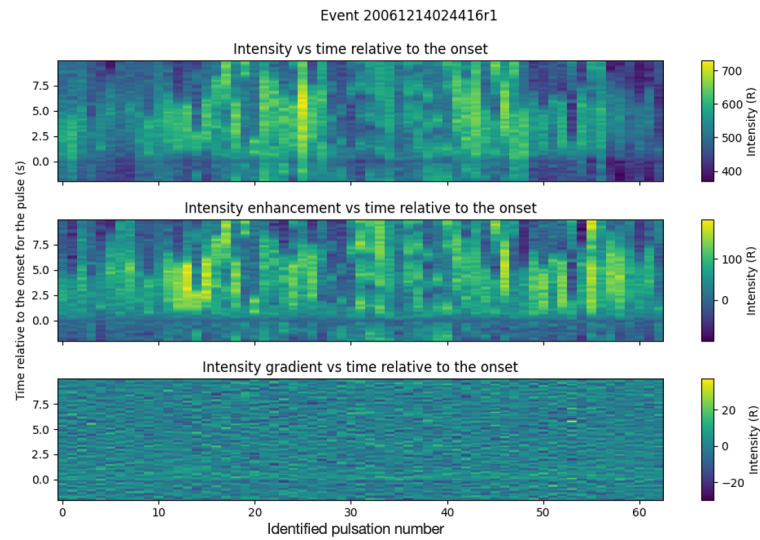


Figure 4.8: Event 2: pseudocolour plot of emission 5620 Å from camera r1.

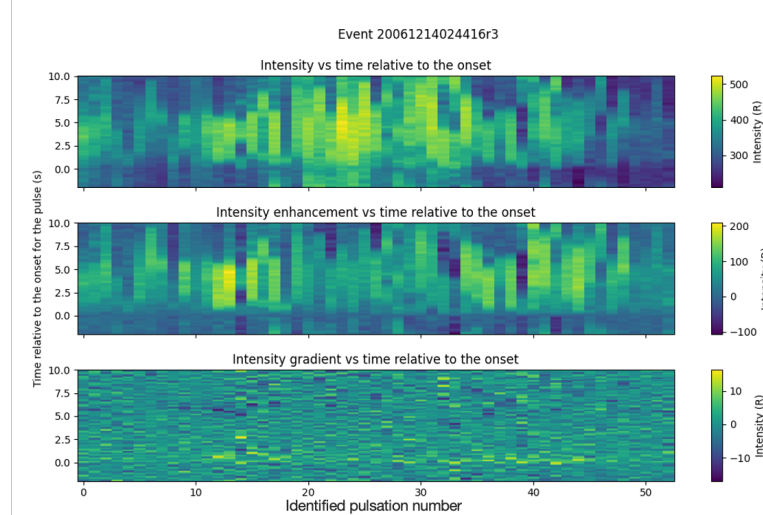


Figure 4.9: Event 2: pseudocolour plot of emission 7774 Å from camera r3.

The line plots presented in Figure 4.10 show the intensity enhancement versus time relative to the onset seen in the top panels, compared with the intensity gradient versus time relative to the onsets, as shown in the lower panels. The two plots illustrate how the gradient changes for the onset of the pulse. For the r1 camera, the pulse is not very distinct compared to background noise. The gradient plot illustrates this by not having any distinct increase and decrease compared to the background intensity. The r3 camera contain more distinct pulses, which is also seen by how the gradient graph has a clear increase and decrease simultaneously as the onset.

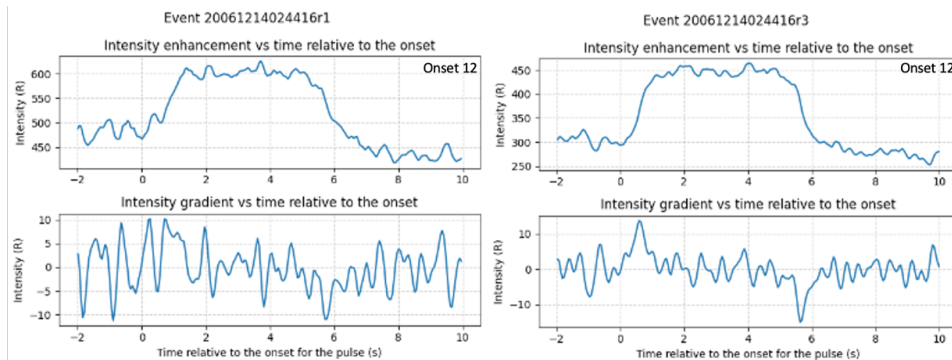


Figure 4.10: Event 2: gradients of onsets shown as line plots. Emission 5620 \AA on the left, and 7774 \AA on the right. For onset number 12.

In Figure 4.10, the upper sections of both plots show two defined onsets. Conversely, Figure 4.11 presents a pulsation onset of varying quality. It shows how there is no defined pulse from the perceived onset at time $t = 0$. Similar selected onsets like this is filtered out when making the final plots.

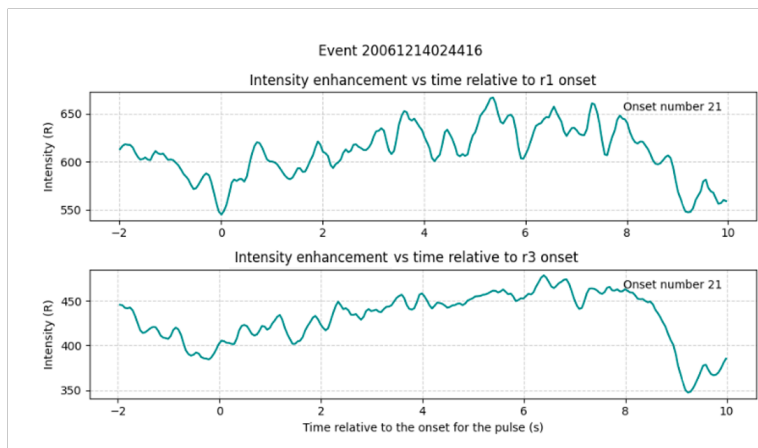


Figure 4.11: Example of a selected pulsation onset of varying quality from event 2.

As shown in Figure 4.12, the top gray plot displays the data incorporating all the initially selected onsets. It is clear that the elimination of inadequately selected onsets, seen in the bottom teal graph, results in a more distinct decreasing trend of the regression line. In this specific event, there were initially 38 paired events, as shown in the gray plot. Subsequently, 27 of these events were removed to create the bottom plots, which now only consist of the most distinct pulsations from this event. In the bottom teal plot, it is evident that the number of distinct onsets were few for event 2.

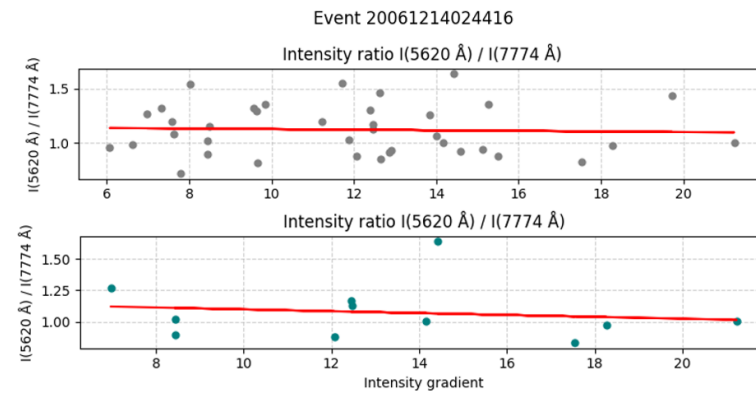


Figure 4.12: Event 2: the plots show the intensity ratio between the intensity at 5620 Å and 7774 Å.

4.1.3 Event 3

The main event plots shown in Figure 4.13, illustrates the 20 minute event starting at 21:55:07, January the 19th, 2007. The manually selected onsets are represented by black dots. Upon observation of the figure, it is evident that the event comprises a combination of distinct pulses occurring predominantly in the middle, and some noise at the beginning of the event.

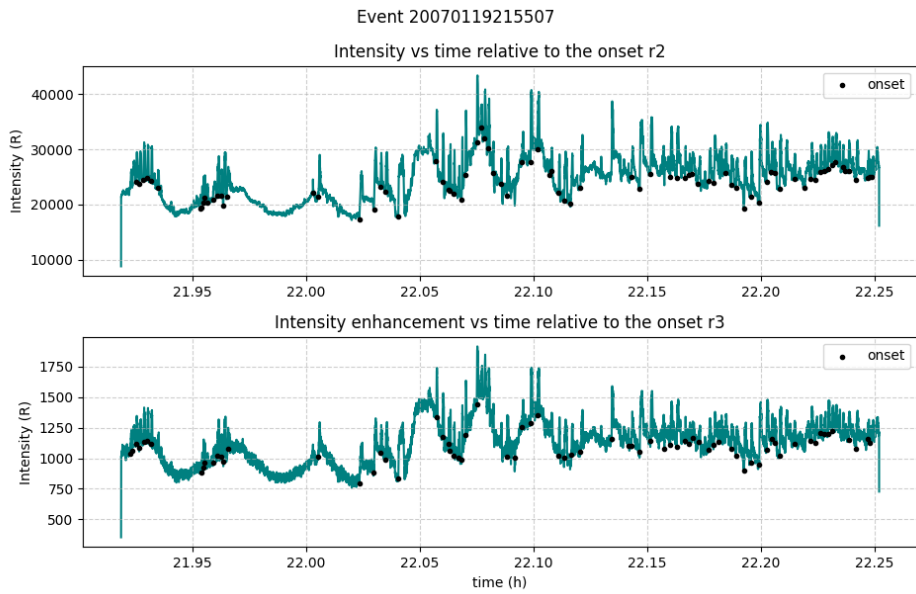


Figure 4.13: Event 3: Main event plots, showing both emissions with black onset markers.

In Figure 4.14 and 4.15, the primary event plots are showcased in a pseudocolour plot, with the total number of samples aligning with the quantity of selected onsets, approximately 80 in these events. As observed in the figures, it appears that there are no pulses in the beginning of the event. The intensity gradient is nearly imperceptible in these plots, except for a few onsets starting at around onset number 30. This pattern is consistent for both emissions.

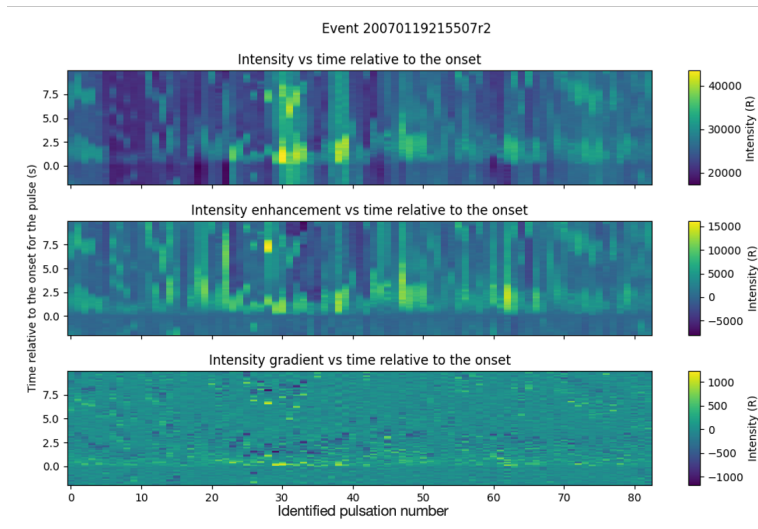


Figure 4.14: Event 3: pseudocolour plot for emission 6730 \AA from camera r2.

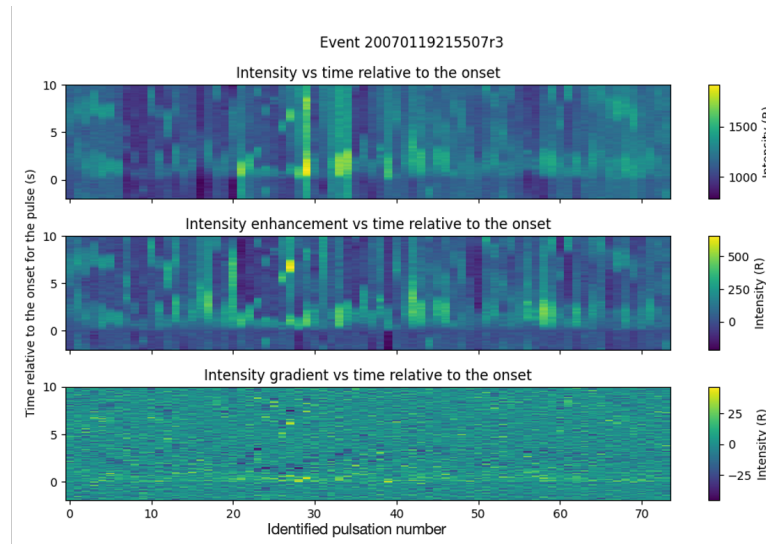


Figure 4.15: Event 3: pseudocolour plot for emission 7774 \AA from camera r3.

The line plots presented in Figure 4.16 show the intensity enhancement versus time relative to the onset seen on the top, compared with the intensity gradient versus time relative to the onset seen on the bottom. The two plots illustrate how the gradient change for the onset of the pulse. Both cameras used in event 3, exhibit distinct intensity gradients that correlates to the pulses. Emission 7774 \AA has less definition compared with emission 6730 \AA .

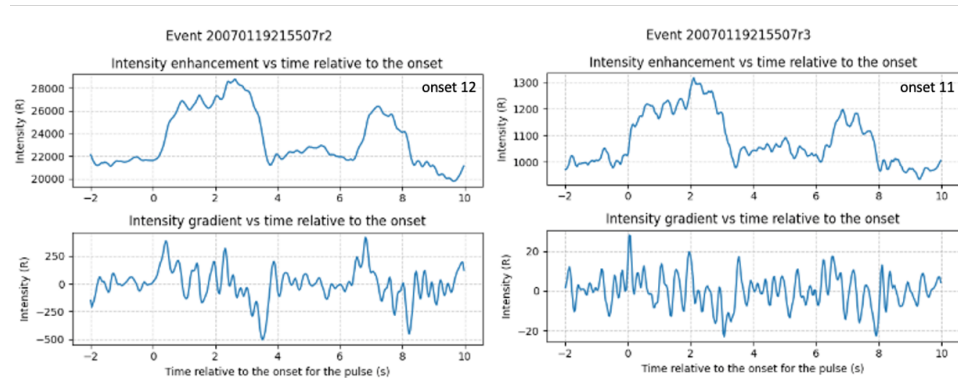


Figure 4.16: Event 3: gradients of onsets shown as line plots. 6730 \AA on the left, and 7774 \AA on the right.

In Figure 4.16, the upper sections of both plots show defined onsets. Figure 4.17 is an example of a pulsation onset of varying quality. It shows a significant decrease in intensity right before the selected onset for emission 6730 \AA . However, for emission 7774 \AA , the pulse lacks a distinct onset and appears to be more indicative of noise rather than a clear onset.

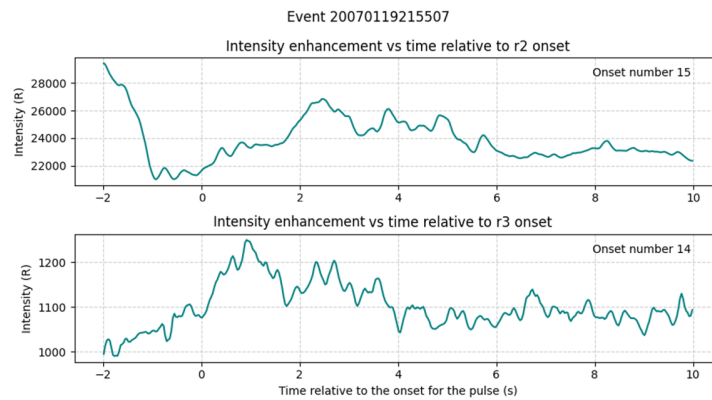


Figure 4.17: Example of a selected pulsation onset of varying quality from event 3.

As shown in Figure 4.18, the top gray plot displays the data incorporating all the initially selected onsets. In the case of this event, the removal of inadequately selected onsets has resulted in a more pronounced increase in the regression line as seen in the plots.

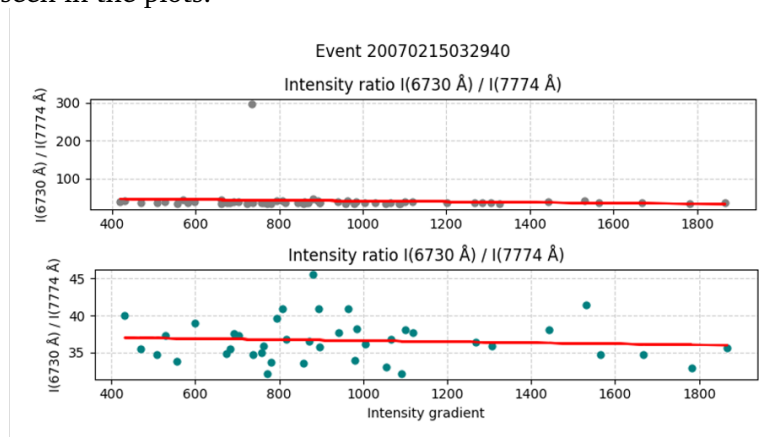


Figure 4.18: Event 3: The plots show the intensity ratio between the intensity at 6730 Å and 7774 Å.

4.1.4 Event 4

The main event plots shown in Figure 4.19, illustrates the 20 minute event starting at 22:35:57, January the 19th, 2007. The manually selected onsets are represented by black dots. When examining this figure, it appears that there are pulsations at the beginning and end, with a window in the middle where pulses seem to be absent from 22:75 h to 22:85 h.

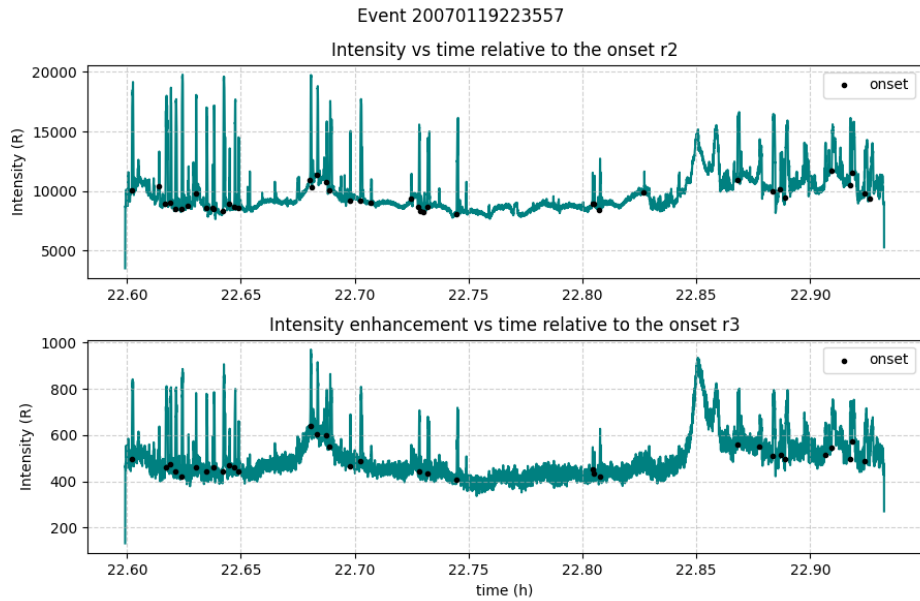


Figure 4.19: Event 4: Main event plots, showing both emissions with black onset markers.

In Figure 4.20 and 4.21, the primary event plots are displayed in a pseudocolour plot, with the total number of samples aligning with the quantity of selected onsets, approximately 40 in these events. In the figures, it seems that there are numerous distinct pulses at the beginning, along with some weaker ones towards the end. This observation aligns well with observations seen in the main event plot in Figure 4.19. However, it appears that some of the selected onsets may have been marked slightly later than the actual onset time, as evidenced by the very first onset. The brighter color, indicative of higher intensity, starts just slightly after $t=0$ on the y-axis.

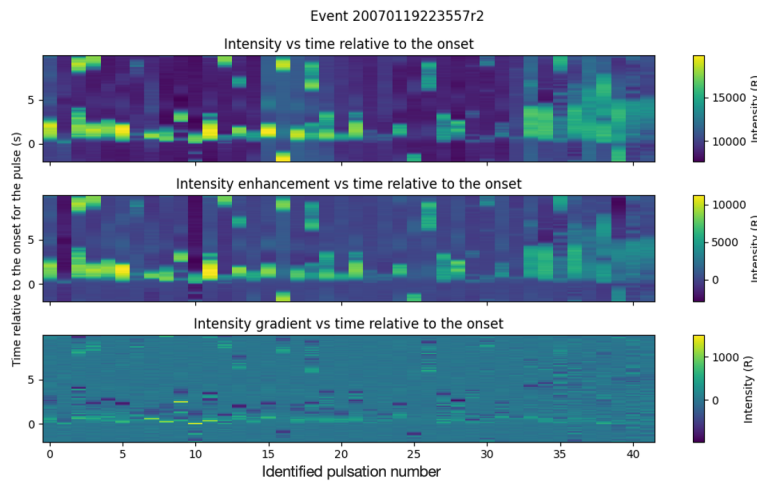


Figure 4.20: Event 4: pseudocolour plot of emission 6730 Å from camera r2.

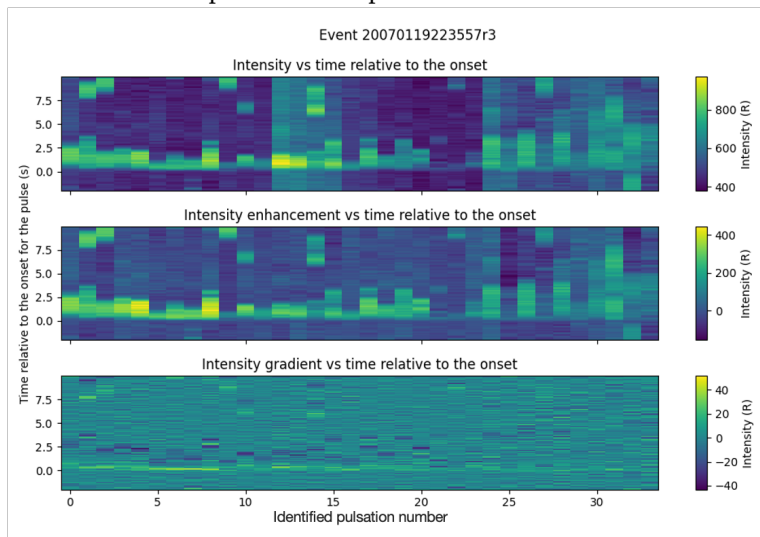


Figure 4.21: Event 4: pseudocolour plot of 7774 Å from camera r3.

The line plots presented in Figure 4.22 show the intensity enhancement versus time relative to the onset seen in the top panels, compared with the intensity gradient versus time relative to the onset seen on the bottom. Both camera r2 and r3, has distinct pulses at onset 0, with corresponding intensity gradients seen on the bottom half of the figure. The $t=0$ missed mark is visible here for the first onset, as seen in both the pseudocolour plots of event 4 and here in the line plot of the same pulse.

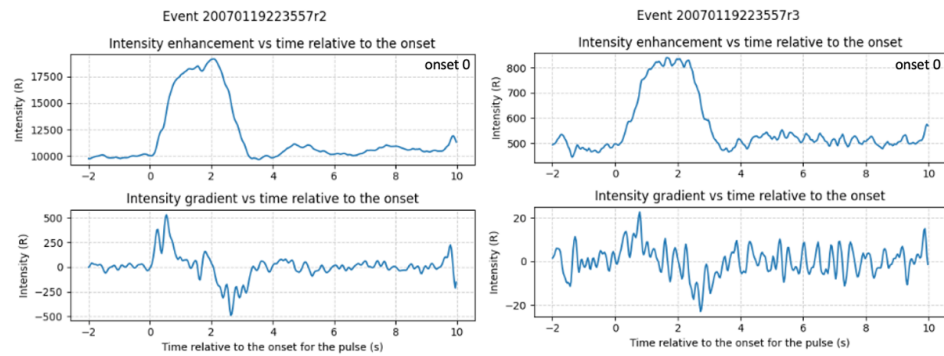


Figure 4.22: Event 4: gradients of onsets shown as line plots. Emission 6730 Å on the left, and 7774 Å on the right.

In Figure 4.22, the upper sections of both plots show defined onsets. Figure 4.23 is an example of an incorrectly chosen onset due to human error during the selection process. The figure shows how the intensities rise slowly, but not as distinct as they should be. It is camera r2 onset 40, and onset 33 for camera r3. Looking back at the pseudocolour plots, it can seem to correlate with the weaker onsets that is visible there.

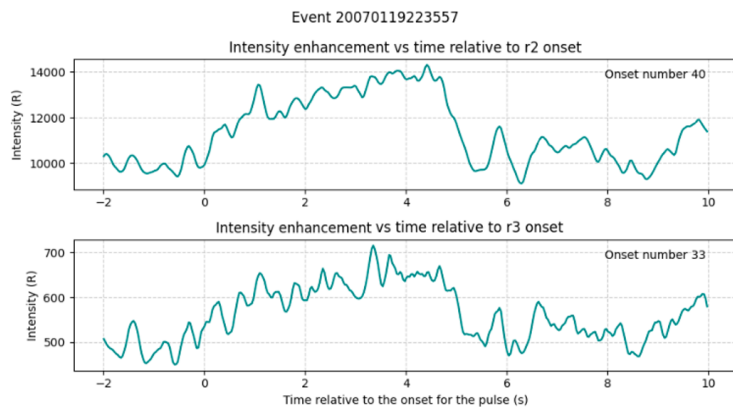


Figure 4.23: Example of selected pulsation onsets of varying quality from event 4

As shown in Figure 4.24, the top gray plot displays the data incorporating all the initially selected onsets. In the context of this event, the removal of inadequately selected onsets did not seem to make a noticeable difference in the resulting regression line plot.

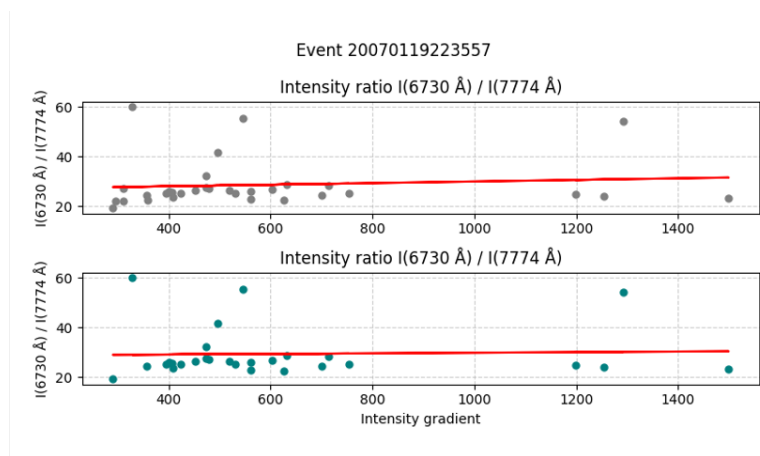


Figure 4.24: Event 4: The plots show the intensity ratio between the intensity at 6730 Å and 7774 Å.

4.1.5 Event 5

The main event plots shown in Figure 4.25, illustrates the 20 minute event starting at 03:18:16, January the 30 th, 2007. The manually selected onsets are represented by black dots. Upon examining this figure, it appears that there is a considerable amount of noise. All the perceived pulsations could potentially be noise, as they appear very similar throughout the entire event. However, it is worth noting that the pulsations do seem distinct and clear, although with some level of uncertainty.

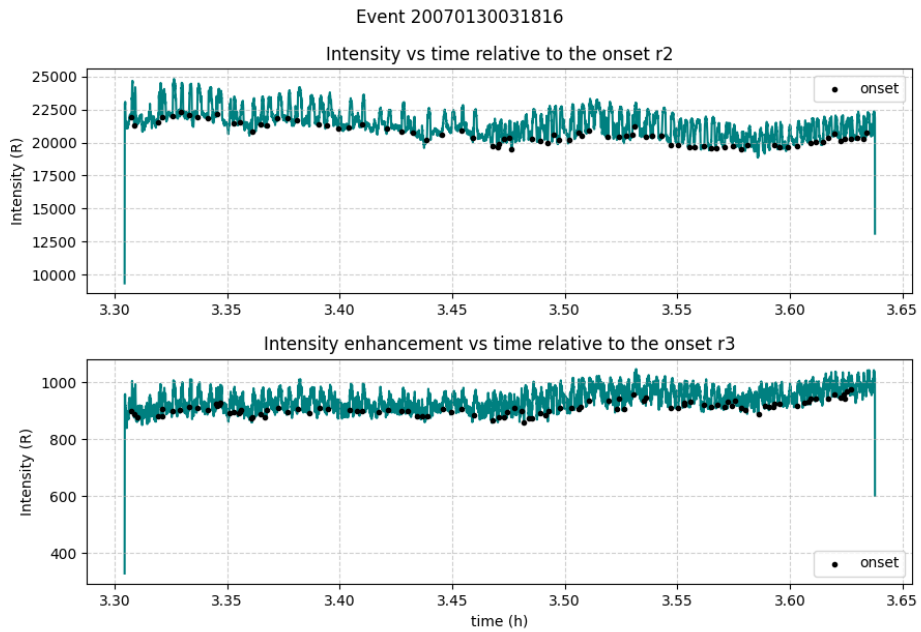


Figure 4.25: Event 5: Main event plots, showing both emissions with black onset markers.

In Figure 4.26 and 4.27, the primary event plots are displayed in a pseudocolour plot, with the total number of samples aligning with the quantity of selected onsets, approximately 80 for emission 6730 \AA from camera r2 and 100 for emission 7774 \AA from camera r3. Examining this figure reveals distinct onsets from start to finish. However, for emission 6730 \AA , the pulsations appear softer and more noisy compared to emission 7774 \AA .

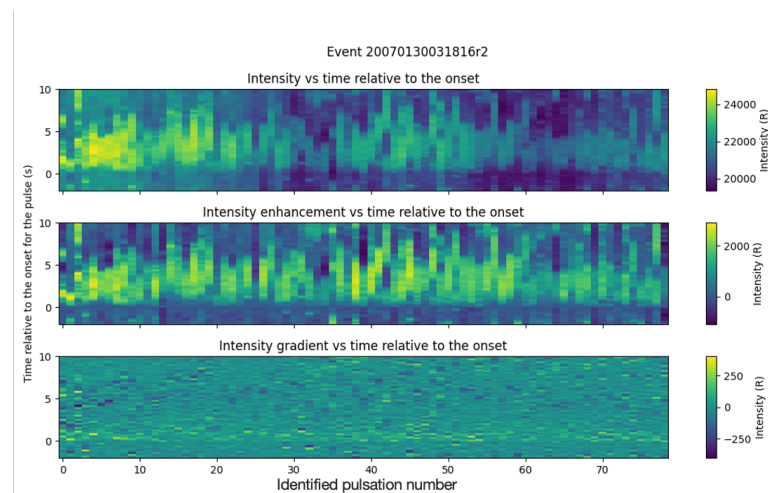


Figure 4.26: Event 5: pseudocolour plot of emission 6730 \AA from camera r2.

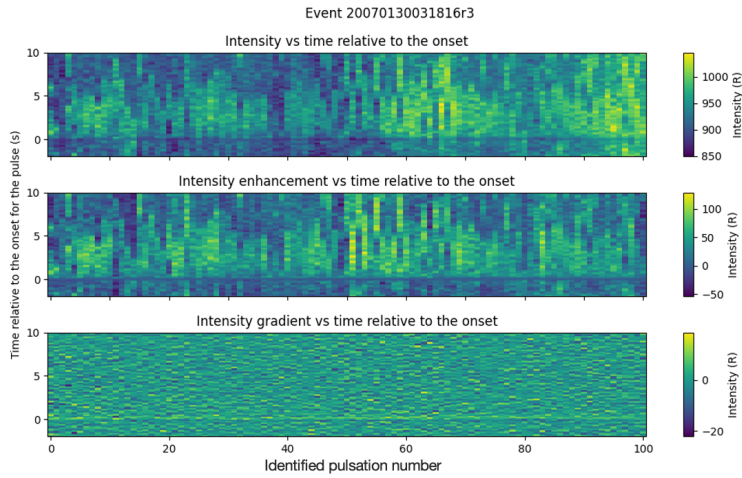


Figure 4.27: Event 5: pseudocolour plot of emission 7774 \AA from camera r3.

The line plots presented in Figure 4.28 show the intensity enhancement versus time relative to the onset seen on the top, compared with the intensity gradient versus time relative to the onset seen on the bottom. For emission 6730 \AA , a distinct pulse is evident with a slightly delayed onset time, as the beginning of the pulse commences slightly after $t = 0$ as seen in the plot. The evolution of the pulse makes it easy to observe the varying gradient. Conversely, for emission 7774 \AA , the pulse is less distinct, leading to a less noticeable change in the intensity gradient. These observations suggest that this event may have increased uncertainty compared to other events, as these are two of the most distinct pulses.

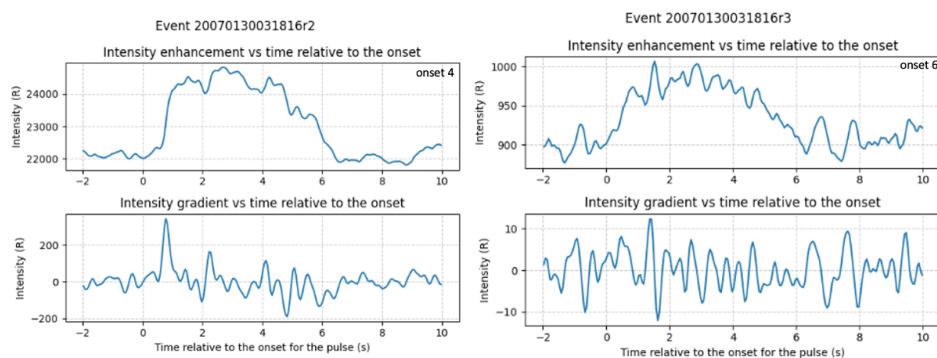


Figure 4.28: Event 5: gradients of onsets shown as line plots. Emission 6730 \AA on the left, and 7774 \AA on the right.

In Figure 4.28, the upper sections of both plots show defined onsets. Figure

4.29 is an example of an incorrectly chosen onset due to human error during the selection process. It is onset 74 from camera r2, and onset 98 for camera r3. When compared with the main event plots, they appear quite similar to the rest of the event. This raises further questions about the uncertainty of this event.

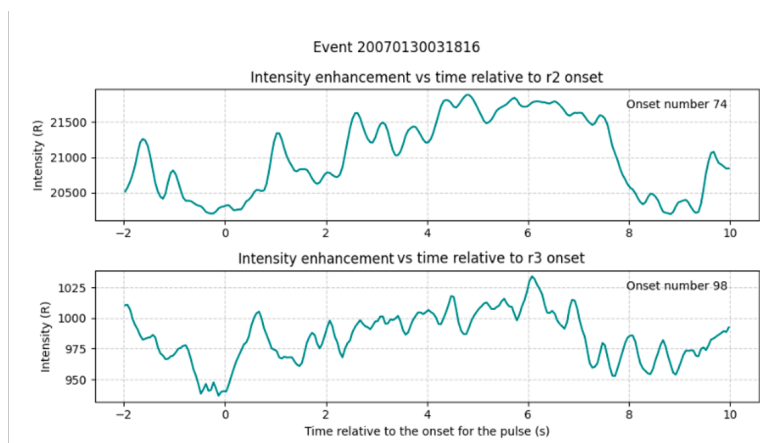


Figure 4.29: Example of a selected pulsation onset of varying quality from event 5.

As shown in Figure 4.30, the top gray plot displays the data incorporating all the initially selected onsets. In the context of this event, the removal of inadequately selected onsets did not seem to make a noticeable difference in the resulting regression line plot, except from decreasing the intensity gradient from a maximum of 400 to a maximum of about 300.

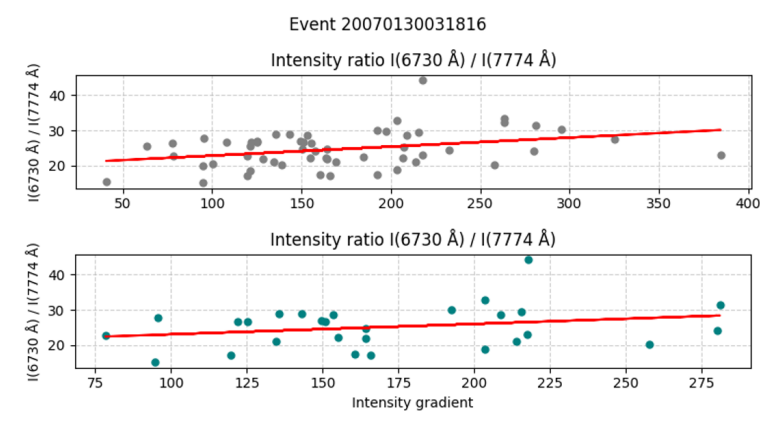


Figure 4.30: Event 5: The plots show the intensity ratio between the intensity at 6730 Å and 7774 Å.

4.1.6 Event 6

The main event plots shown in Figure 4.31, illustrates the 20 minute event starting at 03:38:40, January the 30 th, 2007. The manually selected onsets are represented by black dots. Analyzing this event, it appears that there is noise in the beginning of the event until around 3:70 h, after which pulsations start and proceed to gradually increase throughout the event, becoming more clear and distinct. Up until 3:95 h, where it seems the pulses become more noisy again.

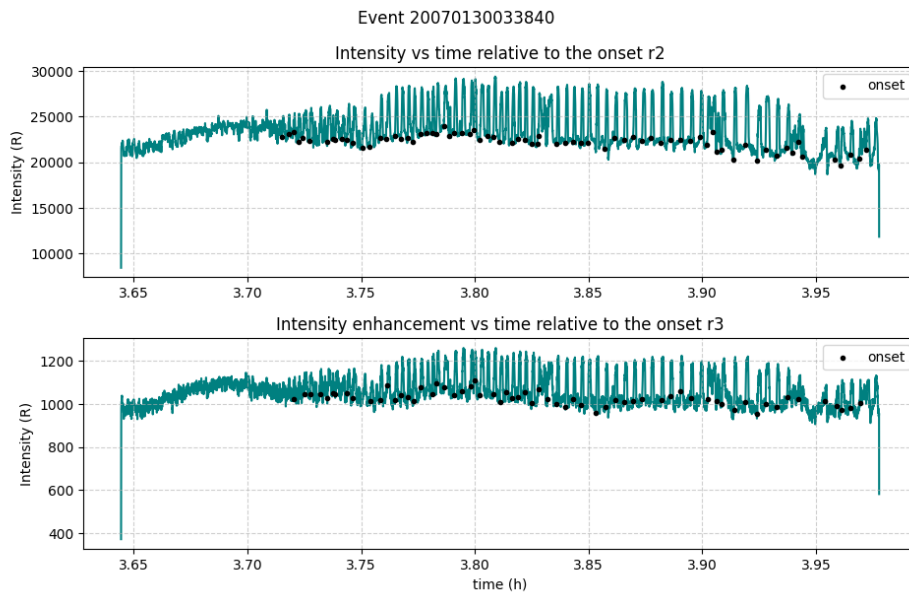


Figure 4.31: Event 6: Main event plots, showing both emissions with black onset markers.

In Figure 4.32 and 4.33, the primary event plots are displayed in a pseudocolour plot, with the total number of samples aligning with the quantity of selected onsets, approximately 70 for emission 6730 \AA from camera r2 and 60 for emission 7774 \AA from camera r3. In the figures, it seems that the first and last 15 onsets are noise, and that there are distinct pulses in the middle caught on both cameras. The intensity gradient especially in camera r2, looks very distinct and nice with an apparent increase around $t = 0$, and then a decrease around $t = 5$.

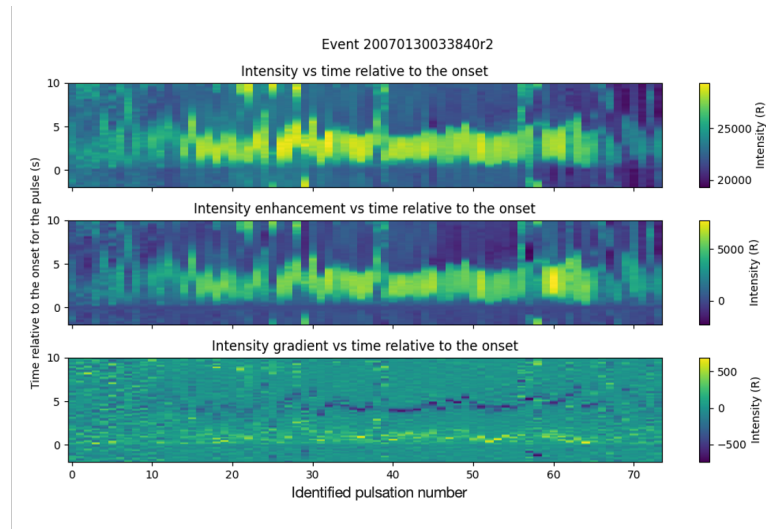


Figure 4.32: Event 6: pseudocolour plot of emission 6730 \AA from camera r2.

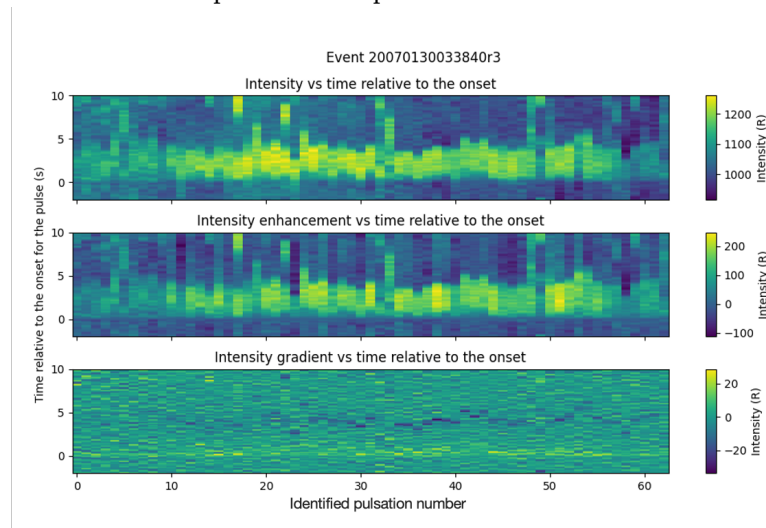


Figure 4.33: Event 6: pseudocolour plot of emission 7774 \AA from camera r3.

The line plots presented in Figure 4.34 show the intensity enhancement versus time relative to the onset seen on the top, compared with the intensity gradient versus time relative to the onset seen in the bottom plot of both figures. Both camera r2 and r3, has distinct pulses and related intensity gradients.

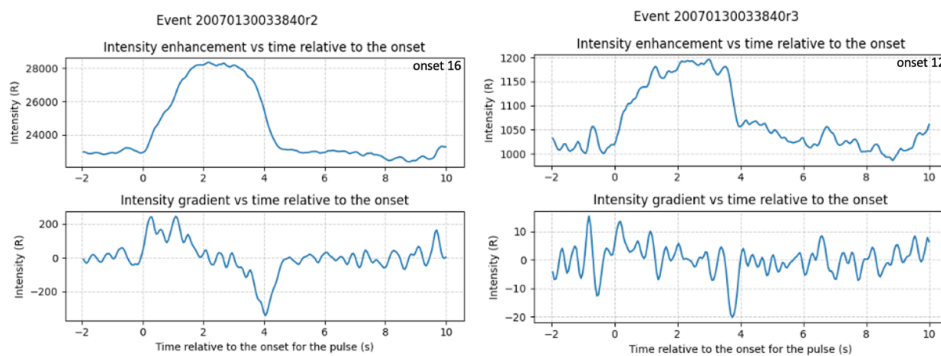


Figure 4.34: Event 6: gradients of onsets shown as line plots. Emission 6730 Å on the left, and 7774 Å on the right.

In Figure 4.34, the upper sections of both plots show defined onsets. Figure 4.35 is an example of an incorrectly chosen onset due to human error during the selection process. It is onset 2 from camera r2, and onset 0 for camera r3. Comparing with the analysis of the main event plots, it seems these are onsets selected at the very start where there was mostly noise, before the distinct pulses started.

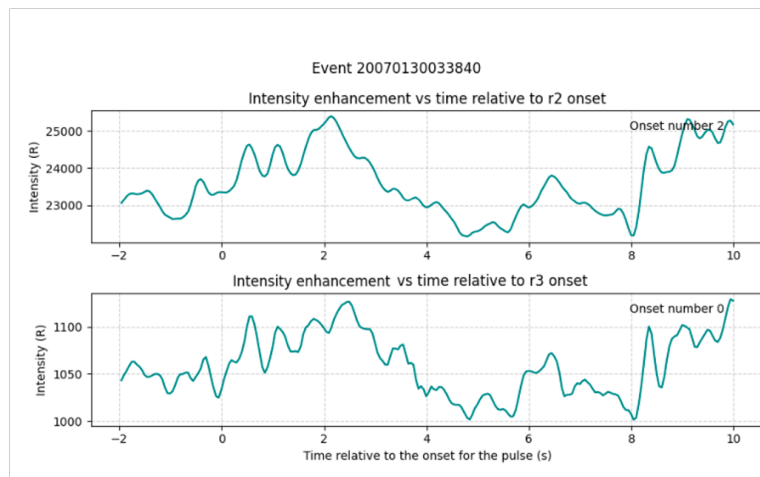


Figure 4.35: Example of a selected pulsation onset of varying quality from event 6

As shown in Figure 4.36, the top gray plot displays the data incorporating all the initially selected onsets. For this event, the removal of inaccurately selected onsets did not seem to make a noticeable difference, except for a possible slight increase in the resulting regression line plot as seen the teal version on the bottom.

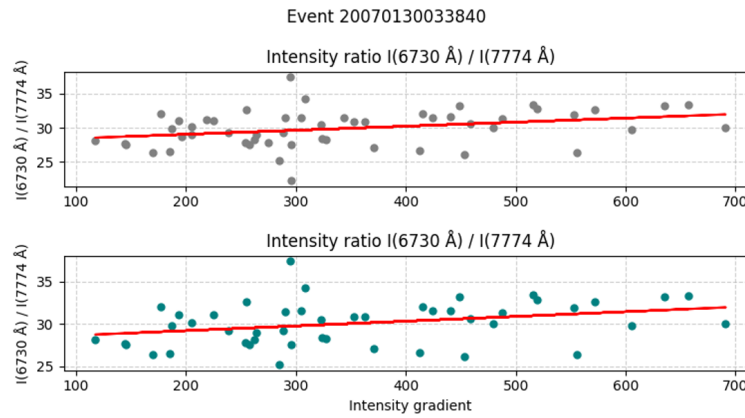


Figure 4.36: Event 6: The plots show the intensity ratio between the intensity at 6730 Å and 7774 Å.

4.1.7 Event 7

The main event plots shown in Figure 4.37, illustrates the 20 minute event starting at 03:29:40, February 15th, 2007. The manually selected onsets are represented by black dots. This event seems to be quite noisy throughout the 20 minutes. It appear to contain some pulses towards the middle and end, but this is questionable due to the consistency of the intensity.

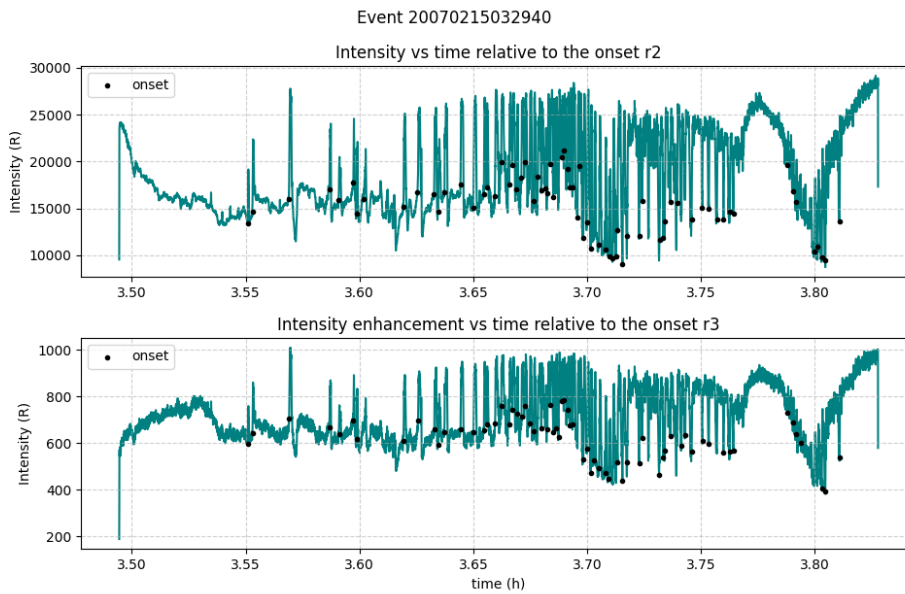


Figure 4.37: Event 7: Main event plots, showing both emissions with black onset markers.

In Figure 4.38 and 4.39, the primary event plots are displayed in a pseudo-colour plot, with the total number of samples aligning with the quantity of selected onsets, approximately 70 for both emissions. It seems the event has some pulses of high intensity as seen in the line main event plot. It appears to be noisy, but has a somewhat distinct intensity gradient line visible at $t=0$ in the figures.

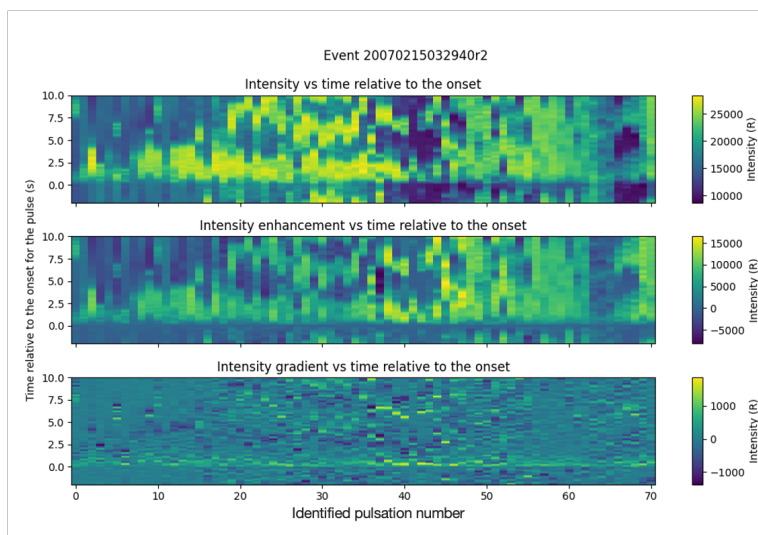


Figure 4.38: Event 7: pseudocolour plot of emission 6730 \AA from camera r2.

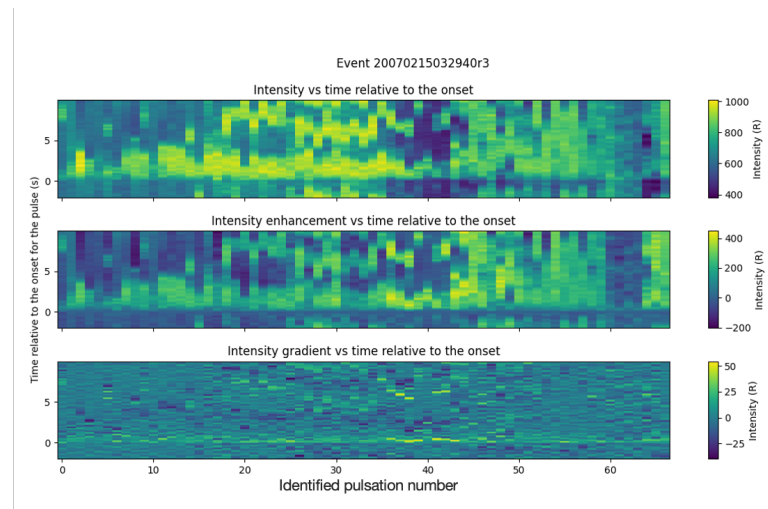


Figure 4.39: Event 7: pseudocolour plot of emission 7774 Å from camera r3.

The line plots presented in Figure 4.40 show the intensity enhancement versus time relative to the onset seen on the top, compared with the intensity gradient versus time relative to the onset seen in the bottom plot of both figures. Both camera r2 and r3, has distinct pulses and related intensity gradients.

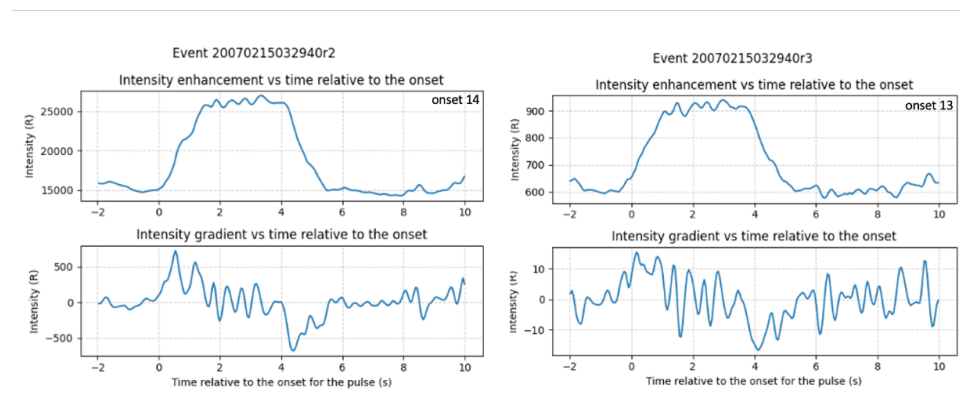


Figure 4.40: Event 7: gradients of onsets shown as line plots. Emission 6730 Å on the left, and emission 7774 Å on the right.

In Figure 4.40, the upper sections of both plots show defined onsets. Figure 4.41 is an example of an incorrectly chosen onset due to human error during the selection process. It is onset 50 from camera r2, and onset 47 for camera r3. When comparing this figure to the main event plots, these onsets around 50 appear to be in the midst of a less distinct area, suggesting the possibility that the area consists of general noise rather than pulsations.

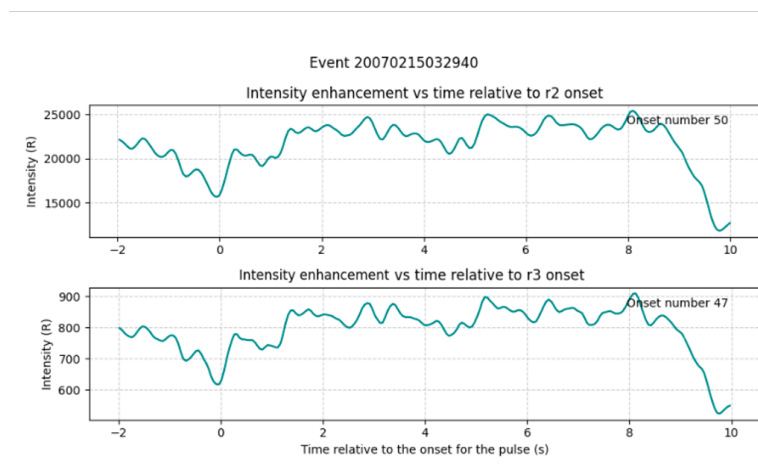


Figure 4.41: Example of a selected pulsation onset of varying quality from event 7

As shown in Figure 4.42, the top gray plot displays the data incorporating all the initially selected onsets. For this event, the elimination of inaccurately selected onsets did not appear to significantly impact the resulting regression line plot. However, it is evident that the highest intensity maximums have been removed, decreasing from an intensity max of 300 down to 45.

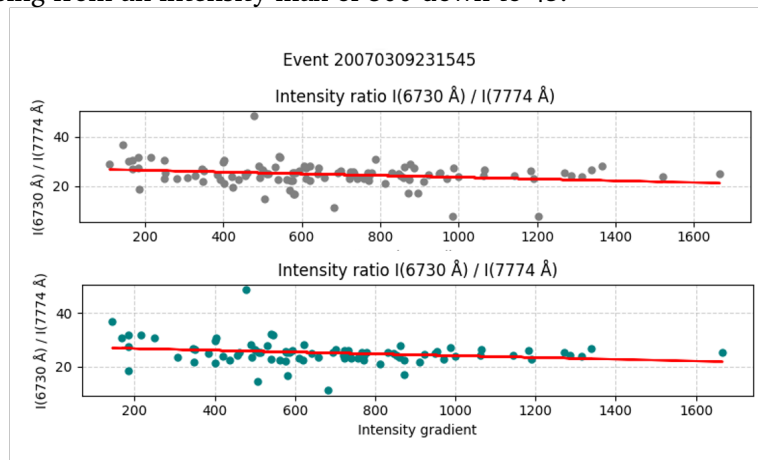


Figure 4.42: Event 7: The plots show the intensity ratio between the intensity at 6730 Å and 7774 Å.

4.1.8 Event 8

The main event plots shown in Figure 4.37, illustrates the 20 minute event starting at 23:15:45, March 9th, 2007. The manually selected onsets are represented by black dots. This event seems to be quite noisy throughout the 20 minutes. It appears that the event contains a substantial amount of noise from

around 23:35 h.

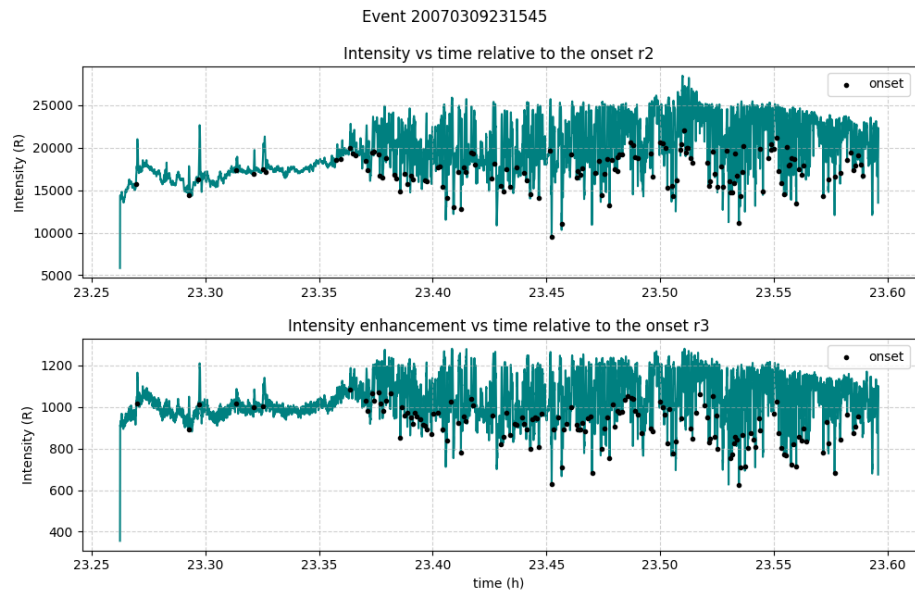


Figure 4.43: Event 8: Main event plots, showing both emissions with black onset markers.

In Figure 4.44 and 4.45, the primary event plots are displayed in a pseudocolour plot, with the total number of samples aligning with the quantity of selected onsets, approximately 140 for both emissions. It appears to be quite noisy, but there is a somewhat distinct intensity gradient line visible in the bottom part of the figures. However, the absence of clear lines in the decline of the gradient supports the notion that it may be noise.

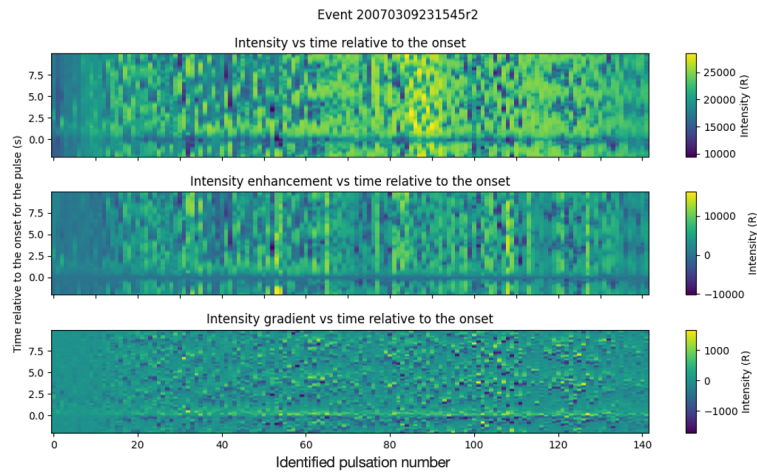


Figure 4.44: Event 8: pseudocolour plot of emission 6730 \AA from camera r2

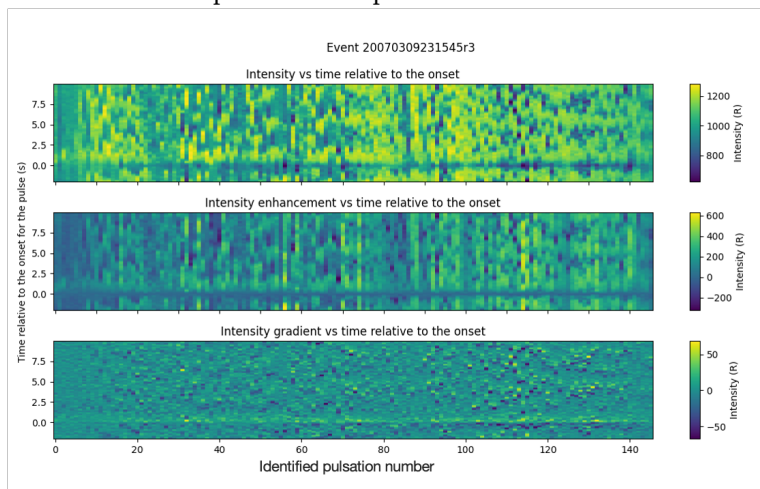


Figure 4.45: Event 8: pseudocolour plot of emission 7774 \AA from camera r3

The line plots presented in Figure 4.46 show the intensity enhancement versus time relative to the onset seen on the top, compared with the intensity gradient versus time relative to the onset seen in the bottom plot of both figures.

Both camera r2 and r3, contain strange pulses. Given these were among the two best ones found in the event it seems to be difficult to identify distinct pulsations from this event. The gradients show the decrease of the selected onset, but all in all it seems like noise.

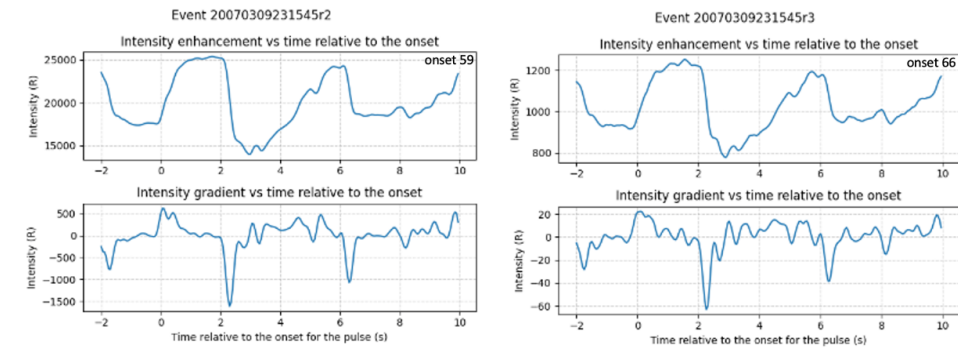


Figure 4.46: Event 8: gradients of onsets shown as line plots. Emission 6730 \AA on the left, and emission 7774 \AA on the right.

In Figure 4.46, the upper sections of both plots show defined onsets. Figure 4.47 is an example of an incorrectly chosen onset due to human error during the selection process. It is onset 32 for both emissions, appearing to be in the beginning of the pulsation noise section of the event starting slightly after 23:35 h as seen in the main event plots.

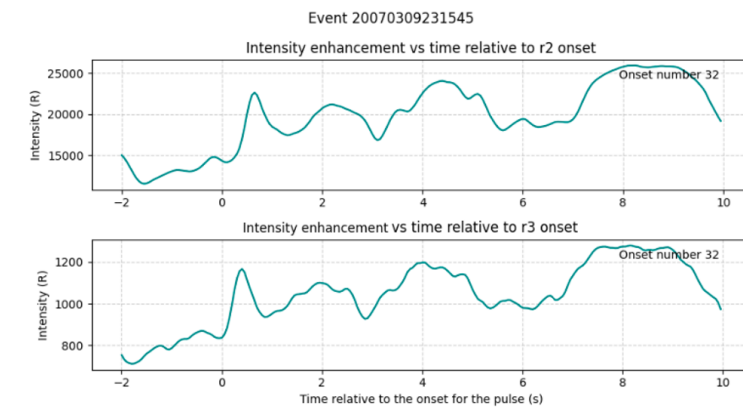


Figure 4.47: Example of a selected pulsation onset of varying quality from event 8

As shown in Figure 4.48, the top gray plot displays the data incorporating all the initially selected onsets. For this event, the elimination of inaccurately selected onsets did not appear to significantly impact the resulting regression line plot.

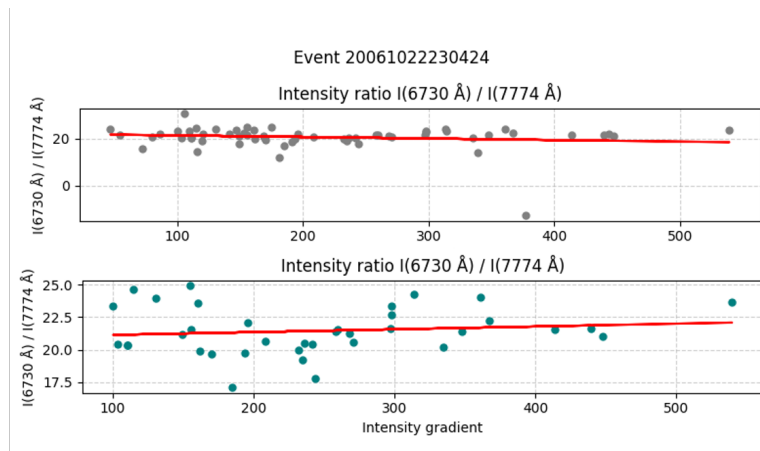


Figure 4.48: Event 8: The plots show the intensity ratio between the intensity at 6730 Å and 7774 Å.

4.2 Results

As evident from the figures, the pulsations in Event 1 are highly distinct, resulting in clean and easily distinguishable pulsations. In Event 2, the pulsations are less distinct, introducing more noise and rendering the plots less clear. Event 3 exhibits more distinct pulsations, with the data showing lower levels of noise. However, the pseudocolour plot indicates that the majority of selected pulsations have very low intensity. In Event 4, the pulsations have higher intensity, especially visible in the pseudocolour plot and the main event plot, containing distinct pulsations, particularly at the beginning. Event 5 appears to have more noise and lacks distinct pulsations compared to other events. The onsets exhibit a weak but distinct increase, as shown in the pseudocolour plot, although the bottom plot of the three suggests that it resembles background noise more than pulses. Event 6 appeared to be noisy, however, it included many distinct pulsations as observed in both the main event plots and the pseudocolour plots. The pseudocolour plots from Event 6 even showcase the intensity gradient lines during the middle of the event, where both the increase and decrease of intensity visible in the plot. Events 7 and 8 contained a lot of noise, with soft and unclear intensity changes in the plots without the distinct pulsations.

The most important findings from the observational study is the numbers found in Table 4.2 and Table 4.3. Table 4.2 display the slope of the regression line along with its variance.

Event	Slope	Variance
1	2.16673127e-03	2.09171573e+01
2	-0.00744144	0.00028716
3	2.16999733e-03	2.65516485e-06
4	1.17809489e-03	4.24464130e-05
5	0.02943631	4.67567844e-04
6	5.58054042e-03	5.90605995e-06
7	-7.05824996e-04	1.63613810e-06
8	-3.34290493e-03	2.54495921e-06

Table 4.2: Slope of the regression lines and their variance for each event.

In Table 4.3, the y-axis intercept numbers for each event is shown as well as its variance.

Event	y-axis intercept	Variance
1	2.09171573e+01	5.77781556e-01
2	1.17352709	0.05608592
3	2.43705006e+01	9.32872007e-01
4	2.86720587e+01	2.03116172e+01
5	20.11324246	1.50410205e+01
6	2.80963206e+01	8.77503613e-01
7	3.72808761e+01	1.69652210e+00
8	2.73845238e+01	1.40522246e+00

Table 4.3: y-axis intercept of the regression line for the events.

In Figure 4.49, the slope values of all the regression lines are presented, along with their respective standard deviation visible in the plot. The standard deviation is a number of uncertainty associated with the estimated slope. As anticipated from analyzing the data, both Event 5 and Event 2 exhibit a high amount of uncertainty.

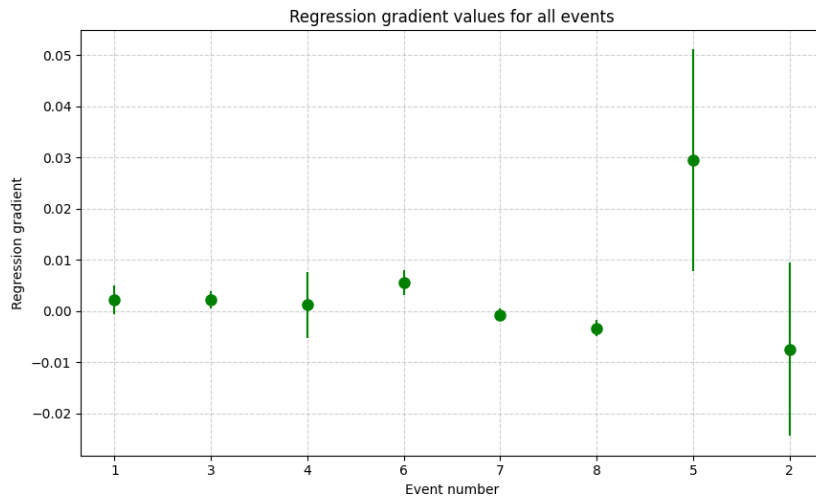


Figure 4.49: Regression slope values for all events with their uncertainty shown as lines going up and down from the slope value marker.

/5

Theoretical Study

The time variation of auroral emission intensity has been computed for abrupt onsets of electron precipitation with a Maxwellian energy distribution. The calculations were performed from the source altitudes of $3 R_E$, $4.4 R_E$, $6.1 R_E$, and $7.6 R_E$ along the Tromsø magnetic field line. These calculations were carried out using AURORA, a time-dependent multi-stream electron transport code developed at UiT. The investigation focused on pulsation onsets of emissions at 4278 \AA , 6730 \AA , 7444 \AA , and 8446 \AA .

In Section 5.1, various plots illustrate the intensity modulation of emissions from the four source altitudes, where the pulsation onsets are compared and discussed. Moving to Section 5.2, the analysis focuses on the intensity ratio between emission lines at 7774 \AA and 6730 \AA , as well as the ratio between 8446 \AA and 4278 \AA .

The data used for these calculations was provided to me personally by Gavazzi (2023-2024), a PhD candidate from the UiT Space Physics group. The model utilized in this study can be accessed on: Gustavsson and Gavazzi (2023).

5.1 Intensity Modulation

The onset of pulsations in the selected auroral emissions, resulting from a burst of pitch angle scattered precipitation at source altitudes of $3 R_E$, $4.4 R_E$,

6.1 R_E , and 7.6 R_E , is illustrated in Figure 5.1 and 5.2. The objective is to examine how the onset varies with time as a function of the source altitude where the pitch angle scattering is assumed to be effective. We can observe the variations in rise characteristics among the different emissions. The 4278 Å emission demonstrates the fastest increase, regardless of the source altitude. The remaining emissions exhibit slightly lower rates of increase, with 6370 Å increasing slightly more rapidly than 7774 Å, and the slowest increase is observed in the 8446 Å emission. This pattern is seen for the onset from all source altitudes.

All intensities are normalized within the range of 0 to 1. The scaling is determined by the maximum intensity observed after 0.5 seconds when the intensities have reached their steady-state levels. Assuming scattering is only effective at one altitude, we observe longer time of flight, energy and time of flight dispersion as the effective source altitude increases. Distinct onset responses are observed for emissions from molecular nitrogen (6730 Å and 4278 Å) and atomic oxygen (7774 Å and 8446 Å), each displaying slightly different energy responses. This implies that emissions from atomic oxygen shift slightly towards higher altitudes. The longer scale height and different excitation thresholds of atomic oxygen contribute to these variations.

In Figure 5.1, the intensity modulation of all the selected emissions and source altitudes is presented. The intensity is shown over time, and it is evident from the plots that after 0.5 seconds, the higher the source altitude, the lower the intensity. For a source altitude of 3 R_E , the intensity reaches almost 1, while for 4.4 R_E , it reaches its maximum at around 0.85. At 6.1 R_E , it reaches 0.8, and at 7.6 R_E , it reaches just below 0.8.

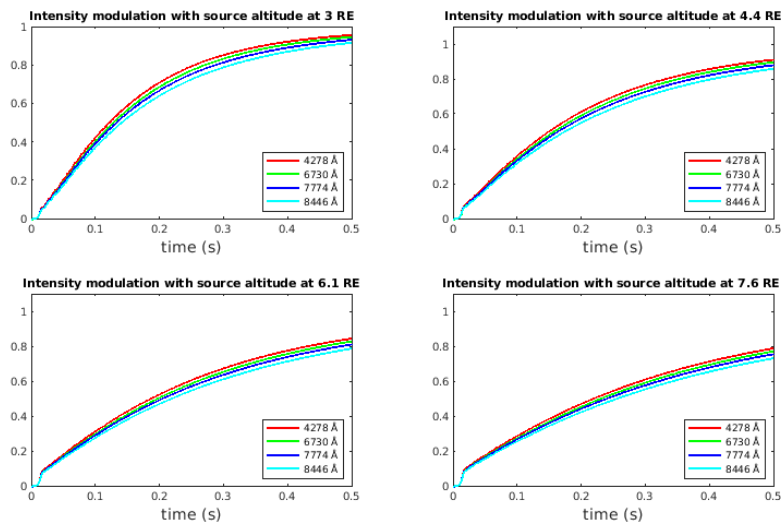


Figure 5.1: Intensity onset for precipitation from sources at $3 R_E$, $4.4 R_E$, $6.1 R_E$ and $7.6 R_E$

In Figure 5.2, the intensity modulation of specific emissions is represented in each plot, with each graph illustrating different source altitudes. Across all subplots, it is clear that the intensity decreases as the source altitude increases.

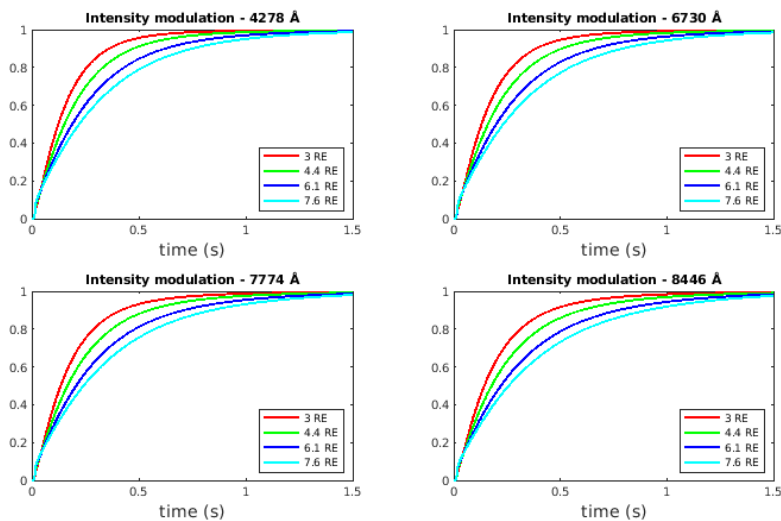


Figure 5.2: Intensity onset for precipitation of emission 4278 \AA , 6730 \AA , 7774 \AA and 8446 \AA .

Figures 5.3 and 5.4 depict the comparison of specific onset pulsations across

the four different source altitudes. It is visible that the onset of the pulsation in the ionosphere can not occur closer than somewhere between $6.1 R_E$ to $7.6 R_E$ during these events.

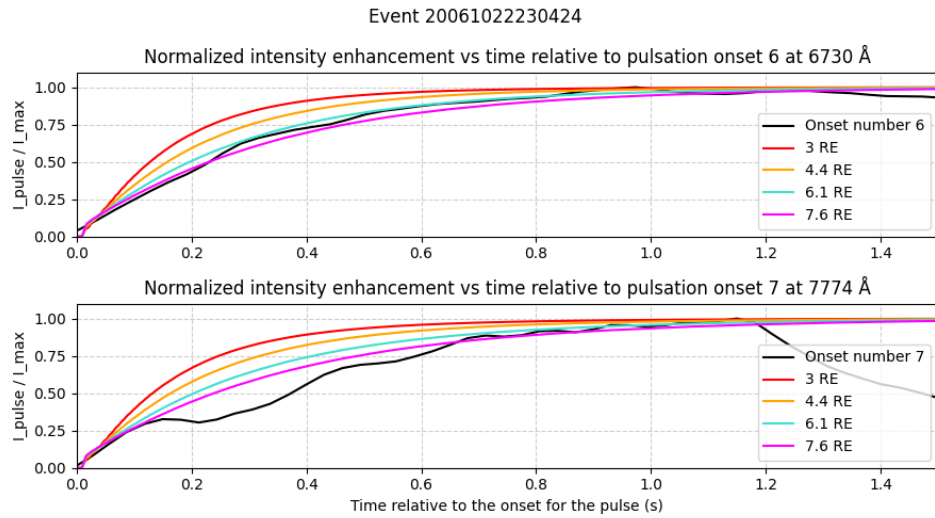


Figure 5.3: The figure show the normalized intensity enhancement as a function of time relative to pulsation onset number 6 at 6730 Å in the top graph, and the corresponding pulsation onset number 7 at 7774 Å.

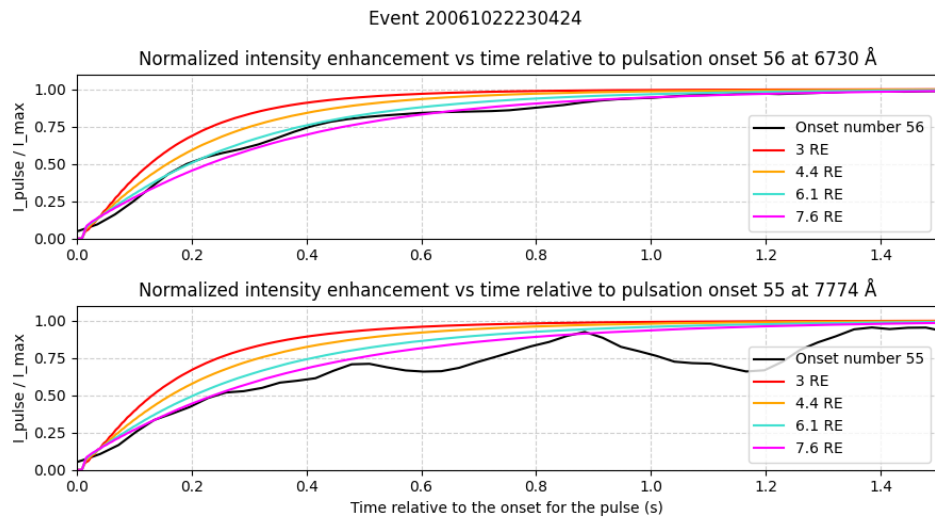


Figure 5.4: The figure show the normalized intensity enhancement as a function of time relative to pulsation onset number 56 at 6730 Å in the top graph, and the corresponding pulsation onset number 55 at 7774 Å.

5.2 Intensity Ratio

In Figure 5.5, the intensity ratio is illustrated between the intensities of the two observed emissions at 6730 and 7774 Å, as well as the molecular nitrogen emissions at 4278 Å and the atomic oxygen emission at 7774 Å, for precipitation originating from the four source altitudes. When comparing the onset ratio of emission 7774 Å and 6730 Å to the ratio of emission 4278 Å and 8446 Å, it is evident that for all source altitudes, the ratio between 7774 Å and 6730 Å is very close to constant.

However, the ratio between the 4278 Å and 8446 Å emissions show some variation with time, for all four source altitudes. The observed variations in the ratio over time suggest that there may be valuable information to extract regarding the variability of the onsets. This is something that should be considered for future studies of pulsating auroras.

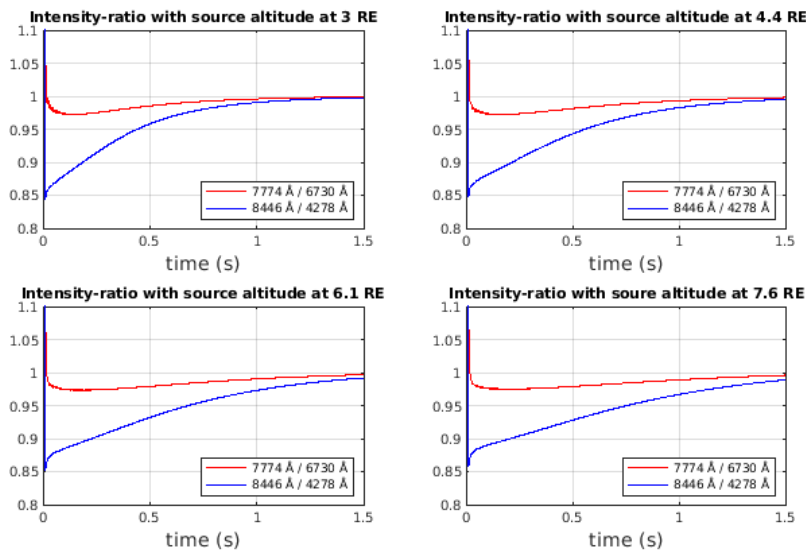


Figure 5.5: The intensity ratio for the precipitation of emission 4278 Å and 8446 Å is shown in blue, while the ratio for 6730 Å and 7774 Å is shown in red.

/6

Discussion

In the observational phase of the thesis, the manual selection of events and pulsations introduces a potential bias. The manual choice of pulsation onsets during the selection process may have inadvertently favored similar onsets, thereby creating a biased selection of the overall data. This potential bias could influence the outcomes derived from this part of the study. It is unclear how the bias affect the study, it seems likely that there is some over-selection of strong and distinctive pulsations relative to fainter and less pronounced ones.

In the modelling part of this thesis, the onset of pulsating aurora has been studied assuming an abrupt filling of the loss cone. The arrival of high-energy particles in the ionosphere precedes that of less energetic particles, resulting in a time-energy dispersion. Moving the source region farther out along the magnetic field line leads to an increase energy-time dispersion. When the filling of the loss cone occurs at a slower, non-prompt rate, the combination of the rate of loss cone filling and time of flight leads to a more gradual increase and a slower rise of auroral emission-intensity in the ionosphere. This prompt loss cone filling is observed from different source altitudes, with the slowest increase originating from the farthest source altitude of 7.6 *RE*.

The findings suggest that a prompt onset, for it to align with our observed data, must come from a further source altitude. Altering the way the loss cone is filled would necessitate a more intricate model design but may introduce bias into the results, impacting the scientific validity. The prompt filling is observed to occur close to the equatorial plane of the magnetosphere. Another possibility to

consider is that a loss cone filled gradually could still result in abrupt pulsation onsets in the ionosphere.

Through observations, it appears that the ratio between 6730 Å and 7774 Å remains relatively constant, exhibiting negligible variation. In contrast, the ratio between 4278 Å and 8446 Å seems to display more variability. This variability suggests that the latter ratio could potentially be utilized to extract additional information about the pulsation onset, making it a noteworthy consideration for future studies.

It is of interest to investigate how the loss cone is filled and to explore the various ways in which this filling could impact pulsating auroras. Additionally, understanding the consequences of stopping the filling of high-energy electrons is a noteworthy area of study. For instance, discontinuing the filling of different parts of the loss cone could result in less effective loss cone pitch angle scattering for high energies. Another interesting scenario to examine, is the aftermath following the event of a perfect loss cone filling.

Since our current analysis solely focuses on the onset of intensity, there has been no exploration of how the pulsation fades off. Future studies should encompass not only the end of auroral pulsations but also the reduction of the filling of the loss cone in the magnetosphere. Additionally, research should investigate how these pulsations transition back to the background intensity.



Summary

In this thesis, I have examined the existing knowledge of pulsating auroras and gained a comprehensive understanding of the underlying mechanisms that govern them.

The distinct pulsations are observed in Event 1, providing clear and interpretable plots. Event 2 shows less distinct pulsations with increased noise. Event 3 exhibits more distinct pulsations, although with lower intensity. Event 4 displays higher-intensity pulsations, especially at the beginning. Event 5 has more noise and less distinct pulsations. Event 6, initially appearing to be noisy, includes distinct pulsations and intensity gradient lines. Events 7 and 8 contain significant noise with soft and unclear intensity changes, lacking distinct pulsations. As expected based on data analysis, both Event 5 and Event 2 show a high degree of uncertainty.

Additionally, I conducted calculations and simulations of electron transport and ionospheric responses. The time-dependent electron transport model, AURORA, was employed to simulate the interactions between electrons and the atmosphere. The simulations considered four distinct source altitudes along the magnetic field line. The electron transport calculations of abrupt onset precipitation of electrons with maxwellian energy-distribution from source altitudes at $3 R_E$, $4.4 R_E$, $6.1 R_E$ and $7.6 R_E$ was performed. The emissions studied are atomic oxygen and molecular nitrogen at the wavelengths 4278 \AA , 6730 \AA , 7774 \AA and 8446 \AA . The onset characteristics of the emissions exhibit variations corresponding to different source altitudes. Therefore, it appears that the source

altitude correlates with the onset characteristics of the pulsating aurora.

Upon comparing the results from the observational aspect of the thesis with the theoretical findings, a correlation was identified. It became apparent that to achieve an abrupt onset in the ionosphere, the source altitude must be within the range of $6.1 R_E$ and $7.6 R_E$. The normalized intensity enhancement, plotted as a function of time relative to pulsation onsets at first 6730 \AA and then 7774 \AA , revealed insights by correlating specific pulsation onsets with the corresponding source altitudes.

During the observational phase, the manual selection of events and pulsations introduces a potential bias. The manual choice may inadvertently favor similar onsets, leading to a skewed selection of pulsations from the overall data. This bias could influence outcomes in this part of the study. In the modeling phase, the thesis explores the onset of pulsating auroras, assuming an abrupt filling of the loss cone. The study delves into understanding how loss cone filling impacts pulsating auroras, exploring consequences of discontinuing high-energy electron filling, and investigating scenarios after a perfect loss cone filling event. The current analysis, focused on onset intensity, lacks exploration of how pulsations fade off. Future studies are encouraged to encompass the decay-phase of auroral pulsations and examine their transition back to background intensity.

Bibliography

- R. L. Arnoldy, K. Dragoon, L. J. Cahill Jr., S. B. Mende, and T. J. Rosenberg. Detailed correlations of magnetic field and riometer observations at $l = 4.2$ with pulsating aurora. *Journal of Geophysical Research: Space Physics*, 87(A12):10449–10456, 1982. doi: <https://doi.org/10.1029/JA087iA12p10449>. URL <https://agupubs.onlinelibrary.wiley.com/doi/abs/10.1029/JA087iA12p10449>.
- H. Dahlgren, B. S. Lanchester, N. Ivchenko, and D. K. Whiter. Variations in energy, flux, and brightness of pulsating aurora measured at high time resolution. *Annales Geophysicae*, 35(3):493–503, 2017. doi: [10.5194/angeo-35-493-2017](https://doi.org/10.5194/angeo-35-493-2017). URL <https://angeo.copernicus.org/articles/35/493/2017/>.
- A. G. Demekhov and V. Y. Trakhtengerts. A mechanism of formation of pulsating aurorae. *Journal of Geophysical Research: Space Physics*, 99(A4):5831–5841, 1994. doi: <https://doi.org/10.1029/93JA01804>. URL <https://agupubs.onlinelibrary.wiley.com/doi/abs/10.1029/93JA01804>.
- E. Gavazzi. Personal communication. August-January 2023-2024.
- E. Grono and E. Donovan. Constraining the source regions of pulsating auroras. *Geophysical Research Letters*, 46(17-18):10267–10273, 2019. doi: <https://doi.org/10.1029/2019GL084611>. URL <https://agupubs.onlinelibrary.wiley.com/doi/abs/10.1029/2019GL084611>.
- E. Grono and E. Donovan. Surveying pulsating auroras. *Annales Geophysicae*, 38(1):1–8, 2020. doi: [10.5194/angeo-38-1-2020](https://doi.org/10.5194/angeo-38-1-2020). URL <https://angeo.copernicus.org/articles/38/1/2020/>.
- B. Gustavsson. Time-dependent electron transport i: Modelling of supra-thermal electron bursts modulated at 5–10 hz with implications for flickering aurora. *Journal of Geophysical Research: Space Physics*, 127(6):e2019JA027608, 2022. doi: <https://doi.org/10.1029/2019JA027608>. URL <https://agupubs.onlinelibrary.wiley.com/doi/abs/10.1029/2019JA027608>.

- B. Gustavsson and E. Gavazzi. AURORA.jl, Apr. 2023. URL <https://github.com/egavazzi/AURORA.jl>.
- M. G. Johnsen. Personal communication. August 2023.
- A. D. Johnstone. Pulsating aurora. *Nature*, 274(5667):119–126, 07/01 1978. ISSN 1476-4687. doi: 10.1038/274119a0. URL <https://doi.org/10.1038/274119a0>.
- S. L. Jones, M. R. Lessard, K. Rychert, E. Spanswick, E. Donovan, and A. N. Jaynes. Persistent, widespread pulsating aurora: A case study. *Journal of Geophysical Research: Space Physics*, 118(6):2998–3006, 2013. doi: <https://doi.org/10.1002/jgra.50301>. URL <https://agupubs.onlinelibrary.wiley.com/doi/abs/10.1002/jgra.50301>.
- S. Kasahara, Y. Miyoshi, S. yokota, T. Mitani, Y. Kasahara, S. Matsuda, A. Kumamoto, A. Matsuoka, y. Kazama, H. u. frey, V. angelopoulos, S. Kurita, K. Keika, K. Seki, and I. Shinohara. Pulsating aurora from electron scattering by chorus waves. *Nature*, 554:337,340, 2018. doi: <https://doi.org/10.1038/nature25505>.
- M. Kosch. Personal communication. August 2023.
- Y. Miyoshi, Y. Katoh, T. Nishiyama, T. Sakanoi, K. Asamura, and M. Hirahara. Time of flight analysis of pulsating aurora electrons, considering wave-particle interactions with propagating whistler mode waves. *Journal of Geophysical Research: Space Physics*, 115(A10), 2010. doi: <https://doi.org/10.1029/2009JA015127>. URL <https://agupubs.onlinelibrary.wiley.com/doi/abs/10.1029/2009JA015127>.
- Y. Miyoshi, S. Saito, K. Seki, T. Nishiyama, R. Kataoka, K. Asamura, Y. Katoh, Y. Ebihara, T. Sakanoi, M. Hirahara, S. Oyama, S. Kurita, and O. Santolik. Relation between fine structure of energy spectra for pulsating aurora electrons and frequency spectra of whistler mode chorus waves. *Journal of Geophysical Research: Space Physics*, 120(9):7728–7736, 2015. doi: <https://doi.org/10.1002/2015JA021562>. URL <https://agupubs.onlinelibrary.wiley.com/doi/abs/10.1002/2015JA021562>.
- N. F. Ness, D. R. Williams, and I. E. Bell. Magnetometer, ace, 10/28 2022. URL <https://nssdc.gsfc.nasa.gov/nmc/experiment/display.action?id=1997-045A-09>.
- NIPR. Thumbnail images of event 2, a. URL <http://133.57.20.115/www/optical/asc/thumbnail/2007/20070213.html>.

- NIPR. Video of event 2, b. URL <http://133.57.20.115/www/optical/asc/movie/2007/20070213.wmv>.
- NIPR. Thumbnail images of event 3, c. URL <http://133.57.20.115/www/optical/asc/thumbnail/2007/20070215.html>.
- NIPR. Video of event 3, d. URL <http://133.57.20.115/www/optical/asc/movie/2007/20070215.wmv>.
- R. Nishimura, M. R. Lessard, Y. Katoh, Y. Miyoshi, E. Grono, N. Partamies, N. Sivadas, K. Hosokawa, M. Fukizawa, M. Samara, R. G. Michell, R. Kataoka, T. Sakanoi, D. K. Whiter, S. ichiro Oyama, Y. Ogawa, and S. Kurita. Diffuse and pulsating aurora. *Space Science Reviews*, 216(1):4, 2020. doi: 10.1007/s11214-019-0629-3. URL <https://doi.org/10.1007/s11214-019-0629-3>.
- T. Nishiyama, T. Sakanoi, Y. Miyoshi, Y. Katoh, K. Asamura, S. Okano, and M. Hirahara. The source region and its characteristic of pulsating aurora based on the reimei observations. *Journal of Geophysical Research: Space Physics*, 116(A3), 2011. doi: <https://doi.org/10.1029/2010JA015507>. URL <https://agupubs.onlinelibrary.wiley.com/doi/abs/10.1029/2010JA015507>.
- S. Nozawa. Personal communication. September 2023.
- Y. Ogawa. Personal communication. September-October 2023.
- S. Oyama. Personal communication. August 2023.
- N. Partamies, D. Whiter, A. Kadokura, K. Kauristie, H. Nesse Tyssøy, S. Massetti, P. Stauning, and T. Raita. Occurrence and average behavior of pulsating aurora. *Journal of Geophysical Research: Space Physics*, 122(5):5606–5618, 2017. doi: <https://doi.org/10.1002/2017JA024039>. URL <https://agupubs.onlinelibrary.wiley.com/doi/abs/10.1002/2017JA024039>.
- M. H. Rees. Coniugate effects of atmospherically scattered auroral electrons. *Radio Science*, 3(7):645–649, 1968. doi: <https://doi.org/10.1002/rds196837645>. URL <https://agupubs.onlinelibrary.wiley.com/doi/abs/10.1002/rds196837645>.
- O. Royrvik and T. N. Davis. Pulsating aurora: Local and global morphology. *Journal of Geophysical Research (1896-1977)*, 82(29):4720–4740, 1977. doi: <https://doi.org/10.1029/JA082i029p04720>. URL <https://agupubs.onlinelibrary.wiley.com/doi/abs/10.1029/JA082i029p04720>.
- F. Tesema, N. Partamies, H. N. Tyssøy, A. Kero, and C. Smith-Johnsen. Observa-

- tions of electron precipitation during pulsating aurora and its chemical impact. *Journal of Geophysical Research: Space Physics*, 125(6):e2019JA027713, 2020. doi: <https://doi.org/10.1029/2019JA027713>. URL <https://agupubs.onlinelibrary.wiley.com/doi/abs/10.1029/2019JA027713>. e2019JA027713 10.1029/2019JA027713.
- D. Whiter. Personal communication. September-November 2023.
- D. Whiter, B. Lanchester, N. Ivchenko, and R. Fear. Ask - auroral structure and kinetics. *Space Environment Physics Group, School of Physics and Astronomy, University of Southampton, UK Space and Plasma Physics, School of Electrical Engineering, KTH, Stockholm, Sweden*, 09/18 2023. URL <http://ask1.esr.eiscat.no/>.
- T. Yamamoto. On the temporal fluctuations of pulsating auroral luminosity. *Journal of Geophysical Research: Space Physics*, 93(A2):897–911, 1988. doi: <https://doi.org/10.1029/JA093iA02p00897>. URL <https://agupubs.onlinelibrary.wiley.com/doi/abs/10.1029/JA093iA02p00897>.
- X. Yu, Z. Yuan, J. Yu, D. Wang, D. Deng, and H. O. Funsten. Diffuse auroral precipitation driven by lower-band chorus second harmonics. *Nature Communications*, 14(1):438, 01/27 2023. ISSN 2041-1723. doi: 10.1038/s41467-023-36095-x. URL <https://doi.org/10.1038/s41467-023-36095-x>.



Python Code

This appendix provides the scripts written in Python 3.8 used to analyze and visualize data, perform calculations and make all the plots for the observational part in this thesis.

Listing A.1 is used to plot the main events. The process involves identifying the pulsation onsets for each event by manually selecting intervals, plotting them, and marking each onset within the intervals. Subsequently, the obtained onset values are saved in separate text files for both time and intensity.

Listing A.2 is used to save MATLAB files of the onset intervals, plotting line plots, pseudocolour plots and separate linear plots of the pulsation onsets. The code provides a comprehensive analysis and visualization of the events, presenting various aspects of intensity, enhancement, and gradient over time relative to the onset. The generated plots offer insights into the characteristics of the analyzed data.

Listing A.3 provides a detailed analysis of intensity and intensity gradient characteristics around the onsets, saving relevant information for further study or visualization.

Listing A.4 is used to plot intensity data and identify paired onsets between two cameras. It involves plotting the onsets for each camera with the corresponding intensity data and saving the paired onset information into a text file. Additionally, it saves each paired line plot into PNG files.

Listing A.5 is designed to analyze and visualize paired onset data from both cameras for each event, facilitating the comparison of intensities. A specific onset is chosen for further analysis, and a linear regression line is applied to the third subplot. The code then displays the paired plots and subplots for more in-depth analysis.

Listing A.6 is utilized to generate a plot that visualizes regression gradient values for different events, incorporating the standard deviation of the values within the plot. The code offers a visual representation of the variation in regression gradient values across different events, facilitating easier comparison and analysis of the data.

Listing A.7 reads and extracts data from magnetometer files corresponding to different events. The resulting visualization provides insights into the magnetic field variations during the specified event, making it easier to analyze and interpret the data.

Listing A.8 is designed to match onset data between MATLAB and Python datasets, generating plots for comparative analysis of intensity enhancements between onsets from the selected emissions during the events. The plots provide insights into the behavior of normalized intensity enhancements at different emissions and onset numbers.

```

1
2 import numpy as np
3 import matplotlib.pyplot as plt
4 from scipy.io import loadmat
5 mat = loadmat('20070309231545r3.mat')
6
7
8 # data variables
9 timeV = mat['timeV'][0:] # shape: (38337, 1)
10 # timeV1 = mat['timeV1'][0:] # shape: (38337, 6)
11 # timeVtest = mat['timeV'][0:]
12 # keo_cam1 = mat['keo_cam1'][0:] # shape: (256, 38337)
13 keo_cam = np.transpose(mat['Keo'][0:]) # shape: (38337, 256)
14 # mean_keo_cam = np.mean(keo_cam[:, 123:132], axis=1) # shape:
15 # (38337, )
16 mean_keo_cam = np.mean(keo_cam[:, 50:300], axis=1) # shape:
17 # (38337, )
18 conv_mean_cam = np.convolve(mean_keo_cam, [0.25, 0.75, 1, 1, 1,
19 # 0.75, 0.25], mode='same')
20
21 plt.figure(figsize=(9, 5))
22 plt.plot(timeV, conv_mean_cam) # plot the main event
23
24 plt.title('Average intensity vs time of the event:

```

```

20070309231545r3')
22 plt.xlabel("Time (h)")
23 plt.ylabel("Intensity (R)")
24 plt.grid(True, linestyle='--', alpha=0.6)
25
26 t_start_stop = np.array([0.5, 1.3])
27 t_start_stop_all = np.zeros((200, 2))
28
29 i_row = 0
30 while t_start_stop[0] < t_start_stop[1]:
31     p1, p2 = plt.ginput(2)
32     t_start_stop = np.array([p1[0], p2[0]])
33     t_start_stop_all[i_row, :] = t_start_stop
34     i_row = i_row + 1
35
36 t_start_stop_all = t_start_stop_all[0:i_row-1, :]
37 # print("intervals selected from the original plot: \n",
38       t_start_stop_all)
39
40 t_onset_x = np.zeros((200, 1))
41 I_onset_y = np.zeros((200, 1))
42
43 idx_onset = 0
44 n_row = i_row - 1
45 for i_current_row in range(n_row):
46     t_start = t_start_stop_all[i_current_row, 0]
47     t_end = t_start_stop_all[i_current_row, 1]
48     intervals = (t_start <= timeV) & (timeV <= t_end)
49     plt.figure()
50     plt.plot(timeV[intervals[:, 0]], conv_mean_cam[intervals[:,
51     0]])
52
53     p = plt.ginput(-1)
54     ip = 0
55     for ip in range(len(p)):
56         t_onset_x[idx_onset] = p[ip][0]      # x coordinate
57         from index/ginput
58         I_onset_y[idx_onset] = p[ip][1]      # y coordinate:
59         I_value at the onset
60         idx_onset = idx_onset + 1
61
62 # save both onset values to a text file
63 with open('20070309231545r3.txt', 'w') as file:
64     for i in range(len(t_onset_x[0:idx_onset])):
65         file.write(f"{float(t_onset_x[i])},{float(I_onset_y[i])
66         }\n")
67
68 # print("t_onset values from zoomed in plots: \n", (t_onset_x
69       [0:idx_onset], I_onset_y[0:idx_onset]))
70
71 plt.title("20070309231545r3.mat")
72 plt.xlabel("Time (h)")
73 plt.ylabel("Intensity (R)")

```

```

69 plt.grid(True, linestyle='--', alpha=0.6)
70 # plt.legend()
71 plt.show()

```

Listing A.1: Code used to get pulsation onset times.

```

1
2 import numpy as np
3 import matplotlib.pyplot as plt
4 from scipy.io import loadmat
5 from scipy.io import savemat
6 mat = loadmat('20070309231545r3.mat')
7
8 # data variables
9 timeV = mat['timeV'][0:] # shape: (38337, 1)
10 keo_cam = np.transpose(mat['Keo'][0:]) # shape: (38337, 256)
11     time, pixels (fra transpose)
12 mean_keo_cam = np.mean(keo_cam[:, 50:300], axis=1) # shape:
13     (38337, )
14 conv_mean_cam = np.convolve(mean_keo_cam, [0.25, 0.75, 1, 1, 1,
15     0.75, 0.25], mode='same')
16
17 t_onset_data = np.loadtxt('20070309231545r3.txt', delimiter=',',
18     ) # time in decimal hours * / 3600 to change units
19
20 # get the time values from the data file
21 t_onset = t_onset_data[:, 0]
22
23 # extra time around the onsets
24 extra_time_before = 2.0 / 3600 # 2 seconds added before the
25     t_onset value in decimal hours
26 extra_time_after = 10.0 / 3600 # 10 seconds added after the
27     t_onset value in decimal hours
28
29 # create a matrix to store the t_point values
30 t_points_matrix = np.zeros((len(t_onset), 1))
31
32 intensity_on = None
33 relative_time = None
34
35 fps = 1 / ((timeV[1] - timeV[0]) * 3600) # frames per second
36 # print('fps', fps)
37
38 d_i_o = 32 * 2 # delta index onset
39 if np.abs(fps - 32) < 0.1:
40     d_i_o = 64
41 elif np.abs(fps - 20) < 0.1:
42     d_i_o = 40
43 elif np.abs(fps - 25) < 0.1:
44     d_i_o = 50
45 # print('dio', d_i_o)
46
47 # looping over the onsets, adding time before and after the
48     t_onset point, and plotting them with the same start point

```

```

42 for i, t_point in enumerate(t_onset):
43     t_start = t_point - extra_time_before
44     t_end = t_point + extra_time_after
45     intervals = (t_start <= timeV) & (timeV <= t_end)
46     i_idx = np.where((t_start <= timeV[:, 0]) & (timeV[:, 0] <=
         t_end))[0]
47     if i == 0:
48         intensity_on = np.zeros([len(t_onset), len(i_idx)])
49         relative_time = (timeV[i_idx, 0] - t_point)*3600
50         intensity_increase = np.zeros([len(t_onset), len(i_idx)
         ])
51         intensity_gradient = np.zeros([len(t_onset), len(i_idx)
         ])
52         intensity_on[i, :] = conv_mean_cam[i_idx]
53         intensity_increase[i, :] = intensity_on[i, :] -
         intensity_on[i, d_i_o] # d_i_o: 2 sek before and 10 after,
         2*fps
54         intensity_gradient[i, :] = np.gradient(conv_mean_cam[i_idx
         ])
55         t_points_matrix[i, 0] = t_point
56
57 # save t_points_matrix as a .mat file
58 savemat('H20070309231545r3_t_intervals.mat', {'
         H20070309231545r3_t_intervals': relative_time})
59 savemat('H20070309231545r3_intensity.mat', {'
         H20070309231545r3_intensity': intensity_on})
60
61 # ----- line plots
62
63
64 plt.figure(figsize=(8, 6))
65 plt.suptitle('Event 20070309231545r3')
66 plt.tight_layout()
67
68 plt.subplot(3, 1, 1)
69 plt.plot(relative_time, intensity_on.T)
70 plt.title('Intensity vs time relative to the onset')
71 plt.tight_layout()
72 plt.grid(True, linestyle='--', alpha=0.6)
73 plt.figlegend(['1', '2', '3', '4', '5', '6', '7', '8', '9', '10
         '], loc='upper right', bbox_to_anchor=(1, 1), ncols=5)
74 plt.ylabel("Intensity (R)") # rayleigh, photon/sec
75
76 plt.subplot(3, 1, 2)
77 plt.plot(relative_time, intensity_increase.T)
78 plt.title('Intensity enhancement vs time relative to the onset'
         )
79 plt.tight_layout()
80 plt.ylabel("Intensity (R)") # rayleigh, photon/sec
81 plt.grid(True, linestyle='--', alpha=0.6)
82 plt.tight_layout()
83
84 plt.subplot(3, 1, 3)
85 plt.plot(relative_time, intensity_gradient.T)

```

```

86 plt.title('Intensity gradient vs time relative to the onset')
87 plt.tight_layout()
88 plt.xlabel("time (s)")
89 plt.ylabel("Intensity (R)")      # rayleigh, photon/sec
90 plt.grid(True, linestyle='--', alpha=0.6)
91 plt.tight_layout()
92
93 plt.show()
94
95 # ----- pcolormesh plots
96
97 t_idx = np.arange(0, len(t_onset))
98 plt.figure(figsize=(8, 6))
99 plt.suptitle('Event 20070309231545r3')
100
101 plt.subplot(3, 1, 1)
102 cba = plt.pcolormesh(t_idx, relative_time, intensity_on.T)
103 plt.title('Intensity vs time relative to the onset')
104 plt.colorbar(cba, label='Intensity (R)', aspect=10)      #
105     rayleigh, photon/sec
106 plt.xticks(ticks=t_idx[::10], labels=[])                #
107     removing x-axis tick labels
108 plt.tight_layout()
109
110 plt.subplot(3, 1, 2)
111 cbb = plt.pcolormesh(t_idx, relative_time, intensity_increase.T
112 )
113 plt.title('Intensity enhancement vs time relative to the onset'
114 )
115 plt.colorbar(cbb, label='Intensity (R)', aspect=10)      #
116     rayleigh, photon/sec
117 plt.ylabel("Time relative to the onset for the pulse (s)")
118 plt.xticks(ticks=t_idx[::10], labels=[])
119 plt.tight_layout()
120
121 plt.subplot(3, 1, 3)
122 cbc = plt.pcolormesh(t_idx, relative_time, intensity_gradient.T
123 )
124 plt.title('Intensity gradient vs time relative to the onset')
125 plt.colorbar(cbc, label='Intensity (R)', aspect=10)      #
126     rayleigh, photon/sec
127 plt.xlabel("Number of samples")
128 plt.tight_layout()
129
130 plt.show()
131
132 # ----- separate line plots of the gradients
133
134 i = 1
135
136 for i, t_point in enumerate(t_onset):
137
138     plt.suptitle('Event 20070309231545r3')

```

```

133
134 plt.subplot(2, 1, 1)
135 plt.plot(relative_time, intensity_on[i, :].T)
136 plt.title('Intensity enhancement vs time relative to the
onset')
137 plt.tight_layout()
138 plt.ylabel("Intensity (R)") # rayleigh, photon/sec
139 plt.grid(True, linestyle='--', alpha=0.6)
140 plt.tight_layout()
141
142 plt.subplot(2, 1, 2)
143 plt.plot(relative_time, np.convolve(intensity_gradient[i,
:].T, [1.0/3.0, 1.0/3.0, 1.0/3.0], 'same'))
144 plt.title('Intensity gradient vs time relative to the onset
')
145 plt.tight_layout()
146 plt.xlabel("Time relative to the onset for the pulse (s)")
147 plt.ylabel("Intensity (R)") # rayleigh, photon/sec
148 plt.grid(True, linestyle='--', alpha=0.6)
149 plt.tight_layout()
150 # plt.show()
151
152 # Save files in pdf and eps format
153 filename = "lines_20070309231545r3_{0:02d}.png".format(i)
154 plt.savefig(filename, format='png')
155 plt.close()

```

Listing A.2: Code used to save MATLAB files containing onset intervals and generate various plots.

```

1
2 import numpy as np
3 from scipy.io import loadmat
4 mat = loadmat('20070309231545r3.mat')
5
6
7 # data variables
8 timeV = mat['timeV'][0:] # shape: (38337, 1)
9 keo_cam = np.transpose(mat['Keo'][0:]) # shape: (38337, 256)
time, pixels
10 mean_keo_cam = np.mean(keo_cam[:, 50:300], axis=1) # shape:
(38337, )
11 conv_mean_cam = np.convolve(mean_keo_cam, [0.25, 0.75, 1, 1, 1,
0.75, 0.25], mode='same')
12
13 t_onset_data = np.loadtxt('20070309231545r3.txt', delimiter=',',
) # time in decimal hours * / 3600 to change units
14
15 # get intensity- and time values for the onsets
16 I_values = t_onset_data[:, 1]
17 t_onset = t_onset_data[:, 0]
18
19 # save I_values at the onsets into a text file
20 with open('20070309231545r3_I_Values.txt', 'w') as file:

```

```

21     for i in range(len(I_values)):
22         file.write(f"{float(I_values[i])}\n")
23
24 # save t_values at onset to a text file
25 with open('20070309231545r3_t_Values.txt', 'w') as file:
26     for i in range(len(t_onset)):
27         file.write(f"{float(t_onset[i]*3600)}\n")
28
29 from_time = 1.0 / 3600
30 to_time = 2.0 / 3600
31
32 # matrix to store the t_point values
33 t_points_matrix = np.zeros((len(t_onset), 1))
34
35 I_max = np.zeros((len(t_onset), 1)) # max
36 I_median = np.zeros((len(t_onset), 1)) # median
37
38 # for gradient
39 dIdt = np.zeros((len(t_onset), 1))
40 dIdt_median = np.zeros((len(t_onset), 1))
41
42 intensity_on = None
43 relative_time = None
44
45 fps = 1 / ((timeV[1] - timeV[0]) * 3600) # frames per second
46 #print('fps', fps)
47
48 d_i_o = 32 * 2 # delta index onset
49 if np.abs(fps - 32) < 0.1:
50     d_i_o = 64
51 elif np.abs(fps - 20) < 0.1:
52     d_i_o = 40
53 elif np.abs(fps - 25) < 0.1:
54     d_i_o = 50
55 #print('dio', d_i_o)
56
57 # looping over the onsets, finding I_max and I_median
58 for i, t_point in enumerate(t_onset):
59     t_start = t_point + from_time
60     t_end = t_point + to_time
61     #print(t_start)
62     #print(t_end)
63     intervals = (t_start <= timeV) & (timeV <= t_end)
64     i_idx = np.where((t_start <= timeV[:, 0]) & (timeV[:, 0] <=
65         t_end))[0]
66     #print('i_index', i_idx)
67     if i == 0:
68         intensity_on = np.zeros([len(t_onset), len(i_idx)])
69         # 2D list/array
70         relative_time = (timeV[i_idx, 0] - t_point) * 3600
71         intensity_increase = np.zeros([len(t_onset), len(i_idx)
72 ])
73     intensity_on[i, :] = conv_mean_cam[i_idx]
74     I_max[i] = max(conv_mean_cam[i_idx])

```



```

72     I_median[i] = np.median(conv_mean_cam[i_idx])
73     t_points_matrix[i, 0] = t_point
74
75
76 # ----- finding the gradient of the pulses
77
78 # looping over the onsets, adding time before and after the
79 # t_onset point, plotting them with the same start point
80 for i, t_point in enumerate(t_onset):
81     t_start = t_point
82     t_end = t_point + 1.0 / 3600
83     #print(t_start)
84     #print(t_end)
85     intervals = (t_start <= timeV) & (timeV <= t_end)
86     i_idx = np.where((t_start <= timeV[:, 0]) & (timeV[:, 0] <=
87                    t_end))[0]
88     #print('i_index', i_idx)
89     if i == 0:
90         intensity_on = np.zeros([len(t_onset), len(i_idx)]) #
91         2D list/array
92         relative_time = (timeV[i_idx, 0] - t_point) * 3600
93         intensity_increase = np.zeros([len(t_onset), len(i_idx)
94                                     ])
95         intensity_on[i, :] = conv_mean_cam[i_idx]
96         dIdt[i] = max(np.gradient(conv_mean_cam[i_idx]))
97         dIdt_median[i] = np.median(np.gradient(conv_mean_cam[i_idx]
98                                     ))
99         t_points_matrix[i, 0] = t_point
100
101 # ----- saving max and median of the pulse (intensity)
102
103 # save I_max_values to a text file
104 with open('20070309231545r3_I_max.txt', 'w') as file:
105     for i in range(len(I_max)):
106         file.write(f"{float(I_max[i])}\n")
107
108 # ----- save I_median to a text file
109 with open('20070309231545r3_I_median.txt', 'w') as file:
110     for i in range(len(I_median)):
111         file.write(f"{float(I_median[i])}\n")
112
113 # ----- saving max and median of gradient
114
115 # save I_max_values to a text file
116 with open('20070309231545r3_I_max_gradient.txt', 'w') as file:
117     for i in range(len(dIdt)):
118         file.write(f"{float(dIdt[i])}\n")
119
120 # save I_median to a text file
121 with open('20070309231545r3_I_median_gradient.txt', 'w') as
122     file:

```

```

120     for i in range(len(dIdt_median)):
121         file.write(f"{float(dIdt_median[i])}\n")

```

Listing A.3: Code used to get intensity average and save the resulting data to text files.

```

1
2 import numpy as np
3 import matplotlib.pyplot as plt
4 from scipy.io import loadmat
5
6 #     20061022230424
7
8 # load files for camera 1
9 mat_r1 = loadmat('20061022230424r1.mat')
10 mat_I_r1 = loadmat('H20061022230424r1_intensity.mat')
11 mat_t_r1 = loadmat('H20061022230424r1_t_intervals.mat')
12
13 onset_data_r1 = np.loadtxt('20061022230424r1.txt', delimiter=',
14                             ')
15 I_onset_data_r1 = np.loadtxt('20061022230424r1_I_Values.txt')
16 t_onset_data_r1 = np.loadtxt('20061022230424r1_t_Values.txt')
17 I_median_data_r1 = np.loadtxt('20061022230424r1_I_median.txt')
18 I_median_gradient_data_r1 = np.loadtxt('20061022230424
19     r1_I_median_gradient.txt')
20 I_max_data_r1 = np.loadtxt('20061022230424r1_I_max.txt')
21 I_max_gradient_data_r1 = np.loadtxt('20061022230424
22     r1_I_max_gradient.txt')
23
24 # load files for camera 2
25 mat_r3 = loadmat('20061022230424r3.mat')
26 mat_I_r3 = loadmat('H20061022230424r3_intensity.mat')
27 mat_t_r3 = loadmat('H20061022230424r3_t_intervals.mat')
28
29 onset_data_r3 = np.loadtxt('20061022230424r3.txt', delimiter=',
30                             ')
31 I_onset_data_r3 = np.loadtxt('20061022230424r3_I_Values.txt')
32 t_onset_data_r3 = np.loadtxt('20061022230424r3_t_Values.txt')
33 I_median_data_r3 = np.loadtxt('20061022230424r3_I_median.txt')
34 I_median_gradient_data_r3 = np.loadtxt('20061022230424
35     r3_I_median_gradient.txt')
36 I_max_data_r3 = np.loadtxt('20061022230424r3_I_max.txt')
37 I_max_gradient_data_r3 = np.loadtxt('20061022230424
38     r3_I_max_gradient.txt')
39
40 # data variables cam1
41 timeV_r1 = mat_r1['timeV'][0:] # shape:
42     (38337, 1)
43 keo_cam = np.transpose(mat_r1['Keo'][0:]) # shape:
44     (38337, 256) time, pixels (fra transpose)
45 mean_keo_cam = np.mean(keo_cam[:, 50:300], axis=1) # shape:
46     (38337, )

```

```

39 conv_mean_cam_r1 = np.convolve(mean_keo_cam, [0.25, 0.75, 1, 1,
1, 0.75, 0.25], mode='same')
40 mat_I_r1 = mat_I_r1['H20061022230424r1_intensity'][0:]
41 mat_t_r1 = mat_t_r1['H20061022230424r1_t_intervals'][0:]
42
43 # data variables cam 2
44 timeV_r3 = mat_r3['timeV'][0:] # shape:
(38337, 1)
45 keo_cam = np.transpose(mat_r3['Keo'][0:]) # shape:
(38337, 256) time, pixels
46 mean_keo_cam = np.mean(keo_cam[:, 50:300], axis=1) # shape:
(38337, )
47 conv_mean_cam_r3 = np.convolve(mean_keo_cam, [0.25, 0.75, 1, 1,
1, 0.75, 0.25], mode='same')
48 mat_I_r3 = mat_I_r3['H20061022230424r3_intensity'][0:]
49 mat_t_r3 = mat_t_r3['H20061022230424r3_t_intervals'][0:]
50
51 plt.figure(figsize=(8, 6))
52 plt.suptitle('Event 20061022230424')
53
54 plt.subplot(2, 1, 1) # 2 rows, 1 column, first subplot
55 plt.scatter(t_onset_data_r1/3600, I_onset_data_r1, marker='.',
color='black', zorder=2, label='onset')
56 plt.plot(timeV_r1, conv_mean_cam_r1, color='teal', zorder=1,
label='')
57 plt.title('Intensity vs time relative to the onset r1')
58 plt.legend()
59
60 plt.tight_layout()
61 plt.grid(True, linestyle='--', alpha=0.6)
62 plt.ylabel("Intensity (R)") # rayleigh, photon/sec
63
64 plt.subplot(2, 1, 2)
65 plt.scatter(t_onset_data_r3/3600, I_onset_data_r3, marker='.',
color='black', zorder=2, label='onset')
66 plt.plot(timeV_r3, conv_mean_cam_r3, color='teal', zorder=1)
67 plt.title('Intensity enhancement vs time relative to the onset
r3')
68 plt.legend()
69
70 plt.tight_layout()
71 plt.ylabel("Intensity (R)") # rayleigh, photon/sec
72 plt.xlabel("time (h)")
73 plt.grid(True, linestyle='--', alpha=0.6)
74 plt.tight_layout()
75
76 plt.show()
77
78
79 i_1 = 1
80 for i_1 in range(len(t_onset_data_r1)):
81     i_r3_best = np.argmin(abs(t_onset_data_r1[i_1] -
t_onset_data_r3))
82     dt_curr = t_onset_data_r1[i_1] - t_onset_data_r3[i_r3_best]

```

```

83
84     if abs(dt_curr) < 1.5:           # 1.5 seconds
85         s = 'onset number in r2: ' + repr(i_1) + ":", " + repr(
t_onset_data_r1[i_1]) + " closest in r3: "
86         s2 = repr(i_r3_best) + ", dt: " + repr(dt_curr)
87         s3 = s + s2
88         print(s3)
89
90         plt.figure(figsize=(9, 5))
91         plt.suptitle('Event 20061022230424')
92
93         plt.subplot(2, 1, 1)
94         plt.plot(mat_t_r1[0, :], mat_I_r1[i_1, :], color='teal'
)
95         plt.title('Intensity enhancement vs time relative to r1
onset')
96         plt.text(0.80, 0.85, f'Onset number {i_1}', color='
black', transform=plt.gca().transAxes)
97
98         plt.tight_layout()
99         plt.ylabel("Intensity (R)")      # rayleigh, photon/sec
100        plt.grid(True, linestyle='--', alpha=0.6) # Adding
grid lines
101        plt.tight_layout()
102
103        plt.subplot(2, 1, 2)
104        plt.plot(mat_t_r3[0, :], mat_I_r3[i_r3_best, :], color=
'teal')
105        plt.title('Intensity gradient vs time relative to r3
onset')
106        plt.text(0.80, 0.85, f'Onset number {i_r3_best}', color
='black', transform=plt.gca().transAxes)
107
108        plt.tight_layout()
109        plt.xlabel("Time relative to the onset for the pulse (s
)")
110        plt.ylabel("Intensity (R)")      # rayleigh, photon/sec
111        plt.grid(True, linestyle='--', alpha=0.6)
112        plt.tight_layout()
113        plt.show()
114
115        # Save both onset indexes to a text file
116        with open('OLD_20061022005940_paired_onsets.txt', 'a')
as file:
117            file.write(f"{int(i_1)},{int(i_r3_best)}\n")
118
119        # save the paired line plots of the onsets, png file
120        filename = "paired_onsets_20061022005940_r2_{0:02d}_r3_
{1:02d}.png".format(i_1, i_r3_best)
121        plt.savefig(filename, format='png')
122        plt.close()

```

Listing A.4: Code used to pair selected onsets and saving indexes into text files.

```

1 import numpy as np
2 import matplotlib.pyplot as plt
3 from scipy.io import loadmat
4
5 # 20070309231545
6
7 # load paired_file
8
9 # paired_onsets = np.loadtxt('20070309231545_paired_onsets.txt
10     ', delimiter=',')
11
12 # Fine selection of favorites only from paired_file
13 paired_onsets = np.loadtxt('new_20070309231545_paired_onsets.
14     txt', delimiter=',')
15
16 # getting the cam values from the data files, separately
17 index_cam1_paired_onset = paired_onsets[:, 0]
18 index_cam2_paired_onset = paired_onsets[:, 1]
19 # print("cam1", index_cam1_paired_onset)
20 # print("cam2", index_cam2_paired_onset)
21
22 # load files for camera 1
23 mat_r2 = loadmat('20070309231545r2.mat')
24 mat_I_r2 = loadmat('H20070309231545r2_intensity.mat')
25 mat_t_r2 = loadmat('H20070309231545r2_t_intervals.mat')
26
27 onset_data_r2 = np.loadtxt('20070309231545r2.txt', delimiter=',
28     ')
29 I_onset_data_r2 = np.loadtxt('20070309231545r2_I_Values.txt')
30 t_onset_data_r2 = np.loadtxt('20070309231545r2_t_Values.txt')
31 I_median_data_r2 = np.loadtxt('20070309231545r2_I_median.txt')
32 I_median_gradient_data_r2 = np.loadtxt('20070309231545
33     r2_I_median_gradient.txt')
34 I_max_data_r2 = np.loadtxt('20070309231545r2_I_max.txt')
35 I_max_gradient_data_r2 = np.loadtxt('20070309231545
36     r2_I_max_gradient.txt')
37
38 # load files for camera 2
39 mat_r3 = loadmat('20070309231545r3.mat')
40 mat_I_r3 = loadmat('H20070309231545r3_intensity.mat')
41 mat_t_r3 = loadmat('H20070309231545r3_t_intervals.mat')
42
43 onset_data_r3 = np.loadtxt('20070309231545r3.txt', delimiter=',
44     ')
45 I_onset_data_r3 = np.loadtxt('20070309231545r3_I_Values.txt')
46 t_onset_data_r3 = np.loadtxt('20070309231545r3_t_Values.txt')
47 I_median_data_r3 = np.loadtxt('20070309231545r3_I_median.txt')
48 I_median_gradient_data_r3 = np.loadtxt('20070309231545
49     r3_I_median_gradient.txt')
50 I_max_data_r3 = np.loadtxt('20070309231545r3_I_max.txt')

```

```

47 I_max_gradient_data_r3 = np.loadtxt('20070309231545
    r3_I_max_gradient.txt')
48
49 # data variables camera 1
50 timeV_r2 = mat_r2['timeV'][0:] # shape:
    (38337, 1)
51 keo_cam = np.transpose(mat_r2['Keo'][0:]) # shape:
    (38337, 256) time, pixels
52 mean_keo_cam = np.mean(keo_cam[:, 50:300], axis=1) # shape:
    (38337, )
53 conv_mean_cam_r2 = np.convolve(mean_keo_cam, [0.25, 0.75, 1, 1,
    1, 0.75, 0.25], mode='same')
54 mat_I_r2 = mat_I_r2['H20070309231545r2_intensity'][0:]
55 mat_t_r2 = mat_t_r2['H20070309231545r2_t_intervals'][0:]
56
57 # data variables camera 2
58 timeV_r3 = mat_r3['timeV'][0:] # shape:
    (38337, 1)
59 keo_cam = np.transpose(mat_r3['Keo'][0:]) # shape:
    (38337, 256) time, pixels
60 mean_keo_cam = np.mean(keo_cam[:, 50:300], axis=1) # shape:
    (38337, )
61 conv_mean_cam_r3 = np.convolve(mean_keo_cam, [0.25, 0.75, 1, 1,
    1, 0.75, 0.25], mode='same')
62 mat_I_r3 = mat_I_r3['H20070309231545r3_intensity'][0:]
63 mat_t_r3 = mat_t_r3['H20070309231545r3_t_intervals'][0:]
64
65 # the index of the onset
66 selected_index = 5
67
68 # get the corresponding onset values
69 selected_onset_r2 = int(index_cam1_paired_onset[selected_index
    ])
70 selected_onset_r3 = int(index_cam2_paired_onset[selected_index
    ])
71 # print(selected_onset_r1)
72 # print(selected_onset_r3)
73
74
75 # get the indices of the onsets in the onset_data arrays
76 index_r1 = np.argmin(np.abs(t_onset_data_r2 - selected_onset_r2
    ))
77 index_r3 = np.argmin(np.abs(t_onset_data_r3 - selected_onset_r3
    ))
78 # print('mat_I_r1', mat_I_r1)
79
80
81 # making pretty paired plots in one to compare
82 for selected_index in range(len(index_cam1_paired_onset)):
83     selected_onset_r2 = int(index_cam1_paired_onset[
    selected_index])
84     selected_onset_r3 = int(index_cam2_paired_onset[
    selected_index])
85     I2_curr = mat_I_r2[selected_onset_r2, :]

```

```

86     I3_curr = mat_I_r3[selected_onset_r3, :] * 20
87
88     plt.figure(figsize=(8, 6))
89     plt.suptitle(f'Event 20070309231545 - paired onset number {
90     selected_index + 1}')
91     plt.plot(mat_t_r2.T, I2_curr.T, label=f'Onset number {
92     selected_onset_r2}')
93     plt.plot(mat_t_r3.T, I3_curr.T, label=f'Onset number {
94     selected_onset_r3}')
95     plt.legend()
96     plt.show()
97
98 # Plot the selected onset and corresponding data
99 plt.figure(figsize=(8, 6))
100 plt.suptitle(f'Event 20070309231545')
101
102 plt.subplot(3, 1, 1)
103 plt.scatter(I_max_gradient_data_r2, I_max_data_r2, color='teal',
104             )
105 plt.title('Peak pulsation intensity vs peak intensity gradient
106           at 6730    ')
107 plt.ylabel('Intensity max')
108 plt.grid(True, linestyle='--', alpha=0.6)
109
110 plt.subplot(3, 1, 2) # 2 rows, 1 column, first subplot
111 # plt.scatter(t_onset_data_r1/3600, I_onset_data_r1, marker
112 #            = '.', color='black', zorder=2, label='onset')
113 # plt.plot(I_max_data_r1[index_r1], I_max_gradient_data_r1[
114 #            index_r1], color='teal', zorder=1)
115 plt.scatter(I_max_gradient_data_r3, I_max_data_r3, color='teal',
116             )
117 plt.title('Peak pulsation intensity vs peak intensity gradient
118           at 7774    ')
119 plt.ylabel('Intensity max')
120 plt.grid(True, linestyle='--', alpha=0.6)
121 # plt.legend()
122
123 plt.subplot(3, 1, 3)
124 x4reg = np.full_like(index_cam1_paired_onset, 0)
125 y4reg = np.full_like(index_cam2_paired_onset, 0)
126 # print(len(y4reg))
127 for selected_index in range(len(index_cam1_paired_onset)):
128     selected_onset_r2 = int(index_cam1_paired_onset [
129     selected_index])
130     # print(selected_index)
131     selected_onset_r3 = int(index_cam2_paired_onset [
132     selected_index])
133     I_ratio = (I_max_data_r2[selected_onset_r2] -
134               I_onset_data_r2[selected_onset_r2])/\
135               (I_max_data_r3[selected_onset_r3] -
136               I_onset_data_r3[selected_onset_r3])

```

```

127     y4reg[selected_index] = I_ratio
128     x4reg[selected_index] = I_max_gradient_data_r2[
129         selected_onset_r2]
130     plt.plot(I_max_gradient_data_r2[selected_onset_r2], I_ratio
131             ,
132             marker='o', linestyle='', color='teal', markersize
133             =5, label='max I')
134 # print(index_cam1_paired_onset)
135 # print(index_cam2_paired_onset)
136 # print(y4reg)
137 # print(x4reg)
138
139 # calculate the linear regression line
140 reg_coefficients, reg_cov = np.polyfit(x4reg, y4reg, 1, cov='
141     True')
142
143 print('slope, y-axis intercept: \n ', reg_coefficients)
144 print('variance of the slope and y-axis intercept, first and
145     last number: \n', reg_cov)
146
147 reg_line = np.polyval(reg_coefficients, x4reg)
148
149 plt.plot(x4reg, reg_line, color='red', label='Linear Regression
150     ') # reg line
151
152 # plt.plot(I_median_data_r1[index_r1],
153     I_median_gradient_data_r1[index_r1])
154
155 plt.title('Intensity ratio I(6730 ) / I(7774 )')
156 plt.xlabel('Intensity gradient')
157 plt.ylabel('I(6730 ) / I(7774 )')
158
159 plt.tight_layout()
160 plt.grid(True, linestyle='--', alpha=0.6)
161 plt.tight_layout()
162
163 plt.show()

```

Listing A.5: Code used to visualize paired onset data from both cameras for each event, including a regression line.

```

1
2 import numpy as np
3 import matplotlib.pyplot as plt
4 from scipy.io import loadmat
5
6 # lists of gradients and its variance
7 reg_gradient_values = [2.16673127e-03, -0.00744144, 2.16999733e
8     -03, 1.17809489e-03, 0.02943631, 5.58054042e-03,
9     -7.05824996e-04, -3.34290493e-03]
10 grad_variances = [8.03542930e-06, 0.00028716, 2.65516485e-06,
11     4.24464130e-05, 4.67567844e-04, 5.90605995e-06,
12     1.63613810e-06, 2.54495921e-06]

```



```

12
13 stdev_values = np.sqrt(grad_variances)      # standard deviation
14 event_order = [1, 3, 4, 6, 7, 8, 5, 2]
15
16 # extract values based on the specified order
17 ordered_gradients = [reg_gradient_values[i - 1] for i in
18     event_order]
19 ordered_stdev_values = [stdev_values[i - 1] for i in
20     event_order]
21
22 # plotting
23 plt.figure(figsize=(8, 6))
24 plt.errorbar(range(1, len(ordered_gradients) + 1),
25     ordered_gradients, yerr=ordered_stdev_values,
26     marker='o', linestyle='', color='green',
27     markersize=8)
28 plt.title('Regression gradient values for all events')
29 plt.xlabel('Event number')
30 plt.ylabel('Regression gradient')
31 plt.xticks(range(1, len(event_order) + 1), event_order)
32 plt.grid(True, linestyle='--', alpha=0.6)
33 plt.show()

```

Listing A.6: The code is utilized to compute the standard deviation of the slope for the regression line.

```

1
2
3 import matplotlib.pyplot as plt
4 import numpy as np
5
6 # loading files
7 file_event_1 = "mag_20061022.txt"
8 file_event_2 = "mag_20061214.txt"
9 file_event_34 = "mag_20070119.txt"
10 file_event_56 = "mag_20070130.txt"
11 file_event_7 = "mag_20070215.txt"
12 file_event_8 = "mag_20070309.txt"
13
14
15 # empty lists to store the extracted data
16 bz_values = []
17 bt_values = []
18
19
20 # read the file and extract relevant data
21 with open(file_event_8, 'r') as file:
22     for _ in range(20):      # skipping the header lines
23         next(file)
24
25     for line in file:
26         data = line.split()
27         bz_values.append(float(data[9]))
28         bt_values.append(float(data[10]))

```

```

29
30 # converting lists to arrays
31 bz_values = np.array(bz_values)
32 bt_values = np.array(bt_values)
33 # print("Bz data \n", bz_values[0])
34 # print("Bt data \n", bt_values[0])
35
36
37 time_minutes = np.arange(len(bz_values))
38 # print(time_minutes[0:10])
39
40 time_hours = time_minutes / 60
41
42
43 plt.figure(figsize=(10, 5))
44 plt.plot(time_hours, bz_values, label='Bz')
45 plt.plot(time_hours, bt_values, label='Bt')
46 plt.ylim(bottom=-8, top=8)
47 plt.axhline(y=0, color='black', linestyle='--', linewidth=1,
48            label='') # adding a solid line at y=0
49
50 # vertical lines at event times
51 plt.axvline(x=23.27, color='#734f8f', linestyle='--', label='
52            Start of event 8')
53 plt.axvline(x=23.60, color='magenta', linestyle='--', label='
54            End of event 8')
55
56 # plt.axvline(x=3.65, color='#734f8f', linestyle=':', label='
57            Start of event 6')
58 # plt.axvline(x=3.98, color='magenta', linestyle=':', label='
59            End of event 6')
60
61 # format x-axis ticks
62 plt.xticks(np.arange(0, max(time_hours)+1, step=3),
63           ['{:02d}:00'.format(int(hour)) for hour in np.arange
64           (0, max(time_hours)+1, step=3)])
65
66 plt.grid(True, linestyle='--', alpha=0.6)
67 plt.xlabel('Time (h)')
68 plt.ylabel('Magnetic Field (nT)')
69 plt.title('Interplanetary Magnetic Field |B| and Bz')
70 plt.text(0, 7, '9.Mar 2007')
71 plt.legend(loc='lower left')
72 plt.show()

```

Listing A.7: The code extracts data from magnetometer files, corresponding to the events.

```

1
2 import numpy as np
3 import matplotlib.pyplot as plt
4 from scipy.io import loadmat
5
6 #      20061022230424

```

```

7 # r1 onset number 6 and r3 number 7
8 # r1 onset number 56 and r3 number 55
9
10
11 # load files for camera 1
12 mat_r1 = loadmat('20061022230424r1.mat')
13 mat_I_r1 = loadmat('H20061022230424r1_intensity.mat')
14 mat_t_r1 = loadmat('H20061022230424r1_t_intervals.mat')
15
16 r1_E1 = loadmat('I6730onsetE1new.mat')
17 t_E1_r1 = r1_E1['t_E1'][0:]
18 I_E1_r1 = r1_E1['I_6730_E1'][0:]
19
20 r1_E2 = loadmat('I6730onsetE2new.mat')
21 t_E2_r1 = r1_E2['t_E2'][0:]
22 I_E2_r1 = r1_E2['I_6730_E2'][0:]
23
24 r1_E3 = loadmat('I6730onsetE3new.mat')
25 t_E3_r1 = r1_E3['t_E3'][0:]
26 I_E3_r1 = r1_E3['I_6730_E3'][0:]
27
28 r1_E4 = loadmat('I6730onsetE4new.mat')
29 t_E4_r1 = r1_E4['t_E4'][0:]
30 I_E4_r1 = r1_E4['I_6730_E4'][0:]
31
32
33 onset_data_r1 = np.loadtxt('20061022230424r1.txt', delimiter=',
34                               ')
35 I_onset_data_r1 = np.loadtxt('20061022230424r1_I_Values.txt')
36 t_onset_data_r1 = np.loadtxt('20061022230424r1_t_Values.txt')
37 I_median_data_r1 = np.loadtxt('20061022230424r1_I_median.txt')
38 I_median_gradient_data_r1 = np.loadtxt('20061022230424
39                               r1_I_median_gradient.txt')
40 I_max_data_r1 = np.loadtxt('20061022230424r1_I_max.txt')
41 I_max_gradient_data_r1 = np.loadtxt('20061022230424
42                               r1_I_max_gradient.txt')
43
44 # load files for camera 2
45 mat_r3 = loadmat('20061022230424r3.mat')
46 mat_I_r3 = loadmat('H20061022230424r3_intensity.mat')
47 mat_t_r3 = loadmat('H20061022230424r3_t_intervals.mat')
48
49 r3_E1 = loadmat('I7774onsetE1new.mat')
50 t_E1_r3 = r3_E1['t_E1'][0:]
51 I_E1_r3 = r3_E1['I_7774_E1'][0:]
52
53 r3_E2 = loadmat('I7774onsetE2new.mat')
54 t_E2_r3 = r3_E2['t_E2'][0:]
55 I_E2_r3 = r3_E2['I_7774_E2'][0:]
56
57 r3_E3 = loadmat('I7774onsetE3new.mat')
58 t_E3_r3 = r3_E3['t_E3'][0:]
59 I_E3_r3 = r3_E3['I_7774_E3'][0:]

```

```

58
59 r3_E4 = loadmat('I7774onsetE4new.mat')
60 t_E4_r3 = r3_E4['t_E4'][0:]
61 I_E4_r3 = r3_E4['I_7774_E4'][0:]
62
63
64 onset_data_r3 = np.loadtxt('20061022230424r3.txt', delimiter=',
    ')
65 I_onset_data_r3 = np.loadtxt('20061022230424r3_I_Values.txt')
66 t_onset_data_r3 = np.loadtxt('20061022230424r3_t_Values.txt')
67 I_median_data_r3 = np.loadtxt('20061022230424r3_I_median.txt')
68 I_median_gradient_data_r3 = np.loadtxt('20061022230424
    r3_I_median_gradient.txt')
69 I_max_data_r3 = np.loadtxt('20061022230424r3_I_max.txt')
70 I_max_gradient_data_r3 = np.loadtxt('20061022230424
    r3_I_max_gradient.txt')
71
72
73 # data variables camera 1
74 timeV_r1 = mat_r1['timeV'][0:] # shape:
    (38337, 1)
75 keo_cam = np.transpose(mat_r1['Keo'][0:]) # shape:
    (38337, 256) time, pixels
76 mean_keo_cam = np.mean(keo_cam[:, 50:300], axis=1) # shape:
    (38337, )
77 conv_mean_cam_r1 = np.convolve(mean_keo_cam, [0.25, 0.75, 1, 1,
    1, 0.75, 0.25], mode='same')
78 mat_I_r1 = mat_I_r1['H20061022230424r1_intensity'][0:]
79 mat_t_r1 = mat_t_r1['H20061022230424r1_t_intervals'][0:]
80
81 # data variables camera 2
82 timeV_r3 = mat_r3['timeV'][0:] # shape:
    (38337, 1)
83 keo_cam = np.transpose(mat_r3['Keo'][0:]) # shape:
    (38337, 256) time, pixels
84 mean_keo_cam = np.mean(keo_cam[:, 50:300], axis=1) # shape:
    (38337, )
85 conv_mean_cam_r3 = np.convolve(mean_keo_cam, [0.25, 0.75, 1, 1,
    1, 0.75, 0.25], mode='same')
86 mat_I_r3 = mat_I_r3['H20061022230424r3_intensity'][0:]
87 mat_t_r3 = mat_t_r3['H20061022230424r3_t_intervals'][0:]
88
89
90 i_1 = 1
91 for i_1 in range(len(t_onset_data_r1)):
92     i_r3_best = np.argmin(abs(t_onset_data_r1[i_1] -
    t_onset_data_r3))
93     dt_curr = t_onset_data_r1[i_1] - t_onset_data_r3[i_r3_best]
94
95     if abs(dt_curr) < 1.5: # 1.5 seconds
96         s = 'onset number in r2: ' + repr(i_1) + ":", " + repr(
    t_onset_data_r1[i_1]) + " closest in r3: "
97         s2 = repr(i_r3_best) + ", dt: " + repr(dt_curr)
98         s3 = s + s2

```

```

99     print(s3)
100
101     if i_1 == 6 and i_r3_best == 7: # plot only onset
102         number 6 from r1 and number 7 from r3
103         plt.figure(figsize=(9, 5))
104         plt.suptitle('Event 20061022230424')
105
106         plt.subplot(2, 1, 1)
107         plt.plot(mat_t_r1[0, :] - 0.05, (mat_I_r1[i_1, :] -
108             mat_I_r1[i_1, 64])
109             / (I_max_data_r1[i_1] - mat_I_r1[i_1, 64])
110             , color='black', label='Onset number 6')
111         plt.plot(t_E1_r1[0, :], I_E1_r1[0, :] / np.max(
112             I_E1_r1[0, :]), color='red', label='3 RE')
113         plt.plot(t_E2_r1[0, :], I_E2_r1[0, :] / np.max(
114             I_E2_r1[0, :]), color='orange', label='4.4 RE')
115         plt.plot(t_E3_r1[0, :], I_E3_r1[0, :] / np.max(
116             I_E3_r1[0, :]), color='turquoise', label='6.1 RE')
117         plt.plot(t_E4_r1[0, :], I_E4_r1[0, :] / np.max(
118             I_E4_r1[0, :]), color='magenta', label='7.6 RE')
119
120         plt.title('Normalized intensity enhancement vs time
121             relative to pulsation onset 6 at 6730 ')
122         plt.tight_layout()
123         plt.ylabel("I_pulse / I_max")
124         plt.ylim(0, 1.1)
125         plt.xlim(0, 1.5)
126         plt.grid(True, linestyle='--', alpha=0.6)
127         plt.tight_layout()
128         plt.legend(loc='lower right')
129
130         plt.subplot(2, 1, 2)
131
132         plt.plot(mat_t_r3[0, :] - 0.01, (mat_I_r3[i_1, :] -
133             mat_I_r3[i_1, 64])
134             / (I_max_data_r3[i_1] - mat_I_r3[i_1, 64])
135             , color='black', label='Onset number 7')
136         plt.plot(t_E1_r3[0, :], I_E1_r3[0, :] / np.max(
137             I_E1_r3[0, :]), color='red', label='3 RE')
138         plt.plot(t_E2_r3[0, :], I_E2_r3[0, :] / np.max(
139             I_E2_r3[0, :]), color='orange', label='4.4 RE')
140         plt.plot(t_E3_r3[0, :], I_E3_r3[0, :] / np.max(
141             I_E3_r3[0, :]), color='turquoise', label='6.1 RE')
142         plt.plot(t_E4_r3[0, :], I_E4_r3[0, :] / np.max(
143             I_E4_r3[0, :]), color='magenta', label='7.6 RE')
144
145         plt.title('Normalized intensity enhancement vs time
146             relative to pulsation onset 7 at 7774 ')
147         plt.tight_layout()
148         plt.xlabel("Time relative to the onset for the
149             pulse (s)")
150         plt.ylabel("I_pulse / I_max")
151         plt.ylim(0, 1.1)
152         plt.xlim(0, 1.5)

```

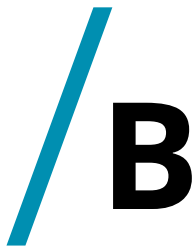
```

137         plt.grid(True, linestyle='--', alpha=0.6)
138         plt.tight_layout()
139         plt.legend(loc='lower right')
140
141         if i_1 == 56 and i_r3_best == 55: # plot only onset
142             number 56 from r1 and number 55 from r3
143             plt.figure(figsize=(9, 5))
144             plt.suptitle('Event 20061022230424')
145
146             plt.subplot(2, 1, 1)
147             plt.plot(mat_t_r1[0, :] - 0.30, (mat_I_r1[i_1, :] -
148                 mat_I_r1[i_1, 64])
149                 / (I_max_data_r1[i_1] - mat_I_r1[i_1, 64])
150                 , color='black', label='Onset number 56')
151             plt.plot(t_E1_r1[0, :], I_E1_r1[0, :] / np.max(
152                 I_E1_r1[0, :]), color='red', label='3 RE')
153             plt.plot(t_E2_r1[0, :], I_E2_r1[0, :] / np.max(
154                 I_E2_r1[0, :]), color='orange', label='4.4 RE')
155             plt.plot(t_E3_r1[0, :], I_E3_r1[0, :] / np.max(
156                 I_E3_r1[0, :]), color='turquoise', label='6.1 RE')
157             plt.plot(t_E4_r1[0, :], I_E4_r1[0, :] / np.max(
158                 I_E4_r1[0, :]), color='magenta', label='7.6 RE')
159
160             plt.title('Normalized intensity enhancement vs time
161                 relative to pulsation onset 56 at 6730 ')
162             plt.tight_layout()
163             plt.ylabel("I_pulse / I_max")
164             plt.ylim(0, 1.1)
165             plt.xlim(0, 1.5)
166             plt.grid(True, linestyle='--', alpha=0.6)
167             plt.tight_layout()
168             plt.legend(loc='lower right')
169
170             plt.subplot(2, 1, 2)
171
172             plt.plot(mat_t_r3[0, :] - 0.15, (mat_I_r3[i_1, :] -
173                 mat_I_r3[i_1, 64])
174                 / (I_max_data_r3[i_1] - mat_I_r3[i_1, 64])
175                 , color='black', label='Onset number 55')
176             plt.plot(t_E1_r3[0, :], I_E1_r3[0, :] / np.max(
177                 I_E1_r3[0, :]), color='red', label='3 RE')
178             plt.plot(t_E2_r3[0, :], I_E2_r3[0, :] / np.max(
179                 I_E2_r3[0, :]), color='orange', label='4.4 RE')
180             plt.plot(t_E3_r3[0, :], I_E3_r3[0, :] / np.max(
181                 I_E3_r3[0, :]), color='turquoise', label='6.1 RE')
182             plt.plot(t_E4_r3[0, :], I_E4_r3[0, :] / np.max(
183                 I_E4_r3[0, :]), color='magenta', label='7.6 RE')
184
185             plt.title('Normalized intensity enhancement vs time
186                 relative to pulsation onset 55 at 7774 ')
187             plt.tight_layout()
188             plt.xlabel("Time relative to the onset for the
189                 pulse (s)")

```

```
175     plt.ylabel("I_pulse / I_max")
176     plt.ylim(0, 1.1)
177     plt.xlim(0, 1.5)
178     plt.grid(True, linestyle='--', alpha=0.6)
179     plt.tight_layout()
180     plt.legend(loc='lower right')
181
182     plt.show()
```

Listing A.8: The code is used to match onset data between MATLAB and Python datasets, generating plots for visual comparison.



Matlab Code

This appendix includes MATLAB scripts for plotting theoretical study data provided by Gavazzi (2023-2024). The corresponding code is accessible on Gustavsson and Gavazzi (2023).

```
1 %%
2 % experiment 1: 3 R_e
3
4 currpwd = pwd; % Current working directory
5 cd /mnt/data/sst141/project_pulsaurora/20240119/experiment_1/ %
   change to directory with modeling-data
6 pwd
7 whos -file I_lambda_of_t.mat % check that file with column
   emission-intensities exists
8 %%
9 load I_lambda_of_t.mat I_4278 I_6730 I_7774 I_8446 t %loadf
   column intensities
10 I_4278_E1 = I_4278; % assign 4278 column intensity for exp1
   to variable
11 I_6730_E1 = I_6730;
12 I_7774_E1 = I_7774;
13 I_8446_E1 = I_8446;
14 t_E1 = t; % time-array-variable for
15 %%
16 % Experiment 2: 4.4 R_e
17
18 cd /mnt/data/sst141/project_pulsaurora/20240119/experiment_2/
19 pwd
20 whos -file I_lambda_of_t.mat
```

```

21
22 %%
23 load I_lambda_of_t.mat I_4278 I_6730 I_7774 I_8446 t
24 I_4278_E2 = I_4278;
25 I_6730_E2 = I_6730;
26 I_7774_E2 = I_7774;
27 I_8446_E2 = I_8446;
28 t_E2 = t;
29 %%
30 % Experiment 3: 6.1 R_e
31
32 cd /mnt/data/sst141/project_pulsaurora/20240119/experiment_3/
   %change to directory with modeling-data
33 pwd
34 whos -file I_lambda_of_t.mat % check that file with column
   emission-intensities exists
35 %%
36 load I_lambda_of_t.mat I_4278 I_6730 I_7774 I_8446 t %loadf
   column intensities
37 I_4278_E3 = I_4278; %assign 4278      column intensity for exp1
   to variable
38 I_6730_E3 = I_6730;
39 I_7774_E3 = I_7774;
40 I_8446_E3 = I_8446;
41 t_E3 = t;           % time-array-variable for
42
43 %%
44 % Experiment 4: 7.6 R_e
45
46 cd /mnt/data/sst141/project_pulsaurora/20240119/experiment_4/
   %change to directory with modeling-data
47 pwd
48 whos -file I_lambda_of_t.mat % check that file with column
   emission-intensities exists
49 %%
50 load I_lambda_of_t.mat I_4278 I_6730 I_7774 I_8446 t %loadf
   column intensities
51 I_4278_E4 = I_4278; %assign 4278      column intensity for exp1
   to variable
52 I_6730_E4 = I_6730;
53 I_7774_E4 = I_7774;
54 I_8446_E4 = I_8446;
55 t_E4 = t;           % time-array-variable for
56
57 %% subplot of all emissions
58
59 figure
60
61 % I_4278
62
63 sph221 = subplot(2,2,1);           %to make one panel per emission
64 ph1 = plot(t_E1, I_4278_E1, 'r');
65 set(ph1, 'linewidth',2)
66 hold on

```

```

67 ph2 = plot(t_E2, I_4278_E2, 'g');
68 set(ph2, 'linewidth',2)
69 hold on
70 ph3 = plot(t_E3, I_4278_E3, 'b');
71 set(ph3, 'linewidth',2)
72 hold on
73 ph4 = plot(t_E4, I_4278_E4, 'c');
74 set(ph4, 'linewidth',2)
75
76 legend([ph1,ph2,ph3,ph4],...
77         {'3 RE', '4.4 RE', '6.1 RE', '7.6 RE'},...
78         'location','southeast')
79
80
81 xlabel('time (s)','fontsize',14)
82 title('Intensity modulation - 4278  ')
83
84
85 % I_6730
86 sph222 = subplot(2,2,2);
87
88 ph5 = plot(t_E1, I_6730_E1, 'r');
89 save('I6730onsetE1.mat','I_6730_E1','t_E1')
90 set(ph5, 'linewidth',2)
91 hold on
92 ph6 = plot(t_E2, I_6730_E2, 'g');
93 save('I6730onsetE2.mat','I_6730_E2','t_E2')
94 set(ph6, 'linewidth',2)
95 ph7 = plot(t_E3, I_6730_E3, 'b');
96 save('I6730onsetE3.mat','I_6730_E3','t_E3')
97 set(ph7, 'linewidth',2)
98 hold on
99 ph8 = plot(t_E4, I_6730_E4, 'c');
100 save('I6730onsetE4.mat','I_6730_E4','t_E4')
101 set(ph8, 'linewidth',2)
102
103 legend([ph5,ph6,ph7,ph8],...
104         {'3 RE', '4.4 RE', '6.1 RE', '7.6 RE'},...
105         'location','southeast')
106 xlabel('time (s)','fontsize',14)
107 title('Intensity modulation - 6730  ')
108
109
110 sph223 = subplot(2,2,3);
111
112 % I_7774
113 ph9 = plot(t_E1, I_7774_E1, 'r');
114 save('I7774onsetE1.mat','I_7774_E1','t_E1')
115 set(ph9, 'linewidth',2)
116 hold on
117 ph10 = plot(t_E2, I_7774_E2, 'g');
118 save('I7774onsetE2.mat','I_7774_E2','t_E2')
119 set(ph10, 'linewidth',2)
120 hold on

```

```

121 ph11 = plot(t_E1, I_7774_E3, 'b');
122 save('I7774onsetE3.mat', 'I_7774_E3', 't_E3')
123 set(ph11, 'linewidth', 2)
124 hold on
125 ph12 = plot(t_E2, I_7774_E4, 'c');
126 save('I7774onsetE4.mat', 'I_7774_E4', 't_E4')
127 set(ph12, 'linewidth', 2)
128
129 legend([ph9, ph10, ph11, ph12], ...
130         {'3 RE', '4.4 RE', '6.1 RE', '7.6 RE'}, ...
131         'location', 'southeast')
132
133 xlabel('time (s)', 'fontsize', 14)
134 title('Intensity modulation - 7774 ')
135
136
137 sph224 = subplot(2,2,4);
138
139
140 % I_8446
141 ph13 = plot(t_E1, I_8446_E1, 'r');
142 set(ph13, 'linewidth', 2)
143 hold on
144 ph14 = plot(t_E2, I_8446_E2, 'g');
145 set(ph14, 'linewidth', 2)
146 hold on
147 ph15 = plot(t_E3, I_8446_E3, 'b');
148 set(ph15, 'linewidth', 2)
149 hold on
150 ph16 = plot(t_E4, I_8446_E4, 'c');
151 set(ph16, 'linewidth', 2)
152
153
154 legend([ph13, ph14, ph15, ph16], ...
155         {'3 RE', '4.4 RE', '6.1 RE', '7.6 RE'}, ...
156         'location', 'southeast')
157
158 xlabel('time (s)', 'fontsize', 14)
159 title('Intensity modulation - 8446 ')
160
161 linkaxes([sph221, sph222, sph223, sph224], 'x')
162 % set(gca, 'xlim', [0 0.5]) % to zoom in time-axis
163
164
165 %% subplot of all emissions
166
167 figure
168
169 % I_4278
170
171 sph221 = subplot(2,2,1); %to make one panel per emission
172 ph1 = plot(t_E1, I_4278_E1/max(I_4278_E1), 'r');
173 set(ph1, 'linewidth', 2)
174 hold on

```

```

175 ph2 = plot(t_E2, I_4278_E2/max(I_4278_E2), 'g');
176 set(ph2, 'linewidth',2)
177 hold on
178 ph3 = plot(t_E3, I_4278_E3/max(I_4278_E3), 'b');
179 set(ph3, 'linewidth',2)
180 hold on
181 ph4 = plot(t_E4, I_4278_E4/max(I_4278_E4), 'c');
182 set(ph4, 'linewidth',2)
183
184 legend([ph1,ph2,ph3,ph4],...
185        {'3 RE', '4.4 RE', '6.1 RE', '7.6 RE'},...
186        'location','southeast')
187
188
189 xlabel('time (s)','fontsize',14)
190 title('Intensity modulation - 4278  ')
191
192
193
194 % I_6730
195 sph222 = subplot(2,2,2);
196
197 ph5 = plot(t_E1, I_6730_E1/max(I_6730_E1), 'r');
198 save('I6730onsetE1new.mat','I_6730_E1','t_E1')
199 set(ph5, 'linewidth',2)
200 hold on
201 ph6 = plot(t_E2, I_6730_E2/max(I_6730_E2), 'g');
202 save('I6730onsetE2new.mat','I_6730_E2','t_E2')
203 set(ph6, 'linewidth',2)
204 ph7 = plot(t_E3, I_6730_E3/max(I_6730_E3), 'b');
205 save('I6730onsetE3new.mat','I_6730_E3','t_E3')
206 set(ph7, 'linewidth',2)
207 hold on
208 ph8 = plot(t_E4, I_6730_E4/max(I_6730_E4), 'c');
209 save('I6730onsetE4new.mat','I_6730_E4','t_E4')
210 set(ph8, 'linewidth',2)
211
212 legend([ph5,ph6,ph7,ph8],...
213        {'3 RE', '4.4 RE', '6.1 RE', '7.6 RE'},...
214        'location','southeast')
215 xlabel('time (s)','fontsize',14)
216 title('Intensity modulation - 6730  ')
217
218
219 sph223 = subplot(2,2,3);
220
221 % I_7774
222 ph9 = plot(t_E1, I_7774_E1/max(I_7774_E1), 'r');
223 save('I7774onsetE1new.mat','I_7774_E1','t_E1')
224 set(ph9, 'linewidth',2)
225 hold on
226 ph10 = plot(t_E2, I_7774_E2/max(I_7774_E2), 'g');
227 save('I7774onsetE2new.mat','I_7774_E2','t_E2')
228 set(ph10, 'linewidth',2)

```

```

229 hold on
230 ph11 = plot(t_E1, I_7774_E3/max(I_7774_E3), 'b');
231 save('I7774onsetE3new.mat','I_7774_E3','t_E3')
232 set(ph11, 'linewidth',2)
233 hold on
234 ph12 = plot(t_E2, I_7774_E4/max(I_7774_E4), 'c');
235 save('I7774onsetE4new.mat','I_7774_E4','t_E4')
236 set(ph12, 'linewidth',2)
237
238 legend([ph9,ph10,ph11,ph12],...
239        {'3 RE', '4.4 RE', '6.1 RE', '7.6 RE'},...
240        'location','southeast')
241
242 xlabel('time (s)','fontsize',14)
243 title('Intensity modulation - 7774  ')
244
245
246 sph224 = subplot(2,2,4);
247
248
249 % I_8446
250 ph13 = plot(t_E1, I_8446_E1/max(I_8446_E1), 'r');
251 set(ph13, 'linewidth',2)
252 hold on
253 ph14 = plot(t_E2, I_8446_E2/max(I_8446_E2), 'g');
254 set(ph14, 'linewidth',2)
255 hold on
256 ph15 = plot(t_E3, I_8446_E3/max(I_8446_E3), 'b');
257 set(ph15, 'linewidth',2)
258 hold on
259 ph16 = plot(t_E4, I_8446_E4/max(I_8446_E4), 'c');
260 set(ph16, 'linewidth',2)
261
262
263 legend([ph13,ph14,ph15,ph16],...
264        {'3 RE', '4.4 RE', '6.1 RE', '7.6 RE'},...
265        'location','southeast')
266
267 xlabel('time (s)','fontsize',14)
268 title('Intensity modulation - 8446  ')
269
270 linkaxes([sph221, sph222, sph223, sph224],'x')
271 % set(gca,'xlim',[0 0.5]) % to zoom in time-axis
272
273
274
275
276 %% subplots:plot of each experiment(1,2,3,4) together in 2x2
      format
277
278 figure
279
280 % experiment 1: 3 RE
281

```

```

282 sph221 = subplot(2,2,1);
283
284 ph1 = plot(t_E1, I_4278_E1/max(I_4278_E1), 'r');
285 set(ph1, 'linewidth', 2)
286 hold on
287 ph2 = plot(t_E1, I_6730_E1/max(I_6730_E1), 'g');
288 set(ph2, 'linewidth', 2)
289 hold on
290 ph3 = plot(t_E1, I_7774_E1/max(I_7774_E1), 'b');
291 set(ph3, 'linewidth', 2)
292 hold on
293 ph4 = plot(t_E1, I_8446_E1/max(I_8446_E1), 'c');
294 set(ph4, 'linewidth', 2)
295
296 legend([ph1,ph2,ph3,ph4],...
297        {'4278', '6730', '7774', '8446'},...
298        'location','southeast')
299
300 xlabel('time (s)','fontsize',14)
301 title('Intensity modulation with source altitude at 3 RE')
302
303
304 % experiment 2: 4.4 RE
305
306 sph222 = subplot(2,2,2);
307
308 ph5 = plot(t_E2, I_4278_E2/max(I_4278_E2), 'r');
309 set(ph5, 'linewidth', 2)
310 hold on
311 ph6 = plot(t_E2, I_6730_E2/max(I_6730_E2), 'g');
312 set(ph6, 'linewidth', 2)
313 hold on
314 ph7 = plot(t_E2, I_7774_E2/max(I_7774_E2), 'b');
315 set(ph7, 'linewidth', 2)
316 hold on
317 ph8 = plot(t_E2, I_8446_E2/max(I_8446_E2), 'c');
318 set(ph8, 'linewidth', 2)
319
320
321 axis([0,1.5,0,1.1])
322
323 legend([ph5,ph6,ph7,ph8],...
324        {'4278', '6730', '7774', '8446'},...
325        'location','southeast')
326
327 xlabel('time (s)','fontsize',14)
328 title('Intensity modulation with source altitude at 4.4 RE')
329
330
331 % experiment 3: 6.1 RE
332
333 sph223 = subplot(2,2,3);
334
335 ph9 = plot(t_E3, I_4278_E3/max(I_4278_E3), 'r');

```

```

336 set(ph9, 'linewidth', 2)
337 hold on
338 ph10 = plot(t_E3, I_6730_E3/max(I_6730_E3), 'g');
339 set(ph10, 'linewidth', 2)
340 hold on
341 ph11 = plot(t_E3, I_7774_E3/max(I_7774_E3), 'b');
342 set(ph11, 'linewidth', 2)
343 hold on
344 ph12 = plot(t_E3, I_8446_E3/max(I_8446_E3), 'c');
345 set(ph12, 'linewidth', 2)
346
347
348 axis([0,1.5,0,1.1])
349
350
351 legend([ph9,ph10,ph11,ph12],...
352        {'4278', '6730', '7774', '8446'},...
353        'location','southeast')
354
355 xlabel('time (s)','fontsize',14)
356 title('Intensity modulation with source altitude at 6.1 RE')
357
358
359 % experiment 4: 7.6 RE
360
361 sph224 = subplot(2,2,4);
362
363 ph13 = plot(t_E4, I_4278_E4/max(I_4278_E4), 'r');
364 set(ph13, 'linewidth', 2)
365 hold on
366 ph14 = plot(t_E4, I_6730_E4/max(I_6730_E4), 'g');
367 set(ph14, 'linewidth', 2)
368 hold on
369 ph15 = plot(t_E4, I_7774_E4/max(I_7774_E4), 'b');
370 set(ph15, 'linewidth', 2)
371 hold on
372 ph16 = plot(t_E4, I_8446_E4/max(I_8446_E4), 'c');
373 set(ph16, 'linewidth', 2)
374
375
376 axis([0,1.5,0,1.1])
377
378 legend([ph13,ph14,ph15,ph16],...
379        {'4278', '6730', '7774', '8446'},...
380        'location','southeast')
381
382 xlabel('time (s)','fontsize',14)
383 title('Intensity modulation with source altitude at 7.6 RE ')
384
385
386 linkaxes([sph221, sph222, sph223, sph224],'x')
387 % set(gca,'xlim',[0 0.5]) % to zoom in time-axis
388
389

```



```

390 %% Individual source altitudes
391
392
393 %% Experiment 1
394 figure % clear figure
395
396
397 ph1 = plot(t_E1, I_4278_E1/max(I_4278_E1), 'r');
398 hold on
399 ph3 = plot(t_E1, I_6730_E1/max(I_6730_E1), 'g');
400 ph5 = plot(t_E1, I_7774_E1/max(I_7774_E1), 'b');
401 ph7 = plot(t_E1, I_8446_E1/max(I_8446_E1), 'c');
402
403 set(ph1, 'linewidth', 2)
404 set(ph3, 'linewidth', 2)
405 set(ph5, 'linewidth', 2)
406 set(ph7, 'linewidth', 2)
407
408 axis([0,1.5,0,1.1])
409
410 legend([ph1,ph3,ph5,ph7], '4278', '6730', '7774', '8446', 'location',
411         , 'southeast')
412
413 xlabel('time (s)', 'fontsize', 14)
414 %title('Intensity modulation with source altitude at 3 RE')
415 title('Column Integrated Intensity with source altitude at 3 RE
416         ')
417
418 grid on
419
420 %% Experiment 2
421 figure % clear figure
422
423
424 ph1 = plot(t_E2, I_4278_E2/max(I_4278_E2), 'r');
425 hold on
426 ph3 = plot(t_E2, I_6730_E2/max(I_6730_E2), 'g');
427 ph5 = plot(t_E2, I_7774_E2/max(I_7774_E2), 'b');
428 ph7 = plot(t_E2, I_8446_E2/max(I_8446_E2), 'c');
429
430 set(ph1, 'linewidth', 2)
431 set(ph3, 'linewidth', 2)
432 set(ph5, 'linewidth', 2)
433 set(ph7, 'linewidth', 2)
434
435 axis([0,1.5,0,1.1])
436
437 legend([ph1,ph3,ph5,ph7], '4278', '6730', '7774', '8446', 'location',
438         , 'southeast')
439
440 xlabel('time (s)', 'fontsize', 14)
441 %title('Intensity modulation with source altitude at 4.4 RE')
442 title('Column Integrated Intensity with source altitude at 4.4
443         RE ')
444
445 grid on

```

```
440
441
442 %% Experiment 3
443 figure % clear figure
444
445 ph1 = plot(t_E3, I_4278_E3/max(I_4278_E3), 'r');
446 hold on
447 ph3 = plot(t_E3, I_6730_E3/max(I_6730_E3), 'g');
448 ph5 = plot(t_E3, I_7774_E3/max(I_7774_E3), 'b');
449 ph7 = plot(t_E3, I_8446_E3/max(I_8446_E3), 'c');
450
451 set(ph1, 'linewidth', 2)
452 set(ph3, 'linewidth', 2)
453 set(ph5, 'linewidth', 2)
454 set(ph7, 'linewidth', 2)
455 axis([0,1.5,0,1.1])
456
457 legend([ph1,ph3,ph5,ph7], '4278', '6730', '7774', '8446', 'location'
      , 'southeast')
458
459 xlabel('time (s)', 'fontsize', 14)
460 %title('Intensity modulation with source altitude at 6.1 RE')
461 title('Column Integrated Intensity with source altitude at 6.1
      RE ')
462 grid on
463
464
465 %% Experiment 4
466 figure % clear figure
467
468 ph1 = plot(t_E4, I_4278_E4/max(I_4278_E4), 'r');
469 hold on
470 ph3 = plot(t_E4, I_6730_E4/max(I_6730_E4), 'g');
471 ph5 = plot(t_E4, I_7774_E4/max(I_7774_E4), 'b');
472 ph7 = plot(t_E4, I_8446_E4/max(I_8446_E4), 'c');
473
474 set(ph1, 'linewidth', 2)
475 set(ph3, 'linewidth', 2)
476 set(ph5, 'linewidth', 2)
477 set(ph7, 'linewidth', 2)
478 axis([0,1.5,0,1.1])
479
480 legend([ph1,ph3,ph5,ph7], '4278', '6730', '7774', '8446', 'location'
      , 'southeast')
481
482 xlabel('time (s)', 'fontsize', 14)
483 %title('Intensity modulation with source altitude at 7.6 RE')
484 title('Column Integrated Intensity with source altitude at 7.6
      RE ')
485 grid on
486
487
488
489
```

```

490 %% Ratio-plots
491
492
493 %% Experiment 1
494 figure % clear figure
495
496 sph221 = subplot(2,2,1);
497 ph1 = plot(t_E1, (I_7774_E1/max(I_7774_E1))./(I_6730_E1/max(
    I_6730_E1)), 'r');
498 hold on
499 ph2 = plot(t_E1, (I_8446_E1/max(I_8446_E1))./(I_4278_E1/max(
    I_4278_E1)), 'b');
500
501 axis([0,1.5,0.8,1.1])
502
503 legend([ph1, ph2], '7774 / 6730 ', '8446 / 4278 ', '
    location', 'southeast')
504
505 xlabel('time (s)', 'fontsize', 14)
506 title('Intensity-ratio with source altitude at 3 RE')
507 grid on
508
509 %% Experiment 2
510 sph222 = subplot(2,2,2);
511 ph3 = plot(t_E2, (I_7774_E2/max(I_7774_E2))./(I_6730_E2/max(
    I_6730_E2)), 'r');
512 hold on
513 ph4 = plot(t_E2, (I_8446_E2/max(I_8446_E2))./(I_4278_E2/max(
    I_4278_E2)), 'b');
514
515 axis([0,1.5,0.8,1.1])
516
517 legend([ph3, ph4], '7774 / 6730 ', '8446 / 4278 ', '
    location', 'southeast')
518
519 xlabel('time (s)', 'fontsize', 14)
520 title('Intensity-ratio with source altitude at 4.4 RE')
521 grid on
522
523
524 %% Experiment 3
525 sph223 = subplot(2,2,3);
526 ph5 = plot(t_E3, (I_7774_E3/max(I_7774_E3))./(I_6730_E3/max(
    I_6730_E3)), 'r');
527 hold on
528 ph6 = plot(t_E3, (I_8446_E3/max(I_8446_E3))./(I_4278_E3/max(
    I_4278_E3)), 'b');
529
530 axis([0,1.5,0.8,1.1])
531
532 legend([ph5, ph6], '7774 / 6730 ', '8446 / 4278 ', '
    location', 'southeast')
533
534 xlabel('time (s)', 'fontsize', 14)

```

```

535 title('Intensity-ratio with source altitude at 6.1 RE')
536 grid on
537
538
539 % Experiment 4
540
541 sph224 = subplot(2,2,4);
542 ph7 = plot(t_E4, (I_7774_E4/max(I_7774_E4))./(I_6730_E4/max(
    I_6730_E4)), 'r');
543 hold on
544 ph8 = plot(t_E4, (I_8446_E4/max(I_8446_E4))./(I_4278_E4/max(
    I_4278_E4)), 'b');
545
546 axis([0,1.5,0.8,1.1])
547
548 legend([ph7, ph8], '7774 / 6730 ', '8446 / 4278 ', '
    location', 'southeast')
549
550 xlabel('time (s)', 'fontsize', 14)
551 title('Intensity-ratio with source altitude at 7.6 RE')
552 grid on
553
554 linkaxes([sph221, sph222, sph223, sph224], 'x')
555 % set(gca, 'xlim', [0 0.5]) % to zoom in time-axis

```

Listing B.1: MATLAB plots of intensity modulation

